Adaptive Formation Control of Cooperative Multi-Vehicle Systems

by

Samet Guler

A thesis
presented to the University of Waterloo
in fulfillment of the
thesis requirement for the degree of
Doctor of Philosophy
in
Mechanical and Mechatronics Engineering

Waterloo, Ontario, Canada, 2015

Author's Declaration

I hereby declare that I am the sole author of this thesis. This is a true copy of the thesis, including any required final revisions, as accepted by my examiners.

I understand that my thesis may be made electronically available to the public.

Abstract

The literature comprises many approaches and results for the formation control of multi-vehicle systems; however, the results established for the cases where the vehicles contain parametric uncertainties are limited. Motivated by the need for explicit characterization of the effects of uncertainties on multi-vehicle formation motions, we study distributed adaptive formation control of multi-vehicle systems in this thesis, focusing on different interrelated sub-objectives. We first examine the cohesive motion control problem of minimally persistent formations of autonomous vehicles. Later, we consider parametric uncertainties in vehicle dynamics in such autonomous vehicle formations. Following an indirect adaptive control approach and utilizing the features of the certainty equivalence principle, we propose control laws to solve maneuvering problem of the formations, robust to parametric modeling uncertainties. Next, as a formation acquisition/closing ranks problem, we study the adaptive station keeping problem, which is defined as positioning an autonomous mobile vehicle A inside a multi-vehicle network, having specified distances from the existing vehicles of the network. In this setting, a single-integrator model is assumed for the kinematics for the vehicle A, and A is assumed to have access to only its own position and its continuous distance measurements to the vehicles of the network. We partition the problem into two sub-problems; localization of the existing vehicles of the network using range-only measurements and motion control of A to its desired location within the network with respect to other vehicles. We design an indirect adaptive control scheme, provide formal stability and convergence analysis and numerical simulation results, demonstrating the characteristics and performance of the design. Finally, we study re-design of the proposed station keeping scheme for the more challenging case where the vehicle A has non-holonomic motion dynamics and does not have access to its self-location information. Overall, the thesis comprises methods and solutions to four correlated formation control problems in the direction of achieving a unified distributed adaptive formation control framework for multi-vehicle systems.

Acknowledgements

First, I would like to thank Baris Fidan. I am indebted to him for all his supports, moral and material, which made the completion of this thesis possible.

I would also like to thank Jan Huissoon, William Melek, Christopher Nielsen and Jorge Cortes for being in my committee and for their helpful comments.

I want to acknowledge the helpful and constructive guidances of Brian Anderson, Soura Dasgupta and Veysel Gazi which were important in achievement of this thesis.

I have had great times in Waterloo. This was possible with those great friends; Nasrettin, Gökhan, Rasit, Kemal, Halit, Elshad, and others. I believe these companionships will last lifetime.

My special thanks go to my lovely family for all their supports.

Dedication

To my family...

Table of Contents

List of Figures

List of Abbreviations

CFSFC	Combined formation shape and flocking control
FF	First follower
GPS	Global positioning system
LS	Least squares
MAS	Multi-agent system
MPF	Minimally persistent formation
OF	Ordinary follower
UAV	Unmanned aerial vehicle

List of Symbols

$\|x\|_p$	$p-$norm of the vector $x \in \Re^n$, $p \in \mathcal{Z}^+$
$\|x\|$	$2-$norm of the vector $x \in \Re^n$
$a \triangleq b$	a equals b by definition
A_i	Agent i
α	Unknown system dynamics parameter vector
β	Unknown system dynamics parameter matrix
$\mathbf{B}$	State matrix of the regulation problem
C	Cycle in a digraph
$\mathcal{C}(r, d)$	Circle with center r and radius d
d_{AT}	Distance between the vehicle A and the target T
d_i	Distance between the vehicles A and A_i
d_i^*	Desired value of d_i
d_i^-	The in-degree of A_i in a digraph
d_i^+	The out-degree of A_i in a digraph
D	The vector of mobile vehicle-stationary vehicle distances d_i
D^*	Desired value of D
$\mathcal{E}_c$	Constraint graph edge set
$\mathcal{E}_f$	Flocking graph edge set
$\mathcal{E}_s$	Sensing graph edge set
$\mathcal{E}_{sh}$	Formation shape graph edge set
γ	Switching function
Γ	Speed profile
$\mathcal{G}_c$	Constraint graph
$\mathcal{G}_f$	Flocking graph
$\mathcal{G}_s$	Sensing graph

$\mathcal{G}_{sh}$	Formation shape graph
$\mathcal{F}(\mathcal{G}, \mathcal{P})$	Formation with graph $\mathcal{G}$ and configuration $\mathcal{P}$
I_n	$n \times n$ identity matrix
J	Cost function
J_{est}	Estimate cost function
$\mathbf{K}$	Control gain matrix
$\lambda_i(A)$	Eigenvalues of the square matrix $A \in \Re^{n \times n}$, $i = \{1, \cdots, n\}$
$\lambda_{\min}(A)$	Minimum eigenvalue of the matrix A
$\lambda_{\max}(A)$	Maximum eigenvalue of the matrix A
$\mathcal{L}$	Laplacian matrix
ν	Linear control input
$\mathcal{N}_i$	The set of neighbors of an agent A_i
ω	Angular velocity
P	Least-squares algorithm covariance matrix
$\mathcal{P}$	Configuration of a multi-agent system
p_A	Position of the vehicle A
p_i	Position of A_i
p_T	Target T location
ϕ	Regressor signal
r_{ij}	Relative position A_i with respect to A_j
$\mathcal{S}$	Multi-agent system
θ	The vector of unknown parameters
$\hat{\theta}$	Estimation vector of θ
$\tilde{\theta}$	Estimation error vector of θ
θ_h	Heading angle of a non-holonomic vehicle
θ_{hi}	Heading deviation from A_i
θ_T	Heading deviation from target T

u	Control input
$\Re^n$	n-dimensional real space
$\Re^+$	Set of nonnegative real numbers
$\mathcal{V}$	Vertex (node) set
v_i	Velocity of A_i
x_i	State vector of A_i
y	Output vector
$\mathcal{Z}^+$	Set of positive integers
$0_{n\times m}$	$n \times m$ zero matrix
ζ	State of the lumped relative position errors

Chapter 1

Introduction

Many creatures in nature behave collectively with the others of the same kind. Birds, ants, and fish show great examples of this behavior. Every one acts in a way that the whole group constitutes a combined structure or shape for advancing some objectives while avoiding collisions. In biological swarms, it is an inherent property that each creature in the swarm makes its movements needed to achieve the desired formation. Among the most interesting instances, there are ants that carry foods from a point to a target point, each keeping a part of the food, an objective which is almost impossible for a single ant. Another amazing instance is a school of fish where every fish moves very close to the others without colliding.

Inspired by this kind of behavior, researchers have worked on setting up swarm architectures to be used in the motion control of multiple mobile systems. Literature comprises many different techniques on this subject. A computer simulation of a flock behavior was introduced in [103], defining the 'rules' that make a group of individuals a swarm: all the members move in the same direction, with the same speed; avoid collisions; and move close to each other. Later, the concepts of control theory and graph theory have been applied to construct coordination schemes that achieve various formation control tasks for mobile robot swarms, including formation acquisition, flocking, consensus, rendezvous, rigid formation maintenance. The methodologies used to solve these problems include virtual-leader based control [93,123], behavior based formation control [6,11], leader-follower formation control [12,32,33,44,45,113,126]. Typical modeling and control tools are brought from the complex systems [83,117], adaptive control [38,65,68,69,137], graph theory [1,17,44,45] frameworks.

Formation control application areas range from multi-robot teams to solving linear algebraic equations. The idea of fractionated space structures is an example to formation control applications. Instead of a monolithic and huge spacecraft, a number of small, but more responsive and effective, spacecrafts are projected to be launched into space. This way, the technical, environmental, and requirement uncertainties will be reduced [15, 16]. These structures are supposed to be integrated by wireless communication in order to make the replacement of a single spacecraft become easier in case of any failure. The problems of information consensus between the spacecrafts and regulation of disturbances need to be studied in parallel as well. Beyond that, another motion problem appears: formation acquisition and maintenance of these structures. Another formation control problem which is not studied explicitly in this thesis is consensus control. Solving systems of linear equations by parallel computers that are coordinated in a distributed way is an application area of consensus control of multi-agent systems (MAS) [4, 97–99]. Given a system $Ax = b$ with the known non-singular matrix A and known vector b, the aim is to solve for the unknown vector x in a distributed fashion. In that setting, each computer tries to find the vector x by solving only a subset of the equation system and communicating with other computers. The distributed way of solving the linear systems of equations brings big advantages in security and computation time [4].

1.1 Motivation

Even though there are numerous theories, methods, and applications on MASs, the control frameworks proposed for MAS motion in a rigid formation are commonly established to be valid for two or three-vehicle formations. However, how the stability is affected when the number of the vehicles increase is not obvious. In fact, the term 'stability of a MAS' has been interpreted dissimilarly in different works; according to some works stability corresponds to stability of the individual vehicles and should be searched for at each individual member, while some others consider this term as having a stable swarm width as time progresses. According to researchers who study formation control of MASs, stability is much related to interactions between vehicles in the formation. As will be discussed in Chapter 2, the difficulty in analyzing the stability properties of a formation control algorithm comes from the lack of convenient and compact *formation models* in the literature. Derivation of a dynamic model for a formation is not trivial indeed. This fact has motivated the authors

to use a system theoretical perspective and study on deriving dynamic models for formations utilizing the features of the graph theory in order to better understand the inherent properties of the formations and ease future control algorithm designs.

There are some dynamical systems that can be modeled by high-order input-affine dynamic model. For this type of systems, consensus and tracking problems have been examined in many works with and without parametric uncertainty, and noisy and time-delayed measurements. When some parameters of the dynamic model are not known exactly, an adaptive or robust method is being used either to estimate the parameters and use this estimation within the controller (indirect method) or to design a controller based on the Lyapunov's theorem achieving the goals even when the parameters do not converge to their correct values (direct method). One witnesses that most of the works in direct or indirect adaptive control structures employ neural or fuzzy approaches in the control design procedure of MASs, which are universal approximators and infamous when it comes to the number of neurons or logics needed to be generated. Sliding mode control technique has also been applied to overcome the effects of uncertainties in dynamic modeling. Although sliding mode control results in a robust system, it leads to high control actions. On the other side, indirect adaptive control approaches rely on the *certainty equivalence principle* and are advantageous in implementation for several reasons. The inspiration of Chapter 4 is utilizing the properties of the certainty equivalence principle through application of the indirect adaptive control approaches to construct systematic adaptive formation control structures when there are parametric modeling uncertainties in vehicle dynamics.

Formation acquisition, or *station keeping*, problem is defined as merging an autonomous vehicle to a multi-vehicle system so that the new vehicle is positioned at desired distances from the existing vehicles. A related objective, the signal source localization, has been treated by many researchers from the control theory and signal processing communities. Advanced results on the target localization problem as well as the problem of reaching to that target exist in the literature. The localization problem is defined as follows: Given a signal source or a target at an unknown location, the main goal is to localize the source in a global coordinate frame by a mobile vehicle using measurements such as position of the mobile vehicle, and the distance to the target or the power of the signal received from the source. In station keeping objective, the target location that the vehicle tries to reach is assumed to be implicitly defined by a multi-vehicle system such that the target point for the mobile vehicle is at desired distances from the existing vehicles. The station keeping objective has been solved for the case of three stationary vehicles on two-dimensional

space, but no result has been established for the N-vehicle case yet in the literature. The motivation of Chapter 5 is to propose a solution method to the station keeping problem for the general, N-vehicle case in both two and three-dimensional space utilizing the *modularity and adaptive* properties of the certainty equivalence principle.

In some real-life application scenarios, a mobile non-holonomic vehicle might be required to achieve the station keeping objective in a GPS-denied environment under the assumption that it does not have access to its own position. In this case, the control techniques derived for systems with the assumption of having the vehicle's own position do not directly apply. So, the control algorithm needs to either employ an adaptive technique or use additional measurements to achieve the objective. In fact, one witnesses that no solution for the target capture problem has been established in the literature for the same measurement setting, i.e., under the assumption that the non-holonomic vehicle cannot sense its self-location information. On the other hand, some control approaches for circumnavigation around a target location by a non-holonomic vehicle for the same measurement setting have recently been established. The motivation of Chapter 6 is to analyze whether the control approaches recently established for the circumnavigation problem can be modified and employed to the target capture and station keeping problems under the same assumptions.

1.2 Contributions of the Thesis

The results of this thesis contribute to the adaptive formation control of multi-vehicle systems literature in many different aspects. Firstly, the background chapter, Chapter 2, summarizes the recent literature on this topic, then four subsequent chapters propose methods for four different, correlated formation control objectives as follows:

Chapter 3: This chapter studies the cohesive motion control problem formally, reviews some formation control approaches integrated to the adaptive control methods in the subsequent sections, and derives a compact state-space motion model for a special class of formations. We formulate the cohesive motion control problem for MPFs of vehicles. We *derive a state-space dynamic model for MPFs* of agents with holonomic point agent kinematics, and *reformulate the cohesive motion control problem as a multivariable regulation problem*. We obtain agent speed conditions in a rigid formation as well.

Chapter 4: We study the cohesive motion control problem of vehicles modeled by high-order dynamics with parametric uncertainty. We integrate the LS parameter estimation

algorithm, which is a commonly used estimation method with well-established convergence results, with a feedback linearization control law to achieve trajectory tracking problem under uncertainty. We prove that the vehicle *perfectly* tracks any smooth trajectory with the proposed controller. Further, we integrate the tracking control law derived for a single vehicle with the virtual-leader based formation control and CFSFC laws, and *propose adaptive formation control schemes for the aforementioned types of vehicles*. The vehicle dynamics need not be homogeneous in the formation, i.e., every vehicle can have different parameter values in the high-order dynamic model.

Chapter 5: We examine the adaptive formation acquisition, or station keeping, problem of a holonomic vehicle. We propose an indirect adaptive control framework which combines the LS estimation algorithm and gradient based motion control law. We use a cost function whose unique minimum corresponds to the target location that the vehicle is desired to reach. *We provide formal stability and convergence results for the proposed controller.* We provide simulation results for different design coefficients and application scenarios.

Chapter 6: *We study the station keeping problem for a more realistic scenario* where the mobile vehicle is modeled by the non-holonomic dynamics and does not have its self-location information. In connection with the station keeping problem setting, we first establish convergence results for the target capture problem for the same measurement setting. The proposed control schemes can be easily employed on non-holonomic vehicles in applications where the vehicle is equipped with only low-cost range sensors.

On the whole, this thesis comprises four different problems and their solution methods, namely, cohesive motion control of MPFs, indirect adaptive formation control of holonomic vehicles with parametric uncertainty, adaptive station keeping, and station keeping of non-holonomic vehicles without self-location information. The key idea of this thesis is (*i*) the need for a compact dynamic model that defines the motion behavior of a formation; (*ii*) the applicability of the certainty equivalence principle to formation control problems through indirect adaptive control architectures; and (*iii*) analysis of formation acquisition for practical scenarios. These topics are inter-dependent topics such that all can be combined under one framework and each can serve as a tool in a cohesive motion control structure for particular application scenarios.

Results of this thesis have been presented in journal and conference papers as well as in a book chapter. The comparative literature survey on formation control algorithms given in Chapter 2 has been published in the book chapter [66]. Adaptive formation control studies

given in Chapter 4 have been demonstrated in [65,69]. The adaptive station keeping results of Chapter 5 has been demonstrated in [64]. The base localization algorithm of Chapter 5 has been presented in [39] in the context of adaptive source localization. The range-based target capture and station keeping results of Chapter 6 have been presented in [67].

1.3 Organization of the Thesis

The thesis mainly consists of five chapters including the background chapter. A chapter is devoted to each of the four topics mentioned so far. Numerical simulation results, discussions, and summaries are provided in each chapter to make every chapter self-contained.

In Chapter 2, basic preliminaries about the graph theory are given in detail. Then, previous works on formation control problem are provided with discussions on how they are related with the current work. Problems that have been considered, assumptions that have been made, and the approaches that have been followed in the literature are presented in detail. Some key results on stability analysis of formations are also given, specifying the drawbacks and applicability to real-time systems.

Chapter 3 is on the cohesive motion control problem of minimally persistent formations. We first state the cohesive motion control problems for minimally persistent formations formally. Then, we review major formation control laws established for general classes of formations in the literature. Later, we derive the system dynamics for formations of agents modeled by point agent kinematics, and convert the cohesive motion control problem to a regulation problem. We then propose an exponentially stabilizing control law to the regulation problem. Finally, we obtain results on agent speed relations in a rigid formation and propose a modified hierarchical leader-follower formation control law.

In Chapter 4, we study vehicles with high-order input-affine dynamics and parametric uncertainty. A special form of dynamic model that is seen in many real-time systems is considered, assuming some parameters in the model are not known. Feedback linearization method together with an indirect least-squares parameter estimation algorithm is employed to make the vehicles track given specified trajectory. We propose two different adaptive formation control frameworks for MASs of these vehicles: the first is based on virtual leader and the other is based on the combined formation shape and flocking control approach of [3]. Finally, formal stability and convergence analysis are provided and numerical simulation results are demonstrated.

Chapter 5 combines two basic algorithms, namely, station keeping and target localization, to derive a systematic framework for the adaptive station keeping problem. Specifically, a mobile sensory vehicle is desired to be added into a network of vehicles by driving the mobile vehicle to a target location which is assumed to be unknown, but uniquely specified by its distances to the stationary vehicles in the network. Only the mobile vehicle's own position and its distances to the stationary vehicles in the network are assumed to be known by the mobile vehicle. Stability and convergence analysis of the algorithm is provided.

Chapter 6 studies the closely related problems of target capturing and station keeping by an autonomous non-holonomic vehicle within the limitations of having access to the measurements of distance from the target only. First, a control law is designed for the target capture problem using the mobile vehicle-target range and range-rate measurement information. Later, the target capture control law is integrated with a linear filter to relax the assumption of range-rate signal availability. Finally, the target capture control law is modified for solving the station keeping objective under the same assumptions. Simulation results for both target capture and station keeping objectives are provided.

Chapter 7 offers conclusions and discussions on the proposed methods.

Chapter 2

Background

In this chapter, we first present the notation used throughout the thesis. We then give some essentials of the graph theory and formation control problem definitions. Later, we review the earlier works on formation control and localization with the open problems in the literature. This chapter is designed based on the book chapter [66].

2.1 Preliminaries and Notation

We now present the notation used throughout the thesis. $\Re^n$ denotes the n-dimensional real space. Matrices are represented by capital letters, e.g., $A \in \Re^{n\times m}$ denotes an $n \times m$ dimensional matrix A. Its transpose and inverse are represented by $A^\top$ and A^{-1}, respectively. We denote $0_{n\times m} \in \Re^{n\times m}$ with all entries zero as zero matrix. I_n stands for the n-dimensional identity matrix. For a square matrix $A \in \Re^{n\times n}$, $\lambda_i(A)$, $i = \{1, \cdots, n\}$, denotes the eigenvalues of A, and we assume that the eigenvalues are ordered such that $\text{Re}\{\lambda_1(A)\} < \cdots < \text{Re}\{\lambda_n(A)\}$. We will denote the minimum $\lambda_1(A)$ and maximum $\lambda_n(A)$ eigenvalues of A by $\lambda_{\min}(A)$ and $\lambda_{\max}(A)$, respectively. $\|x\|_p \in \Re$ where $p \in \mathcal{Z}^+$ denotes the $p-$norm of the vector $x \in \Re^n$. Specifically, we represent the 2-norm of the vector x by $\|x\|$ dropping the subscript. $a \triangleq b$ means 'a equals b by definition'.

$\hat{x}(t) \in \Re^n$ denotes the estimation of the actual vector $x \in \Re^n$ at time instant t. The term "estimation" refers to a process of updating a vector by some rules to get the best approximation of the actual vector x which can be time-varying based on specific quadratic

cost functions. In this thesis, the estimation processes are the commonly known gradient and least-squares parameter estimation schemes.

2.1.1 Graph Theoretical Modeling of Multi-Vehicle Systems

This section gives some definitions from the graph theory and is intended to be the base for the rest of the work. The definitions given here can be found in any book on basic graph theory such as [10]. We start with the description of graphs.

Consider an MAS $\mathcal{S}$ composed of N agents $A_1, \cdots, A_N$ which is required to maintain a certain formation. For this formation control task, $\mathcal{S}$ is represented by a graph $\mathcal{G}(\mathcal{V}, \mathcal{E})$, with the vertex (or node) set $\mathcal{V} = \{1, \cdots, N\}$ and an edge (or link) set $\mathcal{E}$. Each agent A_i is represented by the vertex $i \in \mathcal{V}$. The edge set $\mathcal{E}$ characterizes the agent *interactions* in $\mathcal{S}$. Here what is meant by "*interactions*" needs to be well specified for the particular problem setting as well as whether the interaction between a pair of agents is one way or mutual. Typically, the interaction can be *sensing, communication,* or *formation constraint*, leading $\mathcal{G}(\mathcal{V}, \mathcal{E})$ to be the *sensing graph* $\mathcal{G}_s(\mathcal{V}, \mathcal{E}_s)$, *communication graph* $\mathcal{G}_{com}(\mathcal{V}, \mathcal{E}_{com})$, or *constraint graph* $\mathcal{G}_c(\mathcal{V}, \mathcal{E}_c)$ of $\mathcal{S}$, respectively. In an MAS $\mathcal{S}$, $\mathcal{G}_s$ is the supergraph of $\mathcal{G}_c$. A one way interaction between agents A_i and A_j is represented by a directed edge (i, j), and a mutual interaction between A_i and A_j is represented by an undirected edge (i, j). Accordingly, based on considering the interactions being one way or mutual, the graph $\mathcal{G}(\mathcal{V}, \mathcal{E})$ can be selected to be a *directed graph* (or *digraph*) or *undirected graph*, respectively. For example, if the communication graph $\mathcal{G}_{com}$ of an MAS is undirected, it means that any pair of agents, say $\{A_i, A_j\}$, connected with the communication link $(i, j) \in \mathcal{E}_{com}$ communicate with each other, that is, both send data to and receive data from each other by communication.

In a digraph $\mathcal{G}_c$, the in-degree d_i^- and out-degree d_i^+ represent the number of edges that are incoming to and outgoing from a vertex i, respectively. If $d_i^+ = d_i^-$ for all i in a graph, the graph is said to be *balanced*. If there is an edge from every vertex to every other, then the graph is called *strongly connected*, or a *complete graph*. The analogue of strongly connected graph in undirected graphs is simply termed as connected graph. A *cycle* C in a digraph is the set of vertices and edges in the order such that there is a directed closed path from the first element to the last element of the set.

A *formation* $\mathcal{F}$ of $\mathcal{S}$ additionally represents the structure the agents form in the space, which is characterized by the constraint graph $\mathcal{G}_c$ and the *configuration* $\mathcal{P} = [p_1, \ldots, p_N]^\top \in$

$\Re^{Nn}$ of the formation, where $p_i \in \Re^n$ is the position vector of A_i. A configuration $\mathcal{P}$ that satisfies all constraints in the formation (such as distances between agents or angles between agents in the formation) is called *desired configuration*. $\mathcal{N}_i$, the set of neighbors of an agent A_i, denotes the group of agents with which the agent A_i has an interaction, i.e., has an edge towards them in $\mathcal{E}_s$.

The out-degree d_i^+ is also indicator of another phenomenon, namely *degree-of-freedom (DOF)*, which shows how many constraints agent A_i is supposed to fulfill when it moves. Specifically, on $\Re^2$, an agent with $d_i^+ = 0$ has $2-$DOF, meaning that it can move freely in the plane without concerning the other agents. A $1-$DOF agent has one out-degree and is assumed to satisfy one constraint. Finally, an $n-$DOF agent, $n \geq 2$, has zero out-degree, restricting the motion to only satisfying the inter-agent constraints with the agents its outgoing edges point.

The formation control problem is the problem of controller design for individual agents to achieve predefined control objectives. In this notion, normally there is a formation $\mathcal{F}$ with $\mathcal{G}_c$ and configuration $\mathcal{P}$ whose initial value is $\mathcal{P}_0$ at the initial time instant. In its most basic form, the formation control objective is to steer the agents A_i so that the agents acquire the desired formation structure, where the inter-agent constraints defined by $\mathcal{G}_c$ are satisfied, either in finite time or in the asymptotic sense, and maintain this formation as time progresses. The agents are not necessarily kept stationary after the desired formation is acquired, they may be assumed to move through a given trajectory. There are many types of the formation control problem, to name a few, formation acquisition (or stabilization), flocking, and cohesive motion control can be counted. Avoiding obstacles during the motion and achieving the formation objectives with switching network topology can be counted as sub-objectives appearing in real-life scenarios.

The problem of steering all agents in an MAS to a desired formation shape is named *formation stabilization* (or *formation acquisition*). For this objective, speed of the algorithm is an important factor since the main task is to maintain the desired formation shape in the corresponding space (which is $\Re^2$ or $\Re^3$ in real-life applications) as fast as possible, and the paths the agents travel are not of concern as long as the agent motions are stable (here the term 'stable' means that the distances between any pair of agents connected by a link does not grow unbounded with time). This problem has been studied in many works including [2, 91]. A vast majority of the works in this direction assumes distance or bearing measurements as the only sensing capability and applies gradient control to

achieve the stabilization objective for the formations of single and/or double integrator agents, by defining a potential function for the overall system and minimizing it through gradient approach at each agent in a decentralized sense. One of the main drawbacks that appear in this approach is existence of stable false minima which specifically can drive the formation to an undesired arbitrary line formation where the potential function still takes its minimum value.

Swarm aggregation task is defined as steering all the individual agents into a hyper-ball asymptotically [49, 53–55]. In other words, the agents are driven so that the following inequality holds:

$$\lim_{t\to\infty} \|p_i(t) - p_j(t)\| \leq \varepsilon \quad \forall i, j \in \{1, \cdots, N\},$$

where $\varepsilon > 0$ is a small design coefficient. This objective is achieved in finite-time by applying the specifically designed artificial potentials [53–55], or sliding-mode controls [49]. In these works, the agents are assumed to be holonomic points with single-integrator kinematics, and the radius of the desired hyper-ball can be adjusted using the parameters of the swarm model. The extension to swarms of agents with double-integrator dynamics is also considered in [85,86]. Usually, swarms in nature show this behavior while they move towards a favorable region where the living conditions for individuals are supportive or run away from hostile regions or predators.

Flocking is defined as achieving the common desired velocity for all agents in the formation. This common velocity may be predefined and the agents may be informed with this velocity information, or the agents may reach an arbitrary common velocity by averaging their velocity with their neighbor agents. Flocking is generally combined with the formation shape stabilization task to accomplish formation control objectives. Since the flocking objective is related with controlling the agent velocities, it is necessary to have the ability of controlling the acceleration level, which in turn requires each agent having at least a second order plant model. The case where the agents are not informed with the predefined common velocity information is also examined in the literature and will be covered in the subsequent sections as an adaptive formation control framework.

2.1.2 Rigidity and Persistence of Multi-Vehicle Formations

The term 'rigid motion' means an object moving in space without deforming its shape. This motion corresponds to changes in the translations and rotations of the whole object.

The rigidity concept has found many applications in the formation controls as well. A formation $\mathcal{F}$ with the undirected constraint graph $\mathcal{G}_c$ is rigid if the continuous motions of $\mathcal{F}$ alters positions of the agents so that the whole formation only translates or rotates in the space. This can only be achieved provided $\mathcal{G}_c$ is rigid. Accordingly, rigid graph theory [1,84], is employed to analyze whether a formation is rigid.

As an immediate result one can easily conclude that in a rigid formation, if the distance constraints are satisfied for the edges in the set $\mathcal{E}_c$, the formation will move as a rigid object and no flexibility will occur between the agents. On the other hand, a non-rigid formation may be deformed after some agents in the formation move even if all the distance constraints are satisfied during the motion. Rigid formations are not necessarily strongly connected, which would require $(N^2-N)/2$ links for N agents. For an N agent formation, one can obtain a 2-rigid constraint graph (viz., rigid for a 2-D realization) with $2N-3$ edges, and 3-rigid constraint graph (viz., rigid for a 3-D realization) with $3N-6$ edges. *Minimally rigid formation* is the one that is rigid and has the property that removal of any edge in the formation leads to a non-rigid formation. Accordingly, minimally 2-rigid and minimally 3-rigid formations for N agents are made up with $2N-3$ edges and $3N-6$ edges, respectively. Further details on rigid formations can be found in [1], which also provides a detailed description on how to test whether a formation is rigid (Rigidity Matrix Theorem), and how to construct a rigid graph from the beginning (Henneberg construction). *Flip ambiguity* denotes the case where the shape of a rigid formation can change while maintaining rigidity, which is depicted in Fig. 2.1. The following example illustrates the definitions and nomenclature given above.

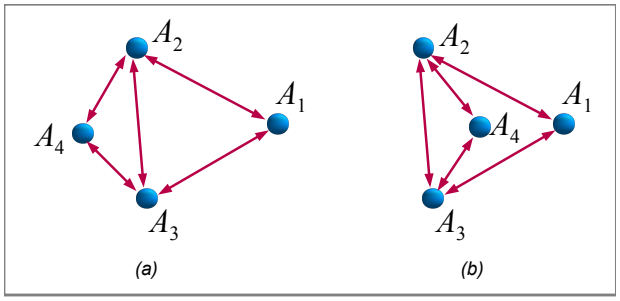

Figure 2.1: Flip ambiguity: A_4 can be positioned in two different locations in the formation, both satisfying the rigidity constraints.

Example 2.1.1. *Consider the 4-agent constraint graphs* $\mathcal{G}_i$, $i = 1, 2, 3, 4, 5$, *in Fig. 2.2.* $\mathcal{G}_1$, $\mathcal{G}_2$, $\mathcal{G}_3$ *are directed and* $\mathcal{G}_5$ *is undirected, while* $\mathcal{G}_4$ *is neither directed nor undirected. Only* $\mathcal{G}_2$ *has cycles,* $C_1 = \{1, 3, 4\}$ *and* $C_2 = \{1, 3, 4, 2\}$. *Observe that only* $\mathcal{G}_3$ *is strongly connected and only* $\mathcal{G}_5$ *is a balanced graph as all undirected graphs are naturally balanced. Among them* $\mathcal{G}_1$ *and* $\mathcal{G}_4$ *are not rigid while the rest are rigid graphs. One can directly observe that moving the nodes* 1 *and* 2 *in* $\mathcal{G}_1$ *without violating distance constraints may destruct the shape of the graph, or exhibits flexibility.*

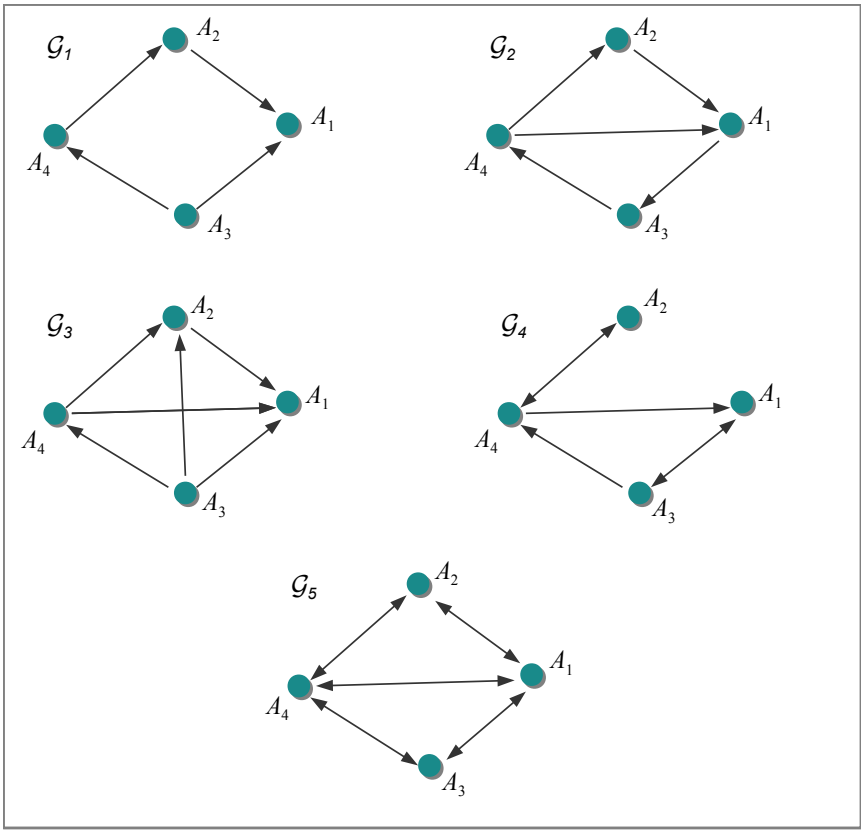

Figure 2.2: Five different constraint graphs with four agents

While in some applications, it is desirable to change the formation *shape* during the motion, in some other applications, the agents may be supposed to reach to a desired formation shape and keep this formation during the rest of the motion (*formation maintaining*). This behavior can be seen in the animals such as bird flocks migrating from a

place to another, moving as a group at a same altitude. They constitute a V-like shape while flying and do not change it until they arrive at the goal location. This type of motion is called as *cohesive whole* motion. We study on formation control algorithms for cohesive motion in Chapter 3 and Chapter 4.

2.1.3 Minimally Persistent Formations

Satisfying the rigidity constraints in a formation $\mathcal{F}$ with a rigid constraint graph $\mathcal{G}_c$ simply corresponds to maintaining the distances between the agent pairs represented by the directed edges in $\mathcal{E}_c$ of $\mathcal{G}_c$ during motion. The analogy of rigidity to directed graphs is *persistence*; however these two terms do not directly give the same meaning, [1, 44]. If every vehicle in $\mathcal{F}$ can satisfy its formation objective such as maintaining the distances to its all leader vehicles at their desired values at the same time, then the formation is called *constraint consistent*. A minimally rigid and constraint consistent formation is called *minimally persistent formation (MPF)* [1]. Since minimally persistent formations of vehicles require the minimum number of edges between a given number of vehicles, a vehicle is required to satisfy the minimum number of motion constraints in a minimally persistent formation.

An acyclic MPF $\mathcal{F}$ has exactly $2N-3$ directed edges on $\Re^2$. In an acyclic MPF $\mathcal{F}$, there is a vehicle with $2-$DOF, meaning that it can move freely in the plane without concerning the other agents, a $1-$DOF vehicle which is assumed to satisfy one constraint, and $N-2$ vehicles with $0-$DOF whose motions are restricted to only satisfying the inter-agent constraints to their leader vehicles.

2.1.4 Agent Model Classification

From a modeling point of view, we may classify the agent models into the following categories: *point agent* model, *point mass* (double integrator) model, *non-holonomic vehicle* model, *Euler-Lagrange vehicle* model, and *high-order dynamic* model. This classification is also related with the space where the motion of the agents flows. Non-holonomic agent models are generally used to describe the motion of wheeled ground vehicles on two-dimensional Euclidean plane, while point or high-order dynamic models are generally used

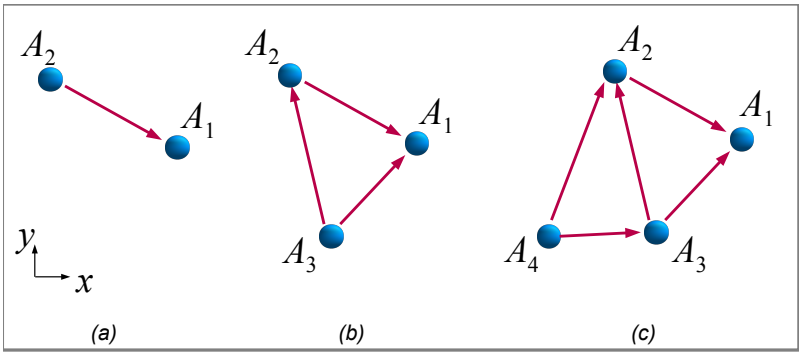

Figure 2.3: Constructing an acyclic minimally persistent formation using the Henneberg construction method: (a) Initial two agent (leader and first follower) formation; (b) Addition of the third (ordinary) agent; (c) Addition of the fourth (ordinary) agent.

to describe the motion of robots moving in a 3D space such as quadrotors and satellites. We now give a brief description for these models.

Definition 2.1.1 (Holonomic point agent and point mass models)**.** *The holonomic point agent (kinematic) model is a first-order one where the motion of the agent in every axis is independent from each other, and thus the agent can move to any point directly in the corresponding space. The model is generally represented by*

$$\dot{p}_i = v_i, \quad i \in \{1, \ldots, N\}, \tag{2.1}$$

where $p_i,\ v_i \in \Re^n,\ n \in \{2, 3\}$, *are the position and the velocity vectors of agent* A_i, *respectively. The input is the velocity vector. Likewise, the point mass model is described by*

$$\dot{p}_i = v_i, \quad \dot{v}_i = u_i, \quad i \in \{1, \ldots, N\}, \tag{2.2}$$

with u_i *the acceleration input.*

Holonomic point agent kinematics is a high-level model. This model is commonly used to simplify the analysis of the overall MAS formation behavior. Real-time systems such as robot vehicles usually have more complicated dynamics such as non-holonomic and fully-actuated Euler-Lagrange dynamics. For real-time implementations, one has to consider these complicated models to characterize the behavior of the robotic system under consideration.

Definition 2.1.2 (Non-holonomic and Dubins vehicle model)**.** *On $\Re^2$, the non-holonomic agent model is given by*

$$\dot{x}_i = v_i \cos(\theta_i) \tag{2.3}$$

$$\dot{y}_i = v_i \sin(\theta_i) \tag{2.4}$$

$$\dot{\theta}_{hi} = \omega_i, \quad i \in \{1, \ldots, N\}, \tag{2.5}$$

where v_i, θ_{hi}, $\omega_i \in \Re$ are the linear speed, heading angle, and angular speed of the agent A_i. Position of the center of the vehicle is denoted by $p_i = [x_i, y_i]^\top \in \Re^2$. The general configuration of this vehicle model for one agent is represented in Fig. 2.4. If the vehicle speed v_i is constant, it is named Dubins vehicle model.

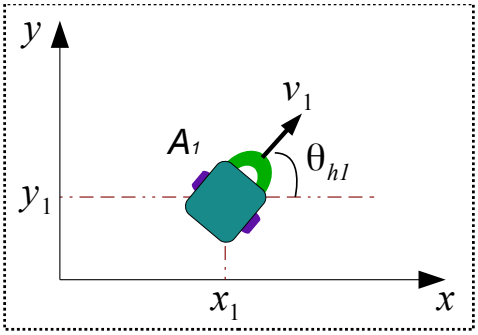

Figure 2.4: Non-holonomic vehicle model

Definition 2.1.3 (Euler-Lagrange vehicle model)**.** *The general fully-actuated Euler-Lagrange vehicle model for A_i is given by*

$$C_i(p_i)\ddot{p}_i + N_i(p_i, \dot{p}_i) = u_i, \tag{2.6}$$

where $C_i \in \Re^{n\times n}$, $u_i \in \Re^n$, and $p_i, \dot{p}_i \in \Re^n$ are the mass matrix, input vector, and output vectors (position and velocity) of A_i, and $N_i \in \Re^n$ denotes the nonlinear effects such as centripetal and coriolis forces, and gravity effects.

Euler-LaGrange model is derived directly from the physical characteristics of the vehicle using kinetic and potential energy conversions. It comprises the coupling forces between different parts of the vehicle, which makes it one of the most comprehensive vehicle model.

Definition 2.1.4 (High-order Dynamic Model)**.** *On $\Re^n$, the high-order dynamic model for the agent A_i is given by*

$$\begin{aligned} \dot{x}_{i,k} &= x_{i,k+1}, \quad k = 1, \ldots, r-1;\ r \geq 2 \\ \dot{x}_{i,r} &= \alpha_i(x_i, t) + \beta_i u_i \\ y_i &= x_{i,1}, \end{aligned}$$

where $x_i = [x_{i,1}^\top, \ldots, x_{i,r}^\top]^\top \in \mathbb{R}^{rm}$. $x_{i,j},\ u_i,\ y_i \in \mathbb{R}^m,\ j = 1, \ldots, r$ are the state, input, and the output vectors, respectively. α_i and β_i are called the parameter vector and gain matrix in the corresponding dimensions.

2.2 Literature on Formation Control

The literature comprises many different techniques and control approaches applied to MASs to achieve the formation objectives. Naturally, a technique performs its job on some certain classes of agents, since any small difference in an agent model requires redesign of the controller. Similarly, assumptions made on sensing and communication topology of the formation separate the earlier works into different classes. For example, a controller designed under the assumption that every agent senses its relative position to its neighbor agents may not be directly applied to formations where agents are only able to sense distances to their neighbors. This section is intended to give a brief summary of the earlier works on MAS formation control, especially the ones of the recent years, mentioning about the assumptions on the agent dynamics and sensing topologies, and their applicability to real-time systems. We classify the earlier works on the formation control of MASs into two groups based on the formation constraint graphs: undirected graphs and directed graphs.

2.2.1 Formation Control Methodologies with Undirected Constraint Graphs

When every agent pair throughout a formation makes mutual effort to maintain their desired inter-agent behaviors, it becomes possible to define a total potential function for the overall formation and derive a control law which employs the gradient of this function at every single agent. Such potential function definition leads to a compact dynamics

representation for the overall formation. In general, the stability analysis of formations with undirected sensing and constraint graphs relies on the mutual behavior between the agent pairs and, in most cases, results in a stable closed-loop dynamics for connected graphs. In this subsection, we review the previous works on the control systems derived for formations with undirected graphs, providing some observations on the results.

[53] studies the swarm aggregation problem, and analyses the stability of multi-agent systems from the 'swarm' perspective. The ultimate objective is forming a cluster around a point. Assuming perfect sensing of each individual member and its neighbors' global position information, it directly designs a control rule for the individuals and further analyses the stability of the whole system using Lyapunov analysis. It is finally shown that in a limited time all the members are driven into a hyperball radius of which can be adjusted changing the parameters of the control signal. It is also proven that the agents become stationary as time progresses. The work gives concrete results on the overall stability of swarms of agents of the same kind. On the other hand, since the objective of the work is forming a group around a point, transient motion of the agents while achieving the aggregation objective is not mentioned. For this reason, the result of the work cannot be directly used in translation of agents from a point to another while achieving formation objectives (cohesive motion).

[91] considers the formation stabilization (or formation acquisition) problem of point agent formations with infinitesimal rigid constraint graphs. Sensing graph and constraint graph are chosen the same. It is shown that for undirected formations, a decentralized gradient-based controller results in a locally stable equilibrium for the formation if the constraint graph is infinitesimally rigid. The key tool applied is the center manifold theory. The result of undirected formations is validated by simulating a polygon example. An extension of the result to the minimally persistent formations constructed by Henneberg insertion technique is also considered. It is shown that if the collinear initial positions are excluded, the same control approach for the minimally persistent formations leads to a closed-loop system equilibrium point which is locally asymptotically stable.

If the objective is to steer a finite number of agents such that they satisfy both formation acquisition and velocity alignment (or *synchronization*), then it becomes necessary to work with a double integrator agent model [125], [3]. It follows from the fact that in the point agent model case the control input is the velocity vector in the same dimension as the position vector, so it is not possible to achieve the control of the velocity dynam-

ics using the velocity vector itself. [125] considers double integrator agents moving on a two-dimensional plane with the objective of both formation acquisition and flocking under randomly switching network topology. Assuming undirected graph structure, the authors apply the summation of two control terms as the control input: first is the well-known gradient control law for cohesion while the second term is for velocity alignment. They prove the convergence of the velocities of the agents to their average value under switching network topology. [3], inspired by [125], applies the same control rule for formations with double integrator agents, introducing a leader. The work is the same as [125] except that a leader agent is added to the formation, and the links between the leader and its neighbors (actually all the other agents are neighbors of the leader) are made directed to the leader, while the other links remain undirected. It is shown that for this kind of formations, assuming the leader velocity is constant, a slight modification of the control law of [125] achieves both the formation acquisition and flocking at the same time.

In [5], the author has used passivity approach to achieve distributed cooperative control for formations with undirected graphs. Specifically, a group of agents are controlled so that they achieve two objectives: (i) The velocity vectors of all agents are driven to a common velocity vector asymptotically, and (ii) the so called difference variables of neighbor agents are driven to a compact invariant set. The former objective is the synchronization of the output variables, while the latter corresponds to the formation stabilization (or *inter-agent distance maintaining*). The work proposes a systematic way to design a generic passivity-based controller to achieve both objectives. The ability to choose the design functions freely as long as they satisfy the given criteria makes the design procedure quite flexible. The desired velocities for all the agents are the same in that work and satisfy a design criterion. However, one may not wish to choose exactly the same desired velocities for all the agents for some objectives. In the hierarchical structure, speed of a follower agent is affected from the agent(s) it follows, and is updated accordingly. Thus, the method of [5] does not fit to formations with digraphs unless some modifications take effect. The results of [5] are extended to include the cases where the reference velocity is not informed to the agents. This extension leads to an adaptive formation control framework and is reviewed in detail in Section 2.3.

Another instance of the works that consider both the synchronization of position variables problem and the velocity alignment problem for N-agent systems is [81]. Using the results of [118], a general class of nonlinear agent models is converted to a suitable form. Combining that model with the results of [5], which applies passivity theorems, [81] solves

both objectives in a centralized manner.

[105] proposes two algorithms for flocking of agents. All the results obtained are for double-integrator agents connected by undirected formation graph, and independent of the number of agents in the formation. Since the control of an agent requires only information about agent's neighbors, the control scheme can be considered as distributed. The first algorithm is on the control of accelerations, that is, for an agent, generated by summation of the gradient control of inter-agent distances and the velocity alignment terms. A potential function to be minimized is then designed based on a new norm function defined to overcome the convexity problem of the commonly used norm functions. The gradient control term is employed so that agent A_i considers others that are within a specified radius of the ball centered at the position of A_i as neighbors and tries to satisfy the inter-agent distance constraint with those agents. It is proved that with the first algorithm all agents achieve inter-agent distance objective as well as velocity alignment and collision avoidance (i.e., satisfy all three conditions of [103]); however, they are still subject to fragmentation group-by-group since they are not navigated. To make the agents achieve a group objective (or flocking) the other algorithm is designed by modifying the control term so that it contains a term related with the group objective. In fact, this addition can be interpreted as an addition of a perfect leader agent to the formation. As opposed to our definition in Section 2.1.1, cohesiveness in this work is defined as formation flow such that agents are within a boundary during motion, regardless of the behavior of the inter-agent metrics.

The case where the inter-agent distance constraints cannot be satisfied is also studied in some works. For instance, [35] mentions about feasibility of formations of agents modeled by single-integrator (2.1) and non-holonomic dynamics (2.3). The feasibility concept is defined as 'being able to satisfy the distance constraints for all edges in a connected graph'. The authors propose controllers for both agent models. For feasible formations of single-integrator agents, the work proposes a control law that achieves inter-agent distance constraints of the formation. It further shows that for infeasible formations the control law makes all the agents reach to specified common velocity, but may not achieve distance constraints even for some agents. The work further shows similar results for the formations of non-holonomic agents.

2.2.2 Directed Constraint Graphs: More Hierarchy

The literature on the control of formations with undirected constraint graphs has generic [1] stability results thanks to the the symmetry the mutual interaction between the agents brings into the formation. In some engineering applications, especially in the control of autonomous mobile vehicles, it may be desirable to construct a formation with directed constraint graph where the agents decide on their motions in a hierarchical framework. This is achieved by introducing a set of so-called *leaders* that direct the formation, and the rest of the formation follows this leader with control actions designed based on their degrees in the hierarchy. Since the stability analysis of a formation mostly based on the edge dynamics, which completely depend on the mutual interactions of agent pairs, analyzing the closed-loop control system of a directed formation lacking these mutual interactions is not a trivial one, and in some cases even intractable. The following intuitive example presents the difficulty of the control design for formations of digraphs: there are two vehicles where one is the leader while the other is the follower whose goal is to follow the leader vehicle at some distance. If the leader moves freely on its own path regardless of the follower vehicle's motion and if the follower vehicle has no a priori information on the leader's path, then no control approach can be derived directly for the follower vehicle to achieve this simple goal. Hence, the works concerning digraphs have to either make some assumptions on the sensing structure or design an adaptive or robust control scheme. Control systems derived for digraphs are mostly for three or four-agent formations. In what follows, we give some control approaches some of which are still lacking full stability analysis.

Point agent formations have been studied heavily in the literature and many techniques have been applied to get strong stability results which are intractable when it comes to more complicated agent models such as non-holonomic ones. We start with the method of [44] which is further developed in [45] integrating it with camera applications. As in many other leader-follower (LF) formation structures, [44] constructs control rules for the agents in a hierarchical fashion; first the control for the first agent is developed, then the control rules for the follower agents are developed consequently. It considers a three-level hierarchical system: there is a leader (A_1), its first follower (FF) (A_2), and the ordinary followers (OF) ($A_3, \ldots, A_N$) (for specific definitions see [44]). Dynamics of all agents are assumed to be holonomic point agent kinematics (2.1) in two-dimensional Euclidean space. The work assumes that each agent is capable of obtaining global position information of

[1] where by 'generic' we mean 'systematic' or 'for an arbitrary number of formation members'.

its own as well as of its leaders. A_1 is required to move to a predefined 'final point' p_{1f} with a proportional control law fed back by the distance to p_{1f}, integrated with a switching threshold function aiming to prevent chattering around a small neighborhood of the final point p_{1f}. For A_2, the same control law is used with the only difference that the feedback signal is the difference between the actual and desired relative positions of A_2 with respect to A_1. Each of $A_3, \ldots, A_N$ with a similar control law, aims to track the closest intersection point of the two circles centered at the two agents it follows with radii corresponding to the inter-agent distance requirements. Since the final points for the agents are assumed to be constant, small neighborhoods of the final points constitute compact discs and fulfill the compact set requirement of Lyapunov stability analysis. In [44], a formal Lyapunov analysis is given to show the stability of A_1 in a sense that it enters the ϵ_1 neighborhood of its final point, for an arbitrarily small positive design constant ϵ_1, and stays there in the limit. A Lyapunov analysis for A_2 and the ordinary followers $(A_3, \ldots, A_N)$ are given in [45] where for simplicity the velocity vector of the leader agent A_1 is assumed to be calculated via interpolation and is added to the control term of A_2. [45] also presents a real-time implementation of the control system on a non-holonomic mobile robot formation. In that paper, follower robots obtain relative position measurements to their leaders using cameras mounted on the vehicles.

When there are cycles in the formation graph, the control design requires more effort [2], [139]. In [2], the inter-agent distance maintaining problem is studied for three point agents, each having 1-DOF and named co-leaders, in a cyclic formation, relaxing the assumption of relative position measurement. Instead, the analysis is based on the inter-agent distances and the orientation of the neighbor agents. Each agent has a unique neighbor, i.e., without loss of generality, it is assumed that $\mathcal{N}_1 = \{A_2\}$, $\mathcal{N}_2 = \{A_3\}$, $\mathcal{N}_3 = \{A_1\}$. A decentralized control scheme is applied to control the orientations of the agents. Another example work that considers cyclic graphs is [139]. The authors of [139] consider minimally persistent formations of point agents with directed graphs containing cycles on a two-dimensional plane and examines the response of the agents to small disturbances that move agents from correct shape by small amounts. The assumption on sensing is relative position measurement through either distance and direction measurements, or distance measurements and communication between certain agents. The agents are supposed to start from positions that form the correct shape and they are disturbed 'sufficiently' small. After disturbance take effect, the leader agent does not move and serves as a reference point for the follower agents. Then, the follower agents make their movements obeying the

hierarchy so that the formation stabilization problem is solved for the resultant simplified dynamics by a suitable gain matrix. Even though the objective is only formation stabilization, the work is important in that it proposes a linear closed-loop dynamic model for the directed cyclic graphs and employs rigidity matrix in finding the gain matrix.

There is a set of pioneer studies by researchers at the University of Pennsylvania that has studied the practical implementations of MASs formed by mobile non-holonomic robots, and introduced some new concepts on *LF formation control* [29, 33, 126]. To name a few, we may mention the so-called $l-l$ and $l-\psi$ control schemes. [33] proposes two types of controllers, $l-l$ and $l-\psi$, for LF formation of non-holonomic robots. The focus is on a pair of non-holonomic mobile robots modeled by (2.3). The system model is then converted to distance l and bearing ψ dynamics, in which the dynamics of both the robots are present explicitly. In order to eliminate the nonlinear effects in the new dynamics, input-output linearization method is applied, so the control law of the follower robot includes the linear and angular speeds of the leader robot. However, no methodology to obtain this information is mentioned in the work. In [33], it is established that if the leading robot moves through a circle path, i.e., with a constant linear and angular speed, then the heading angle of the follower robot locally asymptotically converges to a specified constant. It is further established that when the leading robot moves through a straight path, heading angle of the follower converges to the heading angle of the first robot, a better result for a stronger assumption as expected. It is also stated in [33] that with the distance-distance $l-l$ control law, when the first two robots move on a straight line with constant linear velocity and zero angular velocity, heading angle of the third robot exponentially converges to the initial heading angle of the first two robots. As in $l-\psi$ control, it is assumed that the speeds of the first and second robots as well as their heading angles are available to the third agent without proposing how to obtain them.

The LF control approach of [33] has been developed and integrated with camera applications in [29]. [29] has examined formation control of non-holonomic mobile robots equipped with omni-directional camera systems as only sensor on the robots. Each robot relies on its decentralized control structure, which mainly consists of input-output feedback linearization along with estimation algorithms. The inter-agent distances and bearing angles are chosen as states, thus the linearization procedure requires the knowledge of the control signal of the leader agent as well as the agent itself, as in [33]. Extended Kalman filter is applied to derive the estimation of the required signals. Later, in [126], a stability notion is defined with the name "leader-to-formation" stability (LFS), which is an analogue

to input-to-state (ISS) stability in single-input-single-output (SISO) systems. In that work, directed LF formations are considered, and it is aimed to show how the initial conditions of the formation members and the inputs of the leaders affect the error propagation inside the formation, demonstrating this feature to be a robustness property of formations. A group of agents are assigned as leaders of the formation and the others are assigned as their followers. The leaders are assumed to be controlled with feedback stabilizing controllers and stabilized perfectly. It is proposed that if the follower agents are LFS with respect to the leaders, then the whole formation becomes LFS. The result of this work provides a safety bound on the errors propagated in a LF formation, or conversely, tells about the initial condition bounds for satisfying prescribed safety features. Applications to non-holonomic mobile robots are also given in that work.

The well-known internal model principle has been used as a tool to synchronize MASs of agents with linear system dynamics in a series of works [132–134]. Assuming a complete graph, [134] provides an internal model-based controller for N heterogeneous agents. The models for all agents and their controllers are chosen as linear systems and all the systems are assumed to be stabilizable and detectable. The work also assumes the availability of all the outputs to all the agents. It is shown that if the matrices for the regulation problem of the well-known internal model principle exist, then the outputs synchronize exponentially to a configuration determined by the internal-model principle. The works [132, 133] are also in the same direction.

Besides the numerous works in continuous-time, formation stabilization problem has also been studied in discrete-time domain. [27] has studied global shape stabilization for formations of agents modeled as rigid body dynamics in discrete-time domain: first, the agents equalize their local coordinate frames under the assumption that in the constraint graph there exists a globally reachable vertex. Then, a cost function is introduced in terms of the Laplacian matrix of the graph. By the aid of the so-called Jacobi over-relaxation method, it is shown that the formation with undirected graph globally stabilizes to the desired set with the proposed controller. Further, robustness of the algorithm against the initial frame orientation errors and measurement errors is discussed. Another example work to formation stabilization control in discrete-time is [21], where the authors have analyzed the formation control of MASs with minimally rigid constraint graphs. Assuming all the agents have common clock and range-only measurements to their neighbors, the so-called cyclic stop-and-go strategy is proposed. Applying the vertex-coloring method, the vertices are partitioned into subsets such that no two vertex with the same color are connected

by an edge. Using these two techniques, the work has studied minimization of an energy function whose minimum corresponds to the desired formation if the initial configuration of the agents is inside the neighborhood of the desired equilibrium. Hence, the result is local.

2.2.3 A Discussion on Distributed Controllers in Literature

Previous works on formation control of MASs have mainly focused on the design of control algorithms for each individual agent for the purpose of achieving desirable agent interactions throughout the formation. On the other hand, stability and convergence analyses are examined from the overall system perspective instead of the agent level. Even though there are numerous theories, methods, and applications on MASs, the control frameworks proposed for MAS motion in rigid formations are commonly established for two or three-agent formations. However, how the stability is affected when the number of the agents increase is not obvious. In fact, the term stability of an MAS has been interpreted dissimilarly in different works; according to some works stability corresponds to stability of the individual agents and should be searched for at each individual member, while some others consider this term as having a stable swarm width as time progresses. It is also certain that there is a close correlation between the two points of view.

Motion control for formations with undirected constraint graphs has been studied extensively from different perspectives. Most of the works on this specific topic apply the gradient control taking the advantage of the mutual interactions between agents. As a drawback of the non-convex cost functions considered, there arises the undesired equilibrium issue that mostly correspond to line formations. On the contrary, even though it requires more effort to synthesize systematic control frameworks, formations with directed constraint graphs are more robust to communication failures and more scalable to large number of vehicles in formations. Especially, LF scheme is a very structured control method for directed formations. However, the methods derived for directed formations do not conclude sound stability results for cohesive motion control. Due to the one-sided control laws of vehicles in the formation, the results are heavily based on assumptions such as 'if the leader agent moves on a circle or a line' or 'if the leader agent moves with a specified speed'. So, one needs to observe these restrictions when designing the formation hierarchy and assigning control objectives to agents.

2.3 Literature on Adaptive Formation Control

2.3.1 Perspectives

The term 'adaptive formation control' can be interpreted in various ways. We may classify the recent works on this topic roughly into two parts: (i) The agents which do not know the common objective of the formation learn this objective and adapt itself with respect to this objective, and (ii) every agent in the formation has parametric or non-parametric uncertainties in its system dynamics and makes use of estimation algorithms together with adaptive controller to eliminate the effects of the uncertainties. The latter is in fact the main intention which the adaptive control field has built on for uncertain SISO and MIMO systems. Implementing either of the two categories above in the context of formation control for MASs is challenging although it may seem straightforward at first glance. In this part, we revise some recent results on the adaptive formation control.

We first review the adaptive formation control approaches in the first category. In [70], an adaptive control framework is designed to control spacecraft formation flying. It is assumed that external constant disturbances in a known form enter into each spacecraft system. First, dynamics of the spacecraft system is presented, and how the disturbance enters into system equations is explicitly shown. Then, the adaptive control rule is derived via direct adaptive approach using Lyapunov stability theory.

[8, 9] and Chapter 3 and 4 of [7] translate the word 'adaptation' to mean that some agents inside a formation do not have the common objective information, which is specifically the reference velocity vector that all agents are desired to achieve. Generating the estimate of this vector using the other available information, each agent tries to achieve the common goal. In those works, the results of [5] are further developed for stronger assumptions. Chapter 3 of [7] considers the case where the reference velocity of the formation is known by only the leader agent of the formation. The reference velocity is assumed to be generated by an exo-system of the form $v(t) = H\eta(t)$, where the state vector η is generated by a marginally stable system $\dot{\eta} = A\eta$. It is assumed that the matrix A is skew-symmetric and thus produces constant or periodic η, and is available to all the agents. For each agent, a linear estimation model for the reference velocity is proposed where the matrix A is used as an 'internal model'. Two control designs are then synthesized that integrate the estimation algorithm with the passivity-based design of [5]. The first one shows that

passivity of the closed-loop control system is preserved and the agents converge to an equilibrium set where the distance constraints are satisfied. However, in the first design, the convergence of the velocities to the actual reference velocity of the formation is proved only when $v(t)$ is constant and the formation objective is agreement. In the second (augmented) design, besides the results of the first design, the convergence of all the agents' velocities to the reference velocity is satisfied for any reference velocity at the expense of using the relative velocity information in the control rule, which in real-life scenarios may require synchronous communication between agents.

Adaptive methodologies can be used also in systems in which the multi-agent coordination problem can be formulated as an output regulation (i.e., servomechanism) problem. For example, as discussed in [134], the distributed agreement problem can be formulated as if the agents are tracking a trajectory (the agreement trajectory) generated by an exo-system. Then provided that the agents possess an internal model of the exo-system then agreement can be achieved. However, in general it is really a strong assumption to assume that all the agents know the exo-system (or possess an internal model of it). Instead, it is more realistic to assume that the exo-system is unknown and adaptively construct an internal model to it. This can be done independently in a distributed manner by the agents using their local agreement errors. Such an idea can be used also for the problem of tracking a moving target in a geometric formation. Such an approach is used in a series of studies in [52,61–63] utilizing earlier result on adaptive internal models in [115]. In [61] the problem of formation control and trajectory/target tracking by a group of agents with nonlinear dynamics, unknown parameters, and local external disturbances is considered and adaptive internal model based procedure is developed. This work is later extended in [63] by considering switched exo-systems which allow tracking more complex trajectories as well as various formation maneuvers such as formation expansion/contraction, formation rotation, formation reconfiguration.

[8] and the Chapter 4 of [7] propose parameterization-based velocity estimation model for the same purpose. In these works, the reference velocity is assumed to be generated by the following model $v(t) = \sum_{j=1}^{r} \phi^j(t)\theta^j$, where ϕ^j is the time-dependent regressor signal available to each agent, and $\theta = [\theta^1, \cdots, \theta^r]^\top$ is the parameter vector. The agent A_i, $(i = 1, \ldots, N)$ tries to find the reference velocity by estimating the vector $\hat{\theta}_i = \left[\hat{\theta}_i^1, \cdots, \hat{\theta}_i^r\right]^\top$. As in the internal model-based approach of the Chapter 3 of [7], the formation maintaining objective is achieved with the update rule $\dot{\hat{\theta}}_i = \Lambda(\Phi \otimes I_2)u_i$, where Λ

is the adaptive gain, $\Phi = [\phi^1(t), \cdots, \phi^r(t)]^\top$, and u_i is the control input of A_i. Further, for the constant reference velocities, convergence of the velocity estimates to the actual ones is proved. [130] also considers the tracking control of a linearly parameterized trajectory by the agents with uncertain high-order dynamics assuming the agents can communicate under a communication graph structure.

[9] proposes another augmented design and claims perfect estimation and tracking of any reference velocity. A new directed, strongly connected, and balanced graph $\mathcal{G}^v$ for the communication of velocity information is defined in the formation. Then, it is assumed that an agent has the relative velocity information to its neighbors in $\mathcal{G}^v$. This information is used in the control law of the agent and due to the strongly connectedness of the graph $\mathcal{G}^v$, both the convergence of estimate $\hat{v}(t)$ to the actual reference velocity $v(t)$ objective and the formation maintaining objective are satisfied. However, this design still requires that each agent is aware of the control signal of its neighbors in $\mathcal{G}^v$.

[25] considers the LF formation control of two non-holonomic vehicles, where the linear speed of the leader vehicle is not known by the follower. The follower uses the so-called smooth projection algorithm to estimate the time-varying speed of the leader vehicle. The work proves the uniformly boundedness of the relative distance and bearing between the vehicles with the help of the Lyapunov stability theory, and contributes to the literature of LF framework of non-holonomic vehicles as an adaptive approach.

Adaptive trajectory tracking for double integrator agents is studied in [79]. Although the graph structure is said to represent a LF framework, the overall graph scheme evokes the conventional virtual leader one since the sub-graph representing the followers is bidirectional while the leader connects to that graph with unidirectional links. Adaptivity comes from the need for eliminating the effect of disturbances that are assumed to linearly enter into the system dynamics at the acceleration level and are assumed to be linearly parameterized. Assuming the acceleration of the leader is also parameterized as a linear combination of known basis functions, the work employs an identifier-based adaptive controller together with a consensus controller to synchronize the accelerations of the followers and the leader. So, the work can be considered as a contribution to the adaptive synchronization in MAS literature, rather than LF formation control literature. The same approach for almost the same problem setting is introduced in [138], with a globally uniformly asymptotically convergent result. A drawback that is seen in both works, which appears as a really important phenomenon in real-life applications, is the assumption of the

availability of the instant relative position error descriptions of the agents to their neighbors without delay. In addition, linear parameterization of the non-linear agent dynamics in [138] may not be always straightforward.

In the second category of adaptive formation control approaches, it is assumed that in the MAS the vehicle dynamics contain uncertainties. Here, we review [49, 59, 68, 69, 136] in this direction. [49, 136] consider swarms composed of agents with fully actuated vehicle dynamics in the form of Euler-Lagrange model (2.6). The functions $N_i(p_i, \dot{p}_i)$ represent the disturbances and non-linear effects, and are assumed to be in the form $N_i(p_i, \dot{p}_i) = f_i^k + f_i^u$, where f_i^k, f_i^u are the known and unknown parts, respectively. Moreover, it is assumed that the positive definite matrices $C_i(p_i)$ are unknown with known lower and upper bounds. Sliding-mode control together with the potential function approach is applied to achieve the formation control and the target tracking objectives. The relative position of the target is assumed to be measured by all the agents and the sensing graph is chosen as complete, i.e. every agent senses the relative position to all other agents in the formation. It is shown that the objectives are achieved despite the uncertainties in the agent dynamics. In [59] the results are extended to swarms composed of agents with the non-holonomic vehicle dynamics, containing uncertainties. Note that the case of swarms with non-holonomic vehicle dynamics is in general more involved than the case of swarms with fully actuated agents.

Similar to [49, 136], in [68, 69] the authors use the tools of adaptive control theory to overcome the uncertainties in the system dynamics at the agent level. [68] considers formation control of three UAVs with parametric uncertainties and applies the direct MRAC scheme at each agent. [69] studies a dynamic model in Brunovsky canonical form with parametric uncertainties. Using the feedback linearization technique and least-squares parameter estimation algorithm in an indirect adaptive control scheme formation objectives are achieved for the vehicles with parametric uncertainty. In Chapter 4, we present the approach of [65] where the results of [69] are extended and formal stability analysis are provided.

There are some other adaptive formation control frameworks that are not considered in either of the two categories mentioned above such as [100, 101]. Observing the need that agents have to acquire their own positions in real time for some specific objectives without using positioning systems such as GPS, [100, 101] propose formation maintaining control together with an estimation algorithm for localizing the agents. In these works, each agent

localizes its own position using its sensor information and data obtained from its neighbor agents through communication. The convincing simulation results show the effectiveness of the controller under the given assumptions, and the work is one of the limited works that connect localization with formation control. However, how advantageous applying this approach is uncertain when compared to similar works. Firstly, since the estimation is performed on each agent separately, i.e. in a decentralized fashion, how the desired agent positions are assigned and how the agents are informed with this data are not obvious. Secondly, the work requires a communication topology between agents.

Some researchers have interpreted adaptivity as changing the formation shape during motion based on environmental conditions such as obstacle avoidance. [72] interprets the term adaptivity as having a swarm of autonomous mobile robots avoiding obstacles during motion based on local interactions of individual robots. This is achieved by assigning two neighbor agents to every agent in the formation, leading to multiple rigid triangle formations. The agents fragmentize and move accordingly when to avoid obstacles on the path.

2.3.2 Intelligent Adaptive Approaches

Besides the conventional adaptive control techniques, there are also approaches utilizing intelligent methods such as neural network and fuzzy logic based adaptive controllers for achieving group coordination and/or formation control [38], [131]. In case the uncertainties in the agent or overall swarm dynamics cannot be parameterized conventional techniques based on parametric uncertainties cannot be applied. Neural networks and fuzzy systems are known to be universal approximators [110, 121], which have the property of being able to approximate any smooth function with arbitrary accuracy on a compact set (provided that the parameters of the system are set properly). This property makes them powerful tools which can be employed in function approximation as well as function approximation based adaptive control. In particular, they can be employed to approximate the modeling uncertainties, [120, 121], and eliminate their adverse effects over the system dynamics and controller design. In principle, intelligent adaptive methods can be applied both on agent level and on MAS level. However, most of the works in the literature utilizing such methods on dynamic MAS problems are on the agent level. In other words, most of the neural and/or fuzzy-based formation control or coordination approaches and therefore the corresponding control laws are designed at the agent level and these tools are used to overcome the

uncertainties in the individual agent dynamics such that to achieve the overall swarm coordination and control objectives.

An example work which utilizes an intelligent control approach for multi-agent coordination is [137], where the authors study the containment problem of formations of agents with nonlinear dynamics. The sensing graph is assumed to be directed and the followers need only the position information of their leaders to achieve the formation objective. Neural network based function approximation is applied to estimate the nonparametric uncertainty in the agent dynamics, which may be intractable with the conventional identifier-based adaptive control methods. However, as a deficiency of the utilized function approximation based method, a small function approximation error occurs at steady-state. Such errors can be overcome by adding a robustness signal to the control law as in [78]. A related study is [128] where the output synchronization problem is solved by combining cooperative control, game theory, and reinforcement learning. [111] also makes use of neural network based identifiers to overcome the uncertainties at the agent level and achieve formation control objectives.

A series of studies has also considered the distributed agreement problem (which is known also as the consensus or synchronization problem in the literature) and the formation control problem in a class of multi-agent dynamic systems composed of agents containing non-parametric model uncertainties. In [36], a fuzzy logic based direct adaptive control approach has been developed to solve the MAS formation control problem. In this work a class of multi-agent dynamics systems composed of agents in normal form with model uncertainties is assumed to acquire and maintain a predefined geometric formation as well as to track a reference trajectory. This work utilized earlier results in [120] to suppress the effects of uncertainties and to achieve group objectives. The adaptive term was also augmented with bounding and sliding mode terms in order to achieve robustness. Later, [58] further extended the results by incorporating the high-gain observer in order to estimate the derivatives of the agent errors (which constitutes an important relaxation). Moreover, [58] considered various formation maneuvers such as expansion/contraction, rotation, and formation reconfiguration. Similarly, [50] considered the distributed output agreement problem and utilized similar strategy in order to achieve agreement despite the uncertainties in the agent dynamics.

2.3.3 The Limitations

Despite its settled and solid base, adaptive control theory has not been applied in formation control literature well enough. The fact that in the literature there is no generic system model for persistent formations of MASs may be considered as a reason for this deficiency. Since most of the generic results of the adaptive control theory admit plant dynamics with certain assumptions, either in the time or frequency domain, it appears that there is a need for such a motion model for persistent formations in order to apply the tools of the adaptive control theory and get the most out of its features.

Regarding the discussion on the classification of the adaptive control schemes above, one may expect the future roles of adaptive control theory into formation control in at least two different aspects. The first approach would be overcoming the uncertainties inside the individual agent models by employing the indirect adaptive approach. Here, we should emphasize a disadvantage of the application of this method, since most of the estimation algorithms rely on the persistence of excitation of the regressor signals as a requirement of the parameter convergence, it may be hard to fulfill this condition for every single agent in the formation. The second approach would be the implementation of the direct adaptive control methods [82] in formation models.

In addition, in applying both the indirect and direct adaptive approaches in formation control, another important phenomenon that needs to be taken into consideration is the speed of convergence of parameter estimates or the outputs. Since most adaptive control tools guarantee parameter convergence 'in the asymptotic sense', the initial conditions on the system parameters or outputs would be crucial for transient performance of the overall formation. Besides, although having not been derived generically yet, dynamic models for formations tend to be time-varying. Observing that the adaptive control algorithms derived for time-varying systems have some limitations, controlling a formation with these algorithms would carry the same limitations as well. In summary, although utilizing adaptive control theory into formation control schemes seems promising to overcome the modeling uncertainties and yield better convergence results for formations of agents with uncertain models, it would bring a lot of restrictions and narrow the spectrum of the agent dynamics considered to conclude guaranteed convergence results.

Chapter 3

Cohesive Motion Control: Rigid Formation Maintenance

3.1 Introduction

When a group of vehicles is required to show a cooperative behavior when they move, a formation control algorithm needs to be applied on the individual vehicle controllers. An example to such behaviors is moving the formation of vehicles from an initial to a final configuration preserving the shape (geometry) of the formation, named *cohesive motion control* [1, 12, 44, 45, 113, 139]. The main goal in the design of cohesive motion control structures is to maintain the inter-agent distance constraints between vehicles which are connected by artificial links of the constraint graph of the formation.

Cohesive motion is much related to formation rigidity. For instance, a formation of robots moving in a plane or in a three dimensional space can achieve distance maintaining for all agents in the formation if the constraint graph of the formation is rigid, and all the constraints are satisfied during the motion. The works [29, 32, 33] have studied formation maintenance of multiple non-holonomic mobile robots using LF formation structures. Assuming the availability of relative position measurements between agents, feedback linearization based distance-distance and distance-bearing controllers have been synthesized in these works to achieve desired inter-agent behaviors. Although these works present effective simulation and real-time experimental results, the methods do not conclude with a

comprehensive stability result for cohesive motion of formations, and are prone to singularity issues. In another series of works [12,44,45,113], the task of moving a rigid multi-agent formation to reach a final configuration cohesively, i.e., maintaining the formation rigidity during motion, has been studied. These works also use LF formation structures and propose a set of distributed control schemes for such structures. The leader agent is driven to follow a trajectory or a sequence of way-points which are generated by path planning algorithms, and the followers are required to maintain the inter-agent distances to the agents they follow. To prevent chattering around equilibrium points, switching techniques are employed. Even though [12,44,45,113] present efficient simulation results for the aforementioned control system and have convergence analysis of the leader agent, they still lack the full stability analysis of the overall system. In [44] it is shown that with the proposed control scheme, the leader agent converges to its desired position asymptotically. In [45], stability analysis of the FF agent is also provided, assuming that the FF agent has the knowledge of the velocity vector of the leader agent on-line via interpolation or other techniques. However, no bound on the propagation of the distance keeping errors in the MAS has been established in these works.

In this chapter, we study cohesive motion control of MPFs. We first state the cohesive motion control problems in a formal way for acyclic MPFs. Then, we do a critical review of the formation control approaches in the literature. Later, we derive the system dynamics for formations of agents modeled by point agent kinematics and convert the cohesive motion control problem to a regulation problem in order to ease further control design processes. Then, we design a distributed control law for the acyclic MPF, which results in a simple proportional control law for each agent. Finally, we obtain results on agent speed relations in a rigid formation.

3.2 Problem Definition

We consider a 2-dimensional acyclic MPF $\mathcal{F}$ of an MAS $\mathcal{S} = \{A_1, \cdots, A_N\}$. Assume that each agent is modeled to have single integrator motion kinematics (2.1). The directed *constraint graph* $\mathcal{G}_c$ of $\mathcal{F}$ is assumed to be acyclic and minimally persistent. As is common in the literature, the leader agent A_1 is assumed to be equipped with a GPS, and has more sensing capabilities than the other agents. It is assumed that A_1 knows its own position, $p_1(t)$, for all $t \geq t_0$ in the global coordinate frame. The desired trajectory $p_1^*(t)$

that A_1 is required to follow is assumed to be generated by an exogenous system which we are not concerned in this chapter. We assign the agent A_2 as the FF and the agents $A_i,\ i = \{3, \cdots, N\}$, as the ordinary followers (OF). We emphasize here that to maintain a minimally persistent formation on $\Re^2$, it is necessary and sufficient for each OF agent to follow two agents [44], which we call *its leaders*. Although different assignments for the leader sets of OF agents $A_i,\ i \geq 4$ are possible, in this chapter we assume that the leader set of an OF agent $A_i,\ i = \{3, \cdots, N\}$, is $\{A_{i-1}, A_{i-2}\}$.

The *sensing graph* $\mathcal{G}_s$ of $\mathcal{F}$ is assumed to be the supergraph of the constraint graph $\mathcal{G}_c$, that is, if there is an edge $(i, j) \in \mathcal{E}_c$, then we have $(i, j),\ (j, i) \in \mathcal{E}_s$. So, $\mathcal{G}_s$ is bidirectional and rigid. We assume that the leader A_1 can sense the distances to its followers $A_2,\ A_3$; the LF agent A_2 senses the relative position to the leader A_1; and the OF agents $A_i,\ i = \{3, \cdots, N\}$, senses the distances to its two leaders A_{i-1} and A_{i-2}. We denote the actual and desired relative positions from A_j to A_i by $r_{ij} \triangleq p_i - p_j$ and r^*_{ij}. The actual and desired distances between A_j to A_i are represented by $d_{ij} \triangleq \|r_{ij}\|$ and $d^*_{ij} \triangleq \|r^*_{ij}\|$. The sensing graph being bidirectional means that sensing is mutual, i.e., the agent A_i senses relative position r_{ji} to the agent A_j and the agent A_j senses the relative position r_{ij} to A_i.

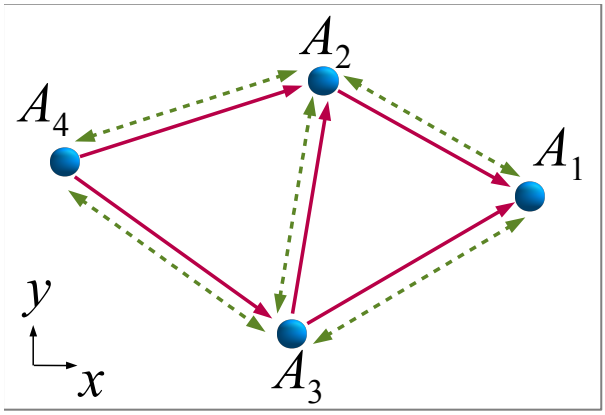

Figure 3.1: Sensing and constraint graphs for a 4-agent formation; solid directed arrows form the constraint graph and dashed undirected arrows form the sensing graph, respectively.

The following design constraint is assumed in this chapter: there are constant maximum

speed bounds $\bar{v}_i > 0$ for every agent $A_i,\ i = \{1, \ldots, N\}$. We define the vector

$$\Gamma(\mathcal{F}) = [\bar{v}_1, \cdots, \bar{v}_N]^\top \tag{3.1}$$

as the *speed profile* of the formation $\mathcal{F}$. One of the objectives of the current work is to analyze the behavior of the formation during motion under the LF scheme, and to analyze the effects of $\Gamma(\mathcal{F})$ on the motion behavior.

The main control task is to design an individual controller producing the velocity of each agent in an acyclic minimally persistent, LF formation $\mathcal{F}$, in order to move the formation to given final position cohesively, i.e., without deforming the shape or violating the distance constraints during the motion. We have the following assumption on the initial formation configuration.

Assumption 3.2.1. *At the initial time instant $t = t_0$, the formation configuration $\mathcal{P}(t_0)$ satisfies the inter-agent distance constraints defined by $\mathcal{G}_c$.*

Assumption 3.2.1 together with a suitable control rule that keeps the formation configuration inside the neighborhood prevents the flip-ambiguity during motion. We are interested in a distributed and hierarchical control design. Here what is meant by distributed control design is designing control law for each level of the formation in a hierarchical order. To facilitate such a design, we consider a leader-first follower-ordinary follower control/constraint architecture. Considering this structure we pose the following problem.

Problem 3.2.1 (LF Formation Cohesive Motion Problem)**.** *Consider an LF formation $\mathcal{F}$ with $N \geq 3$ agents $A_1, \cdots A_N$, the acyclic minimally persistent two-dimensional constraint graph $\mathcal{G}_c$, and rigid, bidirectional sensing graph $\mathcal{G}_s$. Assume that each agent is modeled to have single integrator motion kinematics with the position vector p_i and the control input v_i. Design a distributed control scheme producing $v_1, \ldots, v_N$ such that*

i. A_1 tracks $p_1^*(t)$ asymptotically.

ii. The relative position error $\int_{t_0}^{t} \|r_{12}(\tau) - r_{12}^*\| \mathrm{d}\tau$ between A_1 and A_2 is minimized, that is, A_2 follows A_1 with the desired relative position r_{12}^*.

iii. $A_i,\ i = 3, \ldots, N$, maintains desired distances $d_{i,i-1}^*$ and $d_{i,i-2}^*$ to its leaders A_{i-1} and A_{i-2}, minimizing $\int_{t_0}^{t} \|d_{i,i-1}(\tau) - d_{i,i-1}^*\| \mathrm{d}\tau$ and $\int_{t_0}^{t} \|d_{i,i-2}(\tau) - d_{i,i-2}^*\| \mathrm{d}\tau$.

An important question arises immediately: What would be the velocity bounds for specific agents and how is it related with the level of the agent in the hierarchy? The following problem states this question formally and we search for the answer of this question in the subsequent sections.

Problem 3.2.2 (Agent Speed Bound Problem)**.** *Given an LF formation $\mathcal{F}$ with $N \geq 3$ agents $A_1, \cdots A_N$, the acyclic minimally persistent two-dimensional constraint graph $\mathcal{G}_c$, and rigid, bidirectional sensing graph $\mathcal{G}_s$. Assume that each agent is modeled to have single integrator motion kinematics with the position vector p_i and the control input v_i. Find the conditions on the speed profile $\Gamma(\mathcal{F})$ so that Problem 3.2.1 is solvable.*

3.3 Cohesive Motion Control Design

In this section, we review the major formation control approaches in the literature applicable to the *LF Formation Cohesive Motion Problem*. Two of the approaches presented in this chapter, virtual-leader based formation control and combined formation shape and flocking control approaches, will be extended in Chapter 4, following an indirect adaptive control design procedure, for the more realistic problem setting where the high-order dynamics and parametric uncertainties in vehicle motion are taken into account.

3.3.1 Virtual Leader-based Formation Control

Virtual leader-based formation control approach aims to achieve the goals of Problem 3.2.1 by individual agent tracking of certain assigned reference trajectories. Within the general framework of this approach, which is applicable to settings other than the LF setting as well, a virtual leader A_v is defined inside the formation to well-define the trajectories. As depicted in Fig. 3.2, the desired trajectory $p_i^*(t)$ for agent A_i is defined as

$$p_i^*(t) = p_v^*(t) + r_{iv}^*, \tag{3.2}$$

where p_v^* is the desired trajectory of the virtual leader and r_{iv}^* is the desired relative position of A_i with respect to A_v. Relative positions r_{iv}^* are assigned to define the formation to be maintained, and are assumed to guarantee collision-free motion of $\mathcal{S}$.

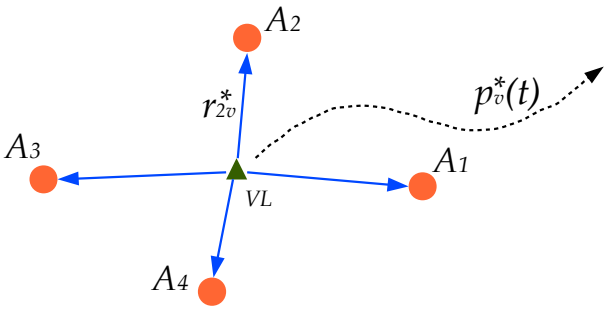

Figure 3.2: Trajectory generation using virtual leader for a four-agent formation.

In the LF formation control approaches, the virtual leader is assumed as the leader agent of the formation, and the follower agents connect to the leader by certain directed edges of the formation constraint graph. For instance, in the formation shown in Fig. 3.1, the leader agent is the virtual leader as well, e.g., $A_1 = A_v$, and it tracks its trajectory $p_1^*(t)$ without concerning the control laws of its followers A_2, A_3. The aim of the follower A_2 is to maintain the desired relative positions r_{12}^* as in the virtual leader-based control scheme. However, the aim of the follower A_3 is to maintain the relative positions r_{13}^* and r_{23}^*, instead of maintaining relative position to one leader.

3.3.2 Combined Formation Shape and Flocking Control

Combined formation shape and flocking control (CFSFC) of systems of multiple double integrator agents with undirected sensing graphs is formally studied in [125]. [3] extends the results of [125] for systems with acyclic directed graphs. Here, we review the framework of [3], and in Chapter 4 we develop an adaptive version of it for vehicles with uncertain dynamics. In [3], a swarm $\mathcal{S}$ of N agents with the double integrator model (2.2) is considered. Two constraint graphs have been considered to achieve the formation shape and flocking control: flocking graph $\mathcal{G}_f(\mathcal{V}, \mathcal{E}_f)$ and formation shape graph $\mathcal{G}_{sh}(\mathcal{V}, \mathcal{E}_{sh})$.

The directed flocking graph $\mathcal{G}_f$ represents the velocity information interaction between the agents. Without loss of generality, the agent A_1 is selected as the flocking leader and all the links $l_{i1}^f \in \mathcal{E}_f$ associated with A_1 are assumed unidirectional and traversed towards A_1, while the other links are assumed to be bidirectional. It is assumed that A_1 tracks its

predefined trajectory $p_1^*(t)$ with a piecewise constant velocity v_1. Let $\mathcal{N}_i^f$ denote the set of neighbors of A_i in $\mathcal{G}_f$. The unidirectional edges $l_{i1}^f \in \mathcal{E}_f$ between the leader A_1 and its neighbors $A_i \in \mathcal{N}_1^f$ mean that $A_i \in \mathcal{N}_1^f$ can sense the leader velocity, but the converse is not true. The bidirectional edges $l_{ij}^f \in \mathcal{E}_f$ between A_i and $A_j \in \mathcal{N}_i^f$, $i, j \neq 1$ mean that A_i is informed with $v_j(t)$ and A_j is informed with $v_i(t)$ at all times. The flocking objective is defined for the followers A_i, $i = (2, \ldots, N)$ as asymptotic tracking of the velocity of the leader. An example of $\mathcal{G}_f$ for a four agent formation is illustrated in Fig. 3.3.

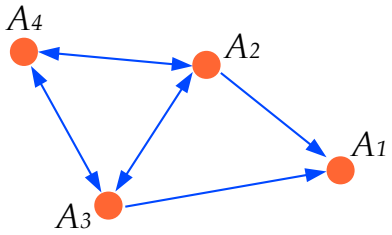

Figure 3.3: An example $\mathcal{G}_f$ for a four-agent formation: All edges associated with A_1 are unidirectional and traversed towards A_1, while the rest of the edges are bidirectional.

On the other hand, the formation shape graph $\mathcal{G}_{sh}$ governs the inter-agent distance constraint structure of the formation. It is assumed that $\mathcal{G}_{sh}$ is undirected and the corresponding formation is rigid. Let $\mathcal{N}_i^{sh}$ denote the set of neighbors of A_i in $\mathcal{G}_s$. Undirected $\mathcal{G}_{sh}$ is interpreted as both A_i and A_j are informed with the desired distance d_{ij}^* if there is a link l_{ij}^{sh} to be maintained between A_i and A_j in $\mathcal{E}_{sh}$.

Denote

$$\begin{aligned} v_r &\triangleq \left[(v_2 - v_1)^\top, \cdots, (v_N - v_1)^\top\right]^\top, \\ p_r &\triangleq \left[(p_2 - p_1)^\top, \cdots, (p_N - p_1)^\top\right]^\top. \end{aligned} \tag{3.3}$$

For CFSFC problem, that is, the problem of converging the velocities v_i, $i \neq 1$, to v_1 and maintaining the formation shape defined by $\mathcal{G}_{sh}$, [3] proposes the following CFSFC law for the follower agents A_i, $i \in \{2, \ldots, N\}$:

$$\dot{v}_r = -\left(\bar{\mathcal{L}} \otimes I_2\right) v_r - \nabla V(p_r), \tag{3.4}$$

where $\bar{\mathcal{L}}$ is the matrix formed by deleting the first row and first column of the Laplacian matrix $\mathcal{L}$ [3] of the flocking graph $\mathcal{G}_f$, and $V(p_r)$ is a potential function invariant to trans-

lation, rotation, and reflection, and having its minimum at zero, p_r being minimizer if and only if it satisfies the rigid formation constraints defined by D_d^*.

Consider a formation $\mathcal{F}$ of three agents $\{A_1, A_2, A_3\}$ with the flocking graph $\mathcal{G}_f$ and formation shape graph $\mathcal{G}_s$ as shown in Fig. 3.4. An example CFSFC control law for $\mathcal{F}$ is given by:

$$\begin{aligned} &\dot{p}_1 = v_1, \quad \dot{v}_1 = 0, \\ &\dot{p}_i = v_i, \\ &\dot{v}_i = -\sum_{j \in \mathcal{N}_i^f} (v_i - v_j) + 4 \sum_{j \in \mathcal{N}_i^s} \left((d_{ij}^*)^2 - d_{ij}^2 \right) (p_i - p_j), \end{aligned} \tag{3.5}$$

where $i = 2, 3$. In [3], it is proven that for the formation setting above, with the control law (3.5), velocities of all follower agents converge to v_1, and all the distance constraints for the links in the edge set $\mathcal{E}_{sh}$ are satisfied, that is, flocking and formation shape objectives are achieved.

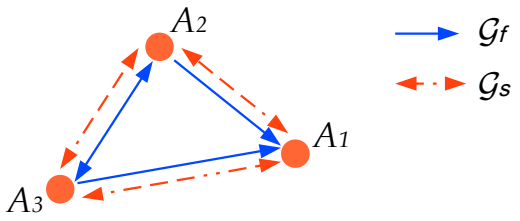

Figure 3.4: The flocking graph $\mathcal{G}_f$ (blue solid) and formation shape graph $\mathcal{G}_s$ (red dashed) of the example three-agent formation.

3.3.3 Hierarchical Cohesive Motion Control

In [44], a distributed control law is proposed to solve Problem 3.2.1. The method of [44] is further enhanced in [45], providing further analysis and vision-based robotic implementation, and in [12] for UAVs with more complex dynamics. In [12], assuming the desired trajectory $p_i^*(t)$ for each agent A_i, $i = \{1 \cdots N\}$, is calculated online based on the rigid

formation constraints, the following control law is proposed for A_i:

$$\begin{aligned} v_i(t) &= \bar{v}_i \gamma(\delta_i(t)) e_i(t), \\ e_i(t) &= \frac{\delta_i(t)}{\|\delta_i(t)\|}, \\ \delta_i(t) &= p_i^*(t) - p_i(t), \end{aligned} \tag{3.6}$$

where $\bar{v}_i$ is the constant maximum speed of A_i, $e_i(t)$ is the unit vector directed towards the desired trajectory at every time instant t, and the switching function $\gamma(t)$ is defined for a function of time $x : \Re^+ \to \Re^2$ and a small positive scalar ϵ_f as follows:

$$\gamma(r) = \begin{cases} 0, & r < \varepsilon_f \\ \frac{r-\varepsilon_f}{\varepsilon_f}, & \varepsilon_f \leq r < 2\varepsilon_f \\ 1, & r \geq 2\varepsilon_f \end{cases} \tag{3.7}$$

In [44], it is assumed that the aim of the leader A_1 is to reach its (predefined) desired final point p_{1f}, and a formal Lyapunov analysis is given to show the stability of A_1 in a sense that it enters a small neighborhood of p_{1f} and stays there in the limit. A Lyapunov analysis for A_2 and the ordinary followers $(A_3, \ldots, A_N)$ are given in [45] where for simplicity the velocity vector of the leader agent A_1 is assumed to be calculated via interpolation and is added to the control term of A_2. [45] also presents a real-time implementation of the control system on a non-holonomic mobile robot formation. In that paper, follower robots obtain relative position measurements to their leaders using cameras mounted on the vehicles.

3.3.4 Sliding Mode Based Formation Control

In [23], first-order and second-order sliding-mode observers have been proposed to estimate the position and velocity of the virtual leader in the formation for tracking objectives. [31] further extends the results of [23] to achieve formation shape and flocking control when an agent is assigned as the leader and there are obstacles in the formation. Both works assume that the sensing graph in the formation is directed and an agent can sense the relative position of its leaders. Here, we translate the control law of [31] for the obstacle-free, minimally persistent formation, and $\Re^2$ case. The agents are modeled to have holonomic point agent kinematics (2.1). The leader A_1 is assumed to move on a trajectory such that

$\dot{p}_1(t) = f_1(t)$, where f_1 is a predefined smooth function. For the first follower A_2, the following control law is proposed:

$$v_2(t) = \alpha e_2(t) + \beta \text{sgn}(e_2(t)), \tag{3.8}$$

where $\alpha \geq 0,\ \beta > 0$ are design constants, and

$$e_2(t) = r_{12}(t) - r^*. \tag{3.9}$$

For the ordinary follower A_3, the following control law is proposed:

$$v_i(t) = \alpha e_i(t) + \beta \text{sgn}(e_i(t)), \tag{3.10}$$

where $\alpha \geq 0,\ \beta > 0$ are design constants, and

$$e_i(t) = \left(r_{i,i-1}(t) - r^*_{i,i-1}\right) + \left(r_{i,i-2}(t) - r^*_{i,i-2}\right). \tag{3.11}$$

3.4 Cohesive Motion Control as a Regulation Problem

In this section, we re-define Problem 3.2.1 as a more generic multivariable regulation problem, deriving the system dynamics of the acyclic MPF $\mathcal{F}$, in order to facilitate application of various other (more generic) approaches. We then design a distributed control law to solve the regulation problem. At the end of this section, we give the simulation results of the synthesized control approach for a five-agent system.

The motion dynamics of the formation will be formulated in state-space, using the lumped state

$$\zeta = \left[\zeta_1^\top, \ldots, \zeta_N^\top\right]^\top \in \Re^{2N}, \tag{3.12}$$

where the state $\zeta_i \in \Re^2$ for each agent A_i is selected as described in the sequel, representing the relative position constraints for rigid formation maintenance together with the assumed single integrator motion kinematics (2.1). ζ_i are defined such that the cohesive motion control goal of Problem 3.2.1 is perfectly met at time instant t if and only if $\zeta(t) = 0$. That

is, the desired value for the lumped state vector ζ will always be zero, leading to a state regulation problem formulation.

The leader agent A_1 has 2-DOF and moves freely in the space to track its desired trajectory. The state for A_1 is selected to be the tracking error in position, i.e.,

$$\zeta_1(t) \triangleq p_1(t) - p_1^*(t), \tag{3.13}$$

and to meet its trajectory tracking task, we assert

$$\dot{p}_1(t) = v_1(\zeta_1(t), v_{1,d}(t)) = v_1^{'}(\zeta_1(t)) - v_{1,d}(t), \tag{3.14}$$

where $v_{1,d} = \dot{p}_1^*$, and $v_1^{'}(\cdot)$ is a static smooth function defining the control law that steers the leader agent according to the tracking error $\zeta_1(t)$.

Assuming a similar state function control law assignment for the FF agent A_2, we derive the dynamics of the relative position r_{12} between the leader and the FF agent, whose desired value is a constant vector, r_{12}^*. We write

$$\dot{r}_{12}(t) = v_1(t) - v_2(\zeta_2(t)) \tag{3.15}$$

where the state

$$\zeta_2(t) \triangleq \tilde{r}_{1,2} \triangleq r_{12}(t) - r_{12}^*, \tag{3.16}$$

of A_2 is defined in terms of the relative distance tracking error, and $v_2(\cdot)$ is a static smooth function defining the control law that steers the FF agent A_2 towards its equilibrium point at each time instant t, at which the relative position constraint is satisfied.

For each OF agent A_i, $(i \geq 3)$, which by the notation convention follows A_{i-1} and A_{i-2}, the state is defined as

$$\zeta_i \triangleq \tilde{r}_{i-1,i} \triangleq r_{i-1,i} - r_{i-1,i}^*, \tag{3.17}$$

considering the relative position of A_{i-1} with respect to A_i. For the relative position of A_{i-2} with respect to A_i, we have

$$\begin{aligned} \tilde{r}_{i-2,i} &\triangleq r_{i-2,i} - r_{i-2,i}^* \\ &= (r_{i-2,i-1} + r_{i-1,i}) - (r_{i-2,i-1}^* + r_{i-1,i}^*) \\ &= \tilde{r}_{i-2,i-1} + \tilde{r}_{i-1,i} \\ &= \zeta_{i-1} + \zeta_i. \end{aligned} \tag{3.18}$$

Noting that (3.16) is also in the form (3.17), the equations (3.17),(3.18) are valid for all $i \in \{2, \dots, N\}$.

Remark 3.4.1. *As clearly seen in (3.13),(3.16), A_1 and A_2 have access to ζ_1 and ζ_2, respectively. Further, for all $i \in \{3, \dots, N\}$, the sensing graph $\mathcal{G}_s$ introduced in Section 3.2 guarantees that A_i can calculate ζ_{i-1}, ζ_i using (3.17),(3.18).*

Using (3.13),(3.17), we obtain the dynamics

$$\begin{aligned}
\dot{\zeta}_1 &= v_1, \\
\dot{\zeta}_2 &= v_1 - v_2, \\
\dot{\zeta}_3 &= v_2 - v_3, \\
&\vdots \\
\dot{\zeta}_N &= v_{N-1} - v_N,
\end{aligned}$$

which can be written in the following compact form:

$$\frac{\mathrm{d}}{\mathrm{d}t}\zeta = \mathbf{B}u, \tag{3.19}$$

where $u = \left[v_1^\top, \cdots, v_N^\top\right]^\top \in \Re^{2N}$ and

$$\mathbf{B} = \begin{bmatrix}
\mathbf{I}_2 & \mathbf{0} & \mathbf{0} & \mathbf{0} & \cdots & \mathbf{0} & \mathbf{0} \\
\mathbf{I}_2 & -\mathbf{I}_2 & \mathbf{0} & \mathbf{0} & \cdots & \mathbf{0} & \mathbf{0} \\
\mathbf{0} & \mathbf{I}_2 & -\mathbf{I}_2 & \mathbf{0} & \cdots & \mathbf{0} & \mathbf{0} \\
 & & & \ddots & & & \\
\mathbf{0} & \mathbf{0} & & \cdots & & \mathbf{I}_2 & -\mathbf{I}_2
\end{bmatrix} \in \Re^{2N \times 2N}. \tag{3.20}$$

The output $y = \left[y_1^\top, \dots, y_N^\top\right]^\top \in \Re^{4N-4}$, of the system is defined as follows:

$$y_1 = \zeta_1, \tag{3.21}$$
$$y_2 = \zeta_2, \tag{3.22}$$
$$y_i = \left[\zeta_{i-1}^\top, \zeta_i^\top\right]^\top, \text{ for } i \in \{3, \dots, N\}. \tag{3.23}$$

Recall Problem 3.2.1 where the objectives are given in more general terms. We now reformulate this problem as an equivalent regulation problem:

Problem 3.4.1. *Consider an acyclic minimally persistent two-dimensional leader-follower formation $\mathcal{F}$, satisfying the constraint, control, sensing, and agent dynamics properties asserted in Section 3.2. For the dynamics (3.19), find a control law u that achieves* $\lim_{t\to\infty} \zeta(t) = 0$.

Problem 3.4.1 is equivalent to Problem 3.2.1 in the sense that any control law u that solves Problem 3.4.1 is also a solution of Problem 3.2.1. Various regulation control methods in the literature can be employed to solve Problem 3.4.1. A linear state-space dynamic model similar to (3.19) has been derived in [139] for MPFs in general, including those having cycles in the constraint graph. In [139], using first-order approximation, a control law is proposed to achieve formation acquisition of agents which are assumed to be perturbed from their equilibrium configuration by small amounts. (3.19) is based on the relative position errors during motion, while the dynamic model in [139] is established for regulation of distance errors caused by small perturbations. In the next subsection, we design a linear distributed output feedback control scheme for the system (3.19)–(3.23) aiming at solving the cohesive motion problem.

3.5 Control Design for the Regulation Problem

3.5.1 Control Design

In this subsection, we design a linear distributed output feedback control scheme to solve Problem 3.4.1. We consider the state feedback control law

$$u = \mathbf{K}\zeta, \tag{3.24}$$

where

$$\mathbf{K} = \begin{bmatrix} -k_1\mathbf{I}_2 & \mathbf{0} & \mathbf{0} & \cdots & \mathbf{0} \\ \mathbf{0} & k_2\mathbf{I}_2 & \mathbf{0} & \cdots & \mathbf{0} \\ \vdots & & \ddots & & \vdots \\ \mathbf{0} & & & k_{N-1}\mathbf{I}_2 & \mathbf{0} \\ \mathbf{0} & & \cdots & \mathbf{0} & k_N\mathbf{I}_2 \end{bmatrix}, \tag{3.25}$$

with

$$k_1, \ldots, k_N > 0. \tag{3.26}$$

Theorem 3.5.1. *The control law (3.24) with the gains selected as in (3.26) solves Problem 3.4.1 exponentially.*

Proof. (3.19),(3.24) result in the closed loop dynamics

$$\begin{aligned} \frac{\mathrm{d}}{\mathrm{d}t}\zeta &= \mathbf{BK}\zeta, \\ &= \begin{bmatrix} -k_1\mathbf{I}_2 & \mathbf{0} & \mathbf{0} & \mathbf{0} & \cdots & \mathbf{0} & \mathbf{0} \\ -k_1\mathbf{I}_2 & -k_2\mathbf{I}_2 & \mathbf{0} & \mathbf{0} & \cdots & \mathbf{0} & \mathbf{0} \\ \mathbf{0} & k_2\mathbf{I}_2 & -k_3\mathbf{I}_2 & \mathbf{0} & \cdots & \mathbf{0} & \mathbf{0} \\ & & & \ddots & & & \\ \mathbf{0} & \mathbf{0} & & \cdots & & k_{N-1}\mathbf{I}_2 & -k_N\mathbf{I}_2 \end{bmatrix} \zeta. \end{aligned} \tag{3.27}$$

Since the matrix $\mathbf{BK}$ is lower block triangular and $k_i > 0$ for all i, we have that $\mathbf{BK}$ is Hurwitz. Hence, $\zeta = 0$ is exponentially stable. □

Note that the control law (3.24) only requires the availability of the state vector ζ_i for agent A_i, making it completely distributed.

Remark 3.5.1. *For the implementation of the control law (3.24), it is sufficient for A_i to have the state ζ_i, which is guaranteed by the structure of the sensing graph $\mathcal{G}_s$. Actually, an OF agent A_i, $i = \{3, \cdots, N\}$ has access to the state ζ_{i-1} as well, as indicated in (3.23). This, in a sense, adds robustness into the system such that in case of a failure in sensing the leader A_{i-1}, the agent A_i, $i = \{3, \cdots, N\}$ can switch to sensing only A_{i-2} for a continuous operation.*

3.5.2 Simulations

In this part, we simulate the behavior of the control system design of Section 3.5.1. Consider an MPF $\mathcal{F}$ of a five-agent system $\mathcal{S} = \{A_1, \cdots, A_5\}$ with the edge set

$$\mathcal{E}_c = \{(2,1), (3,1), (3,2), (4,2), (4,3), (5,3), (5,4)\},$$

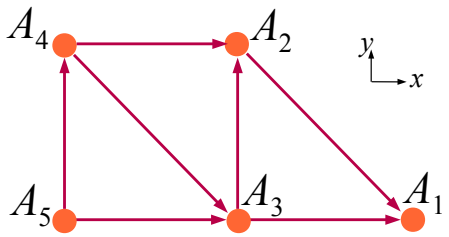

Figure 3.5: The constraint graph $\mathcal{G}_c$ of the 5-agent formation used in simulations.

and with the relative position constraints $r_{12}^* = r_{34}^* = [1, -1]^\top$, $r_{23}^* = r_{45}^* = [0, 1]^\top$. The constraint graph $\mathcal{G}_c$ used in simulations is depicted in 3.5. The desired trajectory for A_1 is $p_1^*(t) = [2 + 0.1t,\ 2\cos(t)]$. The system is simulated for 50 seconds. The gains are chosen as follows:

$$k_1 = 10,\ k_2 = 6,\ k_3 = 8,\ k_4 = 10,\ k_5 = 12.$$

The state vector ζ is bounded and there are periodic relative position errors due to the fact that the leader's trajectory $p_1^*(t)$ has a sinusoidal component.

3.6 Results on the Speed Limitations

In this section, we address Problem 3.2.2 in two parts. The first part is on the speed relations between agents modeled by point agent kinematics moving in a rigid formation. In the second part, we design a hierarchical LF formation control approach for two agents, which is a modified version of the *Hierarchical Cohesive Motion Control* approach given in Section 3.3.3.

3.6.1 Agent Speed Relations in a Rigid Formation

Consider the rigid triangle of the three agents $A_1,\ A_2,\ A_3$ of Fig. 3.1 moving in a two or three-dimensional space. We seek for a relation between the agent velocities. Denote

$$\tilde{d}_{i,i-1}(t) \triangleq \frac{1}{2}\left(d_{i,i-1}^2(t) - (d_{i,i-1}^*)^2\right). \tag{3.28}$$

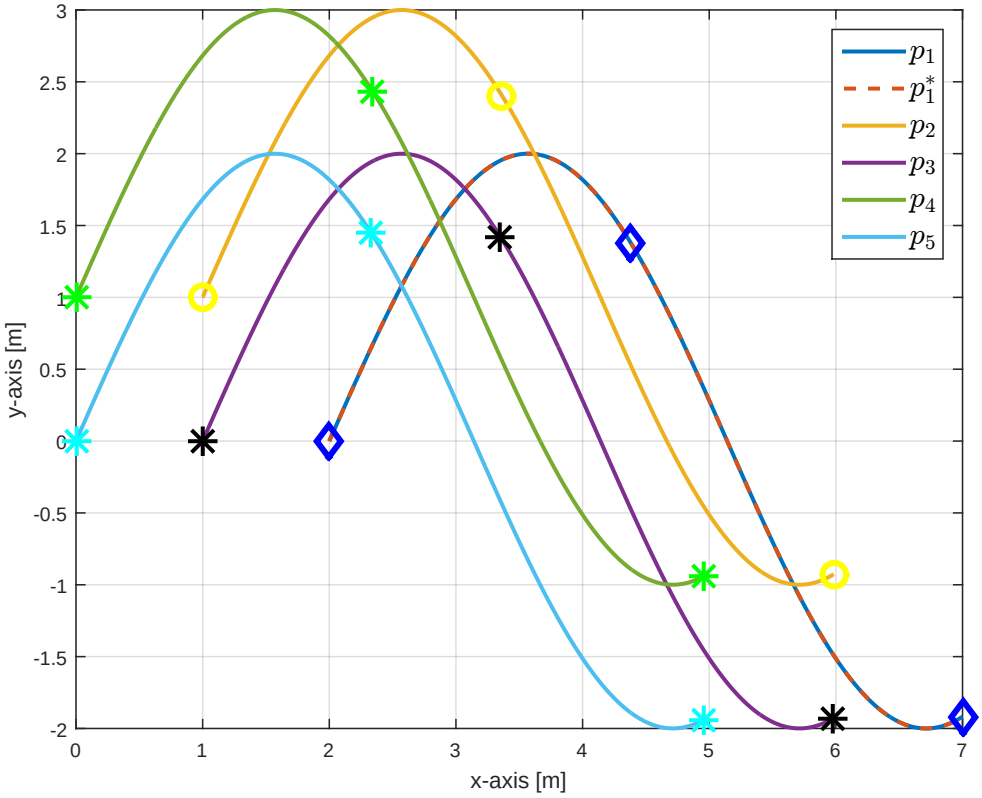

Figure 3.6: Motion of the five-agent system with the control law (3.24): The leader A_1 tracks its desired trajectory while the FF and OF agents follow their leaders to satisfy the constraints imposed by $\mathcal{G}_c$.

The time derivative of $\tilde{d}$ in (3.28) is given by:

$$\begin{aligned}\dot{\tilde{d}}_{ij}(t) &= \frac{\mathrm{d}}{\mathrm{d}t}\frac{1}{2}\left(d_{ij}^2 - (d_{ij}^*)^2\right) = r_{ij}^\top v_{ij} \\ &= (r_i - r_j)^\top (v_i - v_j)\,.\end{aligned} \tag{3.29}$$

Using (3.29) for the agent pairs $\{A_1, A_3\}$ and $\{A_2, A_3\}$, we obtain the following:

$$\begin{bmatrix} r_{31}^\top \\ r_{32}^\top \end{bmatrix} v_3 = \begin{bmatrix} r_{31}^\top v_1 \\ r_{32}^\top v_2 \end{bmatrix}. \tag{3.30}$$

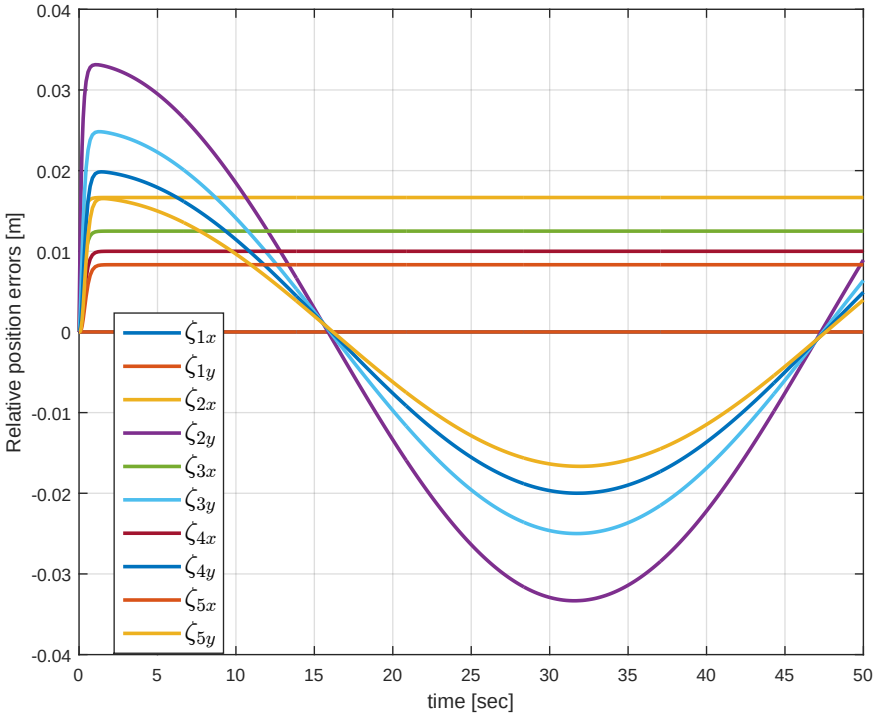

Figure 3.7: The state vector ζ under the control law (3.24): Small, bounded tracking errors are caused by the sinusoidal component of the desired trajectory of A_1.

Lemma 3.6.1. *For the rigid triangle $\{A_1, A_2, A_3\}$ of Fig. 3.1, there holds*

$$\|v_3\|^2 \leq \frac{d_{13}^2\|v_1\|^2 + d_{23}^2\|v_2\|^2}{\lambda_{\min}(r_{31}r_{31}^\top + r_{32}r_{32}^\top)}. \tag{3.31}$$

Proof. (3.30) further yields the equation (3.32).

$$v_3^\top \mathbf{R} v_3 = v_1^\top \mathbf{R}_1 v_1 + v_2^\top \mathbf{R}_2 v_2, \tag{3.32}$$

with

$$\mathbf{R} = \mathbf{R}_1 + \mathbf{R}_2$$
$$\mathbf{R}_1 = r_{31}r_{31}^\top, \quad \mathbf{R}_2 = r_{32}r_{32}^\top.$$

It then follows that

$$\lambda_1\|v_3\|^2 \leq v_3^\top \mathbf{R} v_3 \leq \lambda_2\|v_3\|^2,$$

and thus

$$\frac{v_3^\top \mathbf{R} v_3}{\lambda_2} \leq \|v_3\|^2 \leq \frac{v_3^\top \mathbf{R} v_3}{\lambda_1}, \tag{3.33}$$

where $\lambda_1 := \lambda_{\min}(\mathbf{R})$ and $\lambda_2 := \lambda_{\max}(\mathbf{R})$ are the minimum and the maximum eigenvalue of the matrix $\mathbf{R}$. Note that since the rigid motion assumption eliminates the collinear agent positions in $\Re^2$ and coplanar agent positions in $\Re^3$, we have $\det(\mathbf{R}) \neq 0$, thus $\lambda_1 > 0$. (3.32) also implies that

$$0 \leq v_3^\top \mathbf{R} v_3 \leq \lambda_{\max}(\mathbf{R}_1)\|v_1\|^2 + \lambda_{\max}(\mathbf{R}_2)\|v_2\|^2 \tag{3.34}$$

Since $\lambda_{\min}(\mathbf{R}_i) = 0$ and $\lambda_{\max}(\mathbf{R}_i) = d_{i3}^2$ for $i = \{1, 2\}$, we conclude

$$\|v_3\|^2 \leq \frac{d_{13}^2\|v_1\|^2 + d_{23}^2\|v_2\|^2}{\lambda_1}.$$

□

3.6.2 Speed Control for Rigid Formation Maintenance

In Section 3.3.3, the formation control approach of [44] established for acyclic MPFs is presented. In [44], a leader agent is not affected by the control decision of its followers. Here, we propose an LF formation control law introducing a spring-like action between agents, which is intended to satisfy the feasibility concept within the formation. Specifically, we propose the control law such that the speed of an agent is affected by its followers during motion, which makes the formation robust to the cases where the initial inter-agent distances are much greater than their desired values. We first give definition of the backward function that is employed in the control law: Define the function of time for some $f_{ij} : \Re^+ \to \Re^+$ as

$$f_{ij}(r) = e^{-\frac{r^2}{2\sigma^2}}, \tag{3.35}$$

where σ is design coefficient. Consider Problem 3.2.1 for an acyclic 3-agent MPF $\mathcal{F}$. The control rule for the agent A_i is composed of a speed term s_i and a direction term e_i such that

$$v_i(t) = s_i(t)e_i(t), \tag{3.36}$$

where the speed term satisfies $0 \leq s_i(t) = \|v_i(t)\| \leq \bar{v}_i$ for all $i,\ t$, and the unit vector e_i is the direction term which heads the agent towards its desired position.

Assumption 3.6.1. *Every agent A_i in $\mathcal{F}$ knows the structure of the function f_{ij} with the constant σ, and the speed bounds $\bar{v}_j$ of A_j for all $j \in \mathcal{N}_i^c$.*

Next, we study the sub-objectives described in Problem 3.2.1-(i) and $-(ii)$, considering only agents A_1 and A_2. The leader agent A_1 is required to reach the predefined point p_{1f}. We propose the following control law for the leader agent, which is a revised version of the control law of [44], as follows:

$$\begin{aligned} v_1(t) &= s_1(t)e_1(t) \\ s_1(t) &= \bar{v}_1 f_{12}(\delta_{12}(t))\, \beta(\delta_{1f}(t)), \quad e_1(t) = \frac{-\delta_{1f}(t)}{\|\delta_{1f}(t)\|}, \end{aligned} \tag{3.37}$$

where f_{12} is as in (3.35), the switching term $\gamma(\delta_{1f}(t))$, defined in (3.7), prevents chattering due to small but acceptable errors in the final position of A_1, and

$$\delta_{ij}(t) \triangleq [\tilde{x}_{ij},\ \tilde{y}_{ij}]^\top. \tag{3.38}$$

A_1 moves with two-degree-of-freedom, however, its maximum speed is affected by the relative position r_{12} due to the function f_{12}.

Remark 3.6.1. *Positive definiteness property of f_{12} allows the leader to reach its desired position under the control law (3.37). At the same time, it will decelerate dramatically when the relative position error increases to help the agent A_2 in maintaining the relative position r_{12} at their desired values.*

We assume that A_2 can sense the relative position r_{12}. We take advantage of this assumption in the design of the speed profiles of both of these agents. The goal in Problem 3.2.1$-(ii)$ is to design a control system so that $\lim_{t\to\infty} r_{12}(t) = r_{12}^* = [x_{12}^*,\ y_{12}^*]^\top$, where r_{12}^* is assumed to be a constant vector. For the FF agent we propose control rule

$$\begin{aligned} v_2(t) &= s_2(t)e_2(t) \\ s_2(t) &= (\bar{v}_1 + (1 - f_{12})\alpha_2)\ \beta(\delta_{12}(t)), \quad e_2(t) = \frac{\delta_{12}(t)}{\|\delta_{12}(t)\|}, \end{aligned} \tag{3.39}$$

where $\alpha_2 > 0$ is a small design constant. Note that $\bar{v}_2 = \bar{v}_1 + \alpha_2$. We have the following result for the two-agent formation.

Lemma 3.6.2. *Consider Problem 3.2.1 for a minimally persistent formation $\mathcal{F}$ with leader agent A_1 and first follower agent A_2. Consider the control laws (3.37)-(3.39) for A_1 and A_2, respectively. Then, we have the following:*

i. The equilibrium $\tilde{x}_{1f} = \tilde{y}_{1f} = 0$ is globally asymptotically stable,

ii. The equilibrium $\tilde{x}_{12} = \tilde{y}_{12} = 0$ is globally asymptotically stable,

iii.

$$\lim_{t\to\infty} s_1(t) = \lim_{t\to\infty} s_2(t) = \bar{v}_1. \tag{3.40}$$

Proof. See Appendix B. □

Remark 3.6.2. *Note that the convergence of the FF agent is independent of the convergence of the leader agent to its final point p_{1f} since the control rule (3.39) only uses the speed profile of the leader agent, regardless of its rotation which is determined by e_1.*

Remark 3.6.3. *The convergence of the FF agent's error to zero implies that the FF agent converges to its final destination p_{2f} asymptotically if the leader agent converges to its final destination p_{1f}. Note that in [44], it is also assumed that the FF agent knows p_{2f}, and the control law uses this knowledge. Here, we relax that assumption.*

3.7 Summary and Remarks

In the first part of this chapter, we have formally defined the cohesive motion problem of acyclic MPFs on a two-dimensional plane and reviewed the major formation control algorithms established for this problem. Motivated by the lack of convenient motion models for MPFs, in the second part, we have derived the linear system model (3.19), introducing new state variables with the inter-agent motion variables throughout the formation. This linear multivariable system has allowed us to convert the cohesive motion control problem to a multivariable regulation problem. This conversion is advantageous, because it is a known fact that more generic control structures are available for the regulation problem in the literature. The model (3.19) sets a base for future control derivations for the cohesive motion control problem.

We have designed a linear, easy-to-implement distributed control law for N-agent acyclic MPFs assuming holonomic point agent kinematic models. Taking advantage of the special structure of the system matrix, a completely distributed proportional control scheme has been proposed to regulate the dynamics (3.19). Utilizing the linearity of the system and control gain matrices, exponential convergence rate has been established. Finally, we have analyzed the agent speed relations in rigid body motion. In that context, we have proposed a distributed control law for a two-agent system. Adjusting the speeds of the agents with the introduction of special functions in the control law, feasibility and stability of the system have been established.

Derivation of advanced control laws for the regulation problem stated in Section 3.4 and extending the results of Section 3.6.2 to cover the more general, $N-$agent formations are promising research areas. Further, the system model (3.19), which defines the kinematics of agents, can be integrated with the motion dynamics of agents for real-time implementations.

Chapter 4

Cohesive Motion Control: Uncertain Vehicle Dynamics

4.1 Introduction

In a formation, dynamics of vehicles may vary from vehicle to vehicle and contain uncertain parameters. When there are modeling uncertainties or unknown disturbances acting on the agent dynamics, robust or adaptive control strategies are found to be more convenient and effective. Some formation control works in that direction can be found in [49, 59, 60, 136], where the potential functions method is combined with the sliding mode control technique in order to improve performance and robustness. Similarly, other robust control techniques such as H_∞ based design can also be effectively employed [104]. An alternative approach is to use adaptive techniques and asymptotically overcome or compensate for the adverse effects of the uncertainties and disturbances without a need for high control actions and achieve desired system behavior [82]. Example works on utilizing adaptive techniques for formation control and coordination in multi-agent dynamic systems can be found in [9, 24, 70, 88, 92, 94, 122]. For the cases in which the uncertainties or the disturbances are parametric, the controller can be accordingly parameterized and these parameters can be updated based on the measured errors to achieve the desired objectives. Accordingly, various identification algorithms, such as gradient based and LS based ones, can be used together with adaptive controller. In contrast, if it is not feasible to properly parameterize the uncertainties and/or the controller, universal approximators, such as

polynomials, neural networks, and fuzzy systems, can be used to estimate and to counter effect the uncertainties [120]. Such universal approximators have been utilized in the multi-agent dynamic systems literature for solving various problems including formation control [36, 51, 112, 129] and distributed agreement [50].

In this chapter, we first study the control problem of tracking a predefined smooth trajectory by a single mobile dynamic agent, e.g., an autonomous vehicle, with dynamics in Brunovsky canonical form having parametric uncertainties. Utilizing the certainty equivalence principle, we design a new indirect adaptive control scheme composed of two parts: (i) an LS algorithm with modification for estimating the system parameters with guaranteed performance, and (ii) a Luenberger observer and feedback linearization based trajectory tracking controller. Taking advantage of the fast and robust convergence properties of the LS algorithm, we prove perfect tracking of any smooth trajectory by the mobile agent without any requirement on the persistence of excitation of regressor signals.

Afterwards, we consider the formation control and maintenance problem for swarms of the aforementioned type of mobile vehicles. The overall agent controllers are required to satisfy not only the motion control objectives of the agents but also the desired geometric formation constraints despite the uncertainties in the agent dynamics. We study distributed extension of the proposed adaptive control scheme for the formation control problem using virtual leader approach. As an alternative approach, for the special case of systems of relative degree two, we associate our adaptive control design with the CFSFC algorithm of [3] which was originally derived for double integrator dynamics. We show that, with the proposed controller, the approach of [3] also applies to the systems of relative degree two and with parametric uncertainties, and formation acquisition and maintenance results are established under the same sensing/communication frameworks in the formation. Utilizing the adaptive and robustness feature of the proposed approach, adverse effects of the uncertainty can be overcome in real-time implementations.

4.2 Trajectory Tracking with Parametric Uncertainties

In this section, we present the trajectory tracking control design problem for a single holonomic agent with parametric uncertainties. Many holonomic systems such as quadrotors,

or some of their components, are modeled by the Brunovski canonical form under certain assumptions. We first focus on the objective of trajectory tracking for a single agent. We follow indirect adaptive control approach, that is, we first estimate the unknown parameters and then use these estimated parameter values in the classical feedback linearization law. We use an LS algorithm with modification for parameter estimation. Assuming the desired trajectory is smooth and its derivative is bounded, we prove asymptotic convergence of the single agent to its desired trajectory. A similar problem has been solved by the same method in [127] where the result is said to be valid if the persistence of excitation is assumed, which cannot be directly concluded. We relax that assumption here.

4.2.1 Agent Dynamics

Consider a single holonomic mobile agent A having the following dynamics with relative degree r:

$$\begin{aligned} \dot{\eta} &= f_0(\eta, x) && (4.1)\\ \dot{x}_k(t) &= x_{k+1}(t), \quad k = 1, \ldots, r-1;\ r \geq 2 && (4.2)\\ \dot{x}_r(t) &= \alpha(t) + \beta u(t) \\ y(t) &= x_1(t) \end{aligned}$$

where $u \in \mathbb{R}^m$ is the input vector, $x = [x_1^\top, \ldots, x_r^\top]^\top \in \mathbb{R}^{rm}$ is the state vector, and $x_j \in \mathbb{R}^m$, $j = 1, \ldots, r$. The output $y \in \mathbb{R}^m$ is typically a position vector, i.e., $y(t) = x_1(t) = p(t)$. $\eta \in \mathbb{R}^{n-rm}$ is the state of the zero dynamics. $\alpha : \mathbb{R} \to \mathbb{R}^m$ is unknown, possibly nonlinear, continuous vector function of time. The constant matrix $\beta \in \mathbb{R}^{m \times m}$ is the unknown high-frequency gain. Note that (4.1)-(4.2) is a special case of the high-order dynamics (2.7) where α is a function of time only, and β is constant. We have the following assumptions on the system dynamics.

Assumption 4.2.1.

i. The matrix β is diagonally dominant and the signs of β_{ii} are known.

ii. There exists a very small positive constant ε_M such that $|\beta_{ii}| \geq M_{i,1}$ for all i and $|\beta_{ij}| \leq M_{i,2}$ for all i, j, $i \neq j$ and for some $M_{i,1}$, where $M_{i,2} = \frac{M_{i,1}}{m-1} - \varepsilon_M$.

iii. The agent dynamics (4.1), (4.2) are minimum phase, internally stable, and have well-defined vector relative degree $\{r, \ldots, r\}$. Therefore, the input u always shows up in the $r-th$ derivative of y since the nullity of β is zero.

iv. The entries of α are either constant or slowly time varying, satisfying $\|\alpha(t)\| \leq c_1$ and $\|\dot{\alpha}(t)\| \leq c_2$ for all $t \geq 0$ and for some finite constants $c_1,\ c_2 > 0$.

Assuming internal stability of the zero dynamics we separate it from the rest of the dynamics (4.2) and ignore it in further controller design process. Moreover, from the Gershgorin circle theorem [14], the set of matrices β obeying Assumption 4.2.1-(i) are nonsingular. As a note, the case $\beta_{ii} = 0$ is naturally excluded by the same assumption. The lower and upper bounds $M_{i,1},\ M_{i,2}$ can be selected arbitrarily large based on a priori information.

4.2.2 Trajectory Tracking Problem

Consider the system described by the dynamics (4.1) and (4.2), and the objective of tracking a desired reference trajectory $p^*(t)$. Assume $p^*(t)$ is available for all t. Therefore, the control law aims to ensure that

$$e(t) = p(t) - p^*(t) \tag{4.3}$$

converges to zero asymptotically.

Problem 4.2.1. *Design a control law $u(t)$ that drives the tracking error $e(t)$ in (4.3) of the system (4.2) to zero as $t \to \infty$.*

In the sequel, we propose an indirect adaptive control design approach to solve Problem 4.2.1. The solution requires an adaptive algorithm in the controller design process since the tracking problem setting contains uncertainties in the system dynamics.

4.3 Indirect Adaptive Controller Synthesis

In this section, we design an indirect adaptive controller to overcome the uncertainties and meet the tracking goal. In the context of this section, we denote *channel j* of the mobile

agent A by the vector $[x_{1,j},\ x_{2,j}, \ldots, x_{r,j}]^\top,\ j = \{1, \ldots, m\}$. We use a decentralized control approach and design an individual controller for each channel of the agent. The agent dynamics (4.2) contains nonlinear terms α and β, which constrains the diversity of the controller to be designed unless we apply linearization. For this reason, we first linearize the agent dynamics using feedback linearization. It is a fact that provided the vector $\alpha(t)$ and the matrix β are known exactly, the feedback rule

$$u^\star(t) = \beta^{-1}\left[-\alpha(t) + \nu(t)\right], \tag{4.4}$$

where $\nu(t)$ is the control input to the linearized agent dynamics, perfectly linearizes (4.2), resulting in the following linear model for channel j:

$$\begin{aligned} \dot{x}_{k,j} &= x_{k+1,j}, \quad k = 1, \ldots, r-1;\ r \geq 2 \\ \dot{x}_{r,j} &= \nu_j, \\ y_j &= x_{1,j} = p_j. \end{aligned} \tag{4.5}$$

However, since we do not know exact values of $\alpha(t), \beta$, we perform an adaptive control design to generate the control signal $u(t)$ as an estimate of (4.4). Fundamentally, this can be done in two ways: the first is to estimate $\alpha(t), \beta$ as $\hat{\alpha}(t), \hat{\beta}(t)$ and then use these estimates correspondingly to generate the control signal

$$u(t) = \hat{\beta}^{-1}(t)\left[-\hat{\alpha}(t) + \nu(t)\right], \tag{4.6}$$

and the second is to estimate the optimal control input $u^\star$ directly. In this section, we design an indirect adaptive controller, the former approach, with slight modifications for the single holonomic agent A to solve Problem 4.2.1. The general scheme of the controller we propose is shown in Fig. 4.1.

4.3.1 Parameter Estimation

We now design an estimation algorithm to generate the estimates of the unknown vector α and the unknown matrix β. From the agent dynamics (4.5), we have

$$s^r p_j = \alpha_j + \beta_j^\top u, \quad j = 1, \ldots, m, \tag{4.7}$$

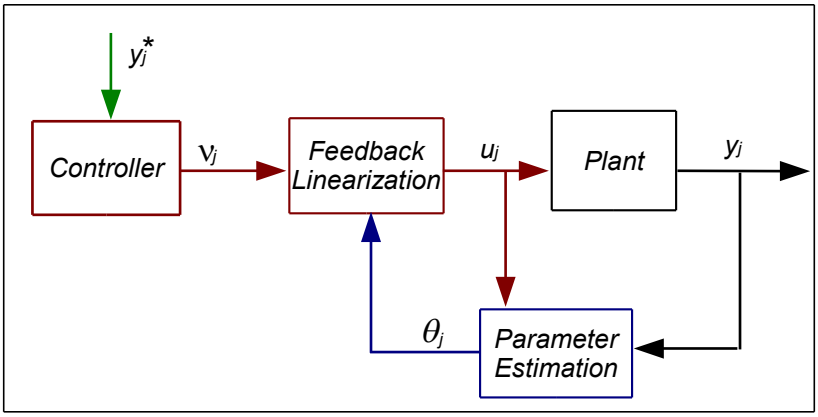

Figure 4.1: The block diagram of the jth channel of the controlled agent system: The parameter estimation vector θ_j formed by $\hat{\alpha}(t)$ and $\hat{\beta}(t)$ is generated in a separate block to be used in the feedback linearization based control law.

where s is the differentiation operator, α_j is the jth entry of the vector α and $\beta_j^\top$ is the jth row of β, i.e., $\beta = [\beta_1 \dots \beta_m]^\top$. We treat the entries of α as piecewise constants and consider the following parametric model:

$$z_j = \theta_j^{*\top} \phi, \tag{4.8}$$

with

$$z_j = \frac{\lambda_{filt}^r s^r}{(s+\lambda_{filt})^r}[p_j], \quad \theta_j^* = [\alpha_j,\ \beta_j^\top]^\top,$$
$$\phi = \left[\frac{\lambda_{filt}^r}{(s+\lambda_{filt})^r}[1],\ \frac{\lambda_{filt}^r}{(s+\lambda_{filt})^r}[u^\top]\right]^\top,$$

where θ_j^* and ϕ are named the parameter vector and the regressor vector of the jth channel, respectively.

In estimation of the matrix β, if the matrix estimate $\hat{\beta}(t)$ converges to a singular matrix, the control input u in (4.6) becomes unbounded. In the literature, the matrix β is generally estimated with neural or fuzzy algorithms, and researchers guarantee boundedness of u using a switching algorithm in the control rule (4.6) such that in the region where $\det(\hat{\beta})$ approaches zero, a bounded signal is used in place of the feedback controller u. Such rules result in a discontinuous control signal, which may cause chattering and lead to intractable

stability analysis. σ-modification is used together with neural network estimation algorithm for single input systems in [135], which leads to a continuous control u. [114] assumes that there is a known set Ω in which the estimated matrix $\hat{\beta}$ lies such that $\Omega = \{\hat{\beta} | \det(\hat{\beta}(t)) \neq 0 \ \forall t\}$. This rule can be implemented by embedding some projections for the estimated matrix $\hat{\beta}$. In Assumption 4.2.1-(i) and (ii), we impose upper and lower bounds on the entries of the matrix β. We use this a priori information and apply parameter projection in the LS update rule of the estimated matrix $\hat{\beta}$ to guarantee the nonsingular property of $\hat{\beta}(t)$ for all time.

In light of the above discussion, we apply the following LS algorithm with parameter projection for estimation of α and β:

$$\begin{aligned} \dot{\hat{\theta}}_j(t) &= \text{Proj}\left\{P(t)\epsilon_j(t)\phi(t)\right\}, \\ \dot{P}(t) &= -P(t)\frac{\phi(t)\phi(t)^\top}{\psi^2(t)}P(t), \quad P(t_{r^+}) = \mu I, \\ \epsilon_j(t) &= \frac{z_j(t) - \hat{z}_j(t)}{\psi^2(t)}, \quad \psi^2(t) = 1 + \phi^\top(t)\phi(t), \end{aligned} \tag{4.9}$$

where $\hat{\theta}_j(0) = \hat{\theta}_{j,0}$, $\hat{\theta}_j = [\hat{\alpha}_j, \ \hat{\beta}_j^\top]^\top$ is the parameter estimate vector, $P \in \mathbb{R}^{(m+1)\times(m+1)}$ is the covariance matrix, $P(0) = P_0$, and ψ is the normalizing signal. We apply covariance resetting [82] in the algorithm such that for all time t after t_r, the time instant where $\lambda_{min}(P) < \mu I, \ \mu > 0$, we settle the covariance matrix at $P(t_{r^+}) = \mu I$, which guarantees $P(t) \geq \mu I$ for all t. Proj$\{.\}$ stands for the parameter projection operator, which is defined for a vector $v \in \Re^{m+1}$, a convex function $g : \Re^m \to \Re$, and the sets $\mathcal{S}^0, \ \delta(\mathcal{S})$ as follows:

$$\text{Proj}\left\{\hat{\beta}_j, v\right\} = \begin{cases} v, & \text{if } \hat{\beta}_j \in \mathcal{S}^0 \\ & \text{or } \hat{\beta}_j \in \delta(\mathcal{S}) \text{ and } v\nabla g \leq 0 \\ v_{pr}, & \hat{\beta}_j \in \delta(\mathcal{S}) \text{ and } v\nabla g \geq 0 \end{cases} \tag{4.10}$$

where $\mathcal{S}^0 = \left\{\hat{\beta}_j \mid g(\hat{\beta}_j) < 0\right\}$ and $\delta(\mathcal{S}) = \left\{\hat{\beta}_j \mid g(\hat{\beta}_j) = 0\right\}$ denote the interior and the boundary of $\mathcal{S}$ which is defined by the following:

$$\begin{aligned} \mathcal{S} &= \mathcal{S}_1 \cap \mathcal{S}_2, \\ \mathcal{S}_1 &= \left\{\hat{\beta}_j \mid \text{sgn}(\beta_{j,j})\hat{\beta}_{j,j} \geq M_{j,1}\right\}, \\ \mathcal{S}_2 &= \left\{\hat{\beta}_j \mid -M_{j,2} \leq \hat{\beta}_{j,k} \leq M_{j,2}\right\}, \end{aligned}$$

with $M_{j,1}$ $M_{j,2}$ obeying the relation in Assumption 4.2.1-(ii). Here, g is a convex function formed by the parameter constraints such that $g(\hat{\beta}_j) \leq 0$. v_{pr} is the modified vector obtained from the original vector v with the following rule: If $\hat{\beta}_{j,k}(t)$ is not in $\mathcal{S}_2$, then the $(k+1)$st entry of v is made zero, and if $\hat{\beta}_{j,j}(t)$ is not in $\mathcal{S}_1$, then the $(j+1)$st entry of v is made zero. The estimation model is then given by

$$\hat{z}_j(t) = \hat{\theta}_j(t)^T \phi(t). \tag{4.11}$$

Remark 4.3.1. *The estimation algorithm* (4.8)-(4.11) *with the parameter projection rule guarantees that the estimated parameters are always inside the given bounds. Since the projection rule is constituted by the convex function* $g(\hat{\beta}_j)$*, the estimation algorithm with projection preserves all its convergence properties of the pure least-squares algorithm, [82].*

We denote the parameter estimation error vector as $\tilde{\theta}_j = \hat{\theta}_j - \theta_j^*$, noting that $\tilde{\theta}_j^\top \phi = -\epsilon_j \psi^2$. The following lemma is a direct consequence of the estimation algorithm defined by (4.8)-(4.11).

Lemma 4.3.1. *[82] Consider Problem 1. The estimation algorithm* (4.8)-(4.11) *applied to the plant model* (4.2) *has the following properties:*

i. $\epsilon_j,\ \epsilon_j\psi,\ \dot{\hat{\theta}}_j \in \mathcal{L}_2 \cap \mathcal{L}_\infty$ *and* $\hat{\theta}_j,\ P \in \mathcal{L}_2$.

ii. $|\hat{\beta}_{ii}| \geq M_{i,1}$ *for all* i *and* $|\hat{\beta}_{ij}| \leq M_{i,2}$ *for all* $i, j,\ i \neq j$.

iii. The vector of the estimated parameters $\hat{\theta}_j$ *converges to a constant vector.*

iv. If ϕ/ψ *is persistently exciting (PE), i.e., for every* T*, there exist positive constants* $c_3,\ c_4$ *such that*

$$c_3 I \leq \int_t^{t+T} \frac{\phi(t)\phi^\top(t)}{\psi^2(t)} \leq c_4 I,$$

then $\hat{\theta}_j \to \theta_j^*$ *as time goes to infinity.*

Lemma 4.3.1 states boundedness of the parameter estimates and other internal signals within the parameter estimation loop (4.8)-(4.11). Convergence to actual parameters requires the PE condition in Part (iv), but such convergence is not necessary for asymptotic tracking, as will be established in Section 4.3.3.

Remark 4.3.2. *Parameter projection applied inside the estimation algorithm guarantees nonsingularity of the estimated matrix $\hat{\beta}(t)$ for all time. This further guarantees the boundedness of the control rule (4.6). Although assuming upper and lower bounds on the entries of an unknown matrix brings restriction on the variety of system dynamics to which the approach can be applied, projecting parameters in the LS algorithm is an explicit approach where each entry of the matrix is updated based on the a priori information.*

Remark 4.3.3. *Number of the gains $P(t)$ to be calculated increases "linearly" with the number of the estimated parameters.*

4.3.2 Tracking Error Dynamics and Observer Design

Substituting (4.6) in (4.2) we obtain

$$\begin{aligned} \dot{x}_{k,j} &= x_{k+1,j}, \quad k = 1, \ldots, r-1, \ r \geq 2, \\ \dot{x}_{r,j} &= \alpha_j + \beta_j^\top \hat{\beta}^{-1}(-\hat{\alpha} + \nu), \\ y_j &= x_{1,j} = p_j, \end{aligned} \tag{4.12}$$

remarking the notation $\alpha = [\alpha_1, \ldots, \alpha_m]^\top$, $\beta = [\beta_1, \ldots, \beta_m]^\top$. Hence,

$$\begin{aligned} \dot{x}_{r,j} &= \alpha_j + (\beta_j - \hat{\beta}_j + \hat{\beta}_j)^\top \hat{\beta}^{-1}(-\hat{\alpha} + \nu) \\ &= \nu_j + (\alpha_j - \hat{\alpha}_j) - \tilde{\beta}_j^\top \hat{\beta}^{-1}(-\hat{\alpha} + \nu) \\ &= \nu_j - \tilde{\theta}_j^\top \bar{\phi}, \end{aligned} \tag{4.13}$$

where $\bar{\phi} = [1, u^\top]^\top \in \Re^{m+1}$ corresponds to the unfiltered version of the regressor signal ϕ. From (4.3) and (4.13), we have

$$\begin{aligned} e_j^{(r)} &= p_j^{(r)} - p_j^{*(r)} \\ &= \nu_j - \tilde{\theta}_j^\top \bar{\phi} - p_j^{*(r)}. \end{aligned} \tag{4.14}$$

Next, we design a Luenberger observer based state-feedback controller to generate an asymptotically stabilizing control signal ν_j:

$$\nu_j = p_j^{*(r)} - c^\top \hat{E}_j, \tag{4.15}$$

where $\hat{E}_j$ is the estimate of the state vector

$$E_j = [e_j, \dot{e}_j, \ldots, e_j^{r-1}]^\top, \tag{4.16}$$

and $c = [c_0, c_1, \ldots, c_{r-1}]^\top$ is chosen such that $\Delta(s) = s^{(r)} + c_{r-1}s^{(r-1)} + \ldots + c_1 s + c_0$ is Hurwitz. The error dynamics based on (4.14), (4.15), and (4.16) can be summarized as

$$\begin{aligned} \dot{E}_j &= A_c E_j + b\left(\nu_j - \tilde{\theta}_j^\top \bar{\phi} - p_j^{*(r)}\right) \\ &= A_c E_j - bc^\top \hat{E}_j - b\tilde{\theta}_j^\top \bar{\phi}, \end{aligned} \tag{4.17}$$

$$A_c = \begin{bmatrix} 0_{r-1\times r-1} & I_{r-1} \\ 0_{1,r-1} & 0 \end{bmatrix} \in \Re^{r\times r}, \quad b = \begin{bmatrix} 0 \\ \vdots \\ 0 \\ 1 \end{bmatrix} \in \Re^r.$$

Defining the state estimation error $\tilde{E}_j = \hat{E}_j - E_j$, (4.17) can be rewritten as

$$\dot{E}_j = AE_j - bc^\top \tilde{E}_j - b\tilde{\theta}_j^\top \bar{\phi}, \tag{4.18}$$

where $A = A_c - bc^\top$. The Luenberger observer design will aim to drive $\tilde{E}_j$ and E_j to zero asymptotically. Similar to c, define $h = [h_{r-1}, \ldots, h_1, h_0]^\top$ such that $\Delta_h(s) = s^{(r)} + h_{r-1}s^{(r-1)} + \ldots + h_1 s + h_0$ is Hurwitz, with faster poles than $\Delta(s)$. Define $c_c = [1, 0, \ldots, 0]^\top$ and $A_o = A_c - hc_c^\top$. Then, defining the observer law

$$\dot{\hat{E}}_j = A_o \hat{E}_j + he_j + b\left(\nu_j - p_j^{*(r)}\right), \tag{4.19}$$

we obtain the following state estimation error dynamics by subtracting (4.17) from (4.19):

$$\dot{\tilde{E}}_j = A_o \tilde{E}_j + b\tilde{\theta}_j^\top \bar{\phi}. \tag{4.20}$$

(4.18) and (4.20) can be combined in a single equation as follows:

$$\begin{bmatrix} \dot{E}_j \\ \dot{\tilde{E}}_j \end{bmatrix} = A_T \begin{bmatrix} E_j \\ \tilde{E}_j \end{bmatrix} + \begin{bmatrix} -b \\ b \end{bmatrix} \tilde{\theta}_j^\top \bar{\phi}, \tag{4.21}$$

$$A_T = \begin{bmatrix} A & -bc^\top \\ 0 & A_o \end{bmatrix}.$$

4.3.3 Stability and Convergence

In this section, we discuss the stability and convergence properties of the adaptive tracking control design of Section 4.3.1 and 4.3.2.

Theorem 4.3.1. *Consider Problem 4.2.1. The adaptive control scheme (4.6) with (4.8)-(4.11), (4.15), and (4.19) steers the output vector p to p^* asymptotically.*

Proof. The main objective, deriving the output vector and its derivatives up to the order r to their desired values asymptotically, is integrated into the equation (4.21). Note that (4.21) is a linear time-invariant system driven by the parameter estimation error term $\tilde{\theta}_j^\top \phi$. From Lemma 4.3.1, we have that with the LS estimation algorithm (4.8)-(4.11), the term $\tilde{\theta}_j^\top \phi = \epsilon_j \psi^2$ converges to zero asymptotically for all $j \in [1, \cdots, m]$. Since A_T is block diagonal and since A, A_o are Hurwitz by definition, we have that E_j, $\tilde{E}_j \to 0$ for all $j \in [1, \cdots, m]$ as $t \to \infty$. Thus, $p(t) \to p^*(t)$ as $t \to \infty$. □

Remark 4.3.4. *For the convergence of the output vector y to its desired value, it is sufficient to employ an estimation algorithm which leads to boundedness of signals in the closed-loop system and convergence of the signal $\tilde{\theta}^\top \phi$ to zero. Gradient and least-squares estimation algorithms satisfy this requirement. Observe that convergence of the estimated parameter $\hat{\theta}$ to its actual value θ^* is not a condition for the tracking objective.*

4.4 Adaptive Formation Control

In this section, we study formation control of swarms of agents of type considered in Section 4.2 and 4.3. Since we employ indirect adaptive control approach, each agent overcomes the parametric uncertainty independently. This choice brings some advantages when we consider the formation control of these agents, specifically it makes the design of decentralized formation control schemes for the formation possible.

We consider a swarm $\mathcal{S}$ of N holonomic agents. For convenience, we denote the ith agent and its state by A_i and x_i $(i = 1, \ldots, N)$, respectively. The system dynamics is given

by (4.1), (4.2), with proper re-indexing of (4.2) for each A_i as follows:

$$\begin{aligned} \dot{x}_{i,k} &= x_{i,k+1}, \quad k = 1, \ldots, r-1;\ r \geq 2 \\ \dot{x}_{i,r} &= \alpha_i(t) + \beta_i u_i \\ y_i &= x_{i,1} = p_i, \end{aligned} \tag{4.22}$$

where $x_{i,k},\ u_i,\ p_i,\ \alpha_i \in \Re^m$, and $\beta_i \in \Re^{m \times m}$. We assume that every agent A_i knows the vectors $x_{i,1}$ and $x_{i,2}$, which, for the $r = 2$ case, corresponds to that every agent knows its own position and velocity vectors. The main objective of the swarm is to move as a cohesive whole from a start point to a final point. We propose two different formation control schemes. In the first approach, we apply the control law derived in Section 4.3 to steer each agent to a reference trajectory generated to satisfy the formation requirements for cohesive whole motion of the agents in n-dimensional space. The second approach employs the combined shape control and flocking algorithm of [3] for systems with relative degree two and in two dimensional Euclidean space.

4.4.1 Adaptive Virtual Leader Based Formation Control

In Section 3.3.1, we summarized the virtual-leader based formation control of $\mathcal{S}$. We now integrate it with the adaptive tracking control law of a single vehicle. For agent A_i, we propose the control rule (4.6) together with (4.8)-(4.11), (4.15), and (4.19). The term $p_j^{*(r)}$ in (4.15) is replaced by $p_{i,j}^{*(r)}$, the jth entry of the reference trajectory p_i^* in (3.2). We reach the following corollary for this setting.

Corollary 4.4.1. *For every agent dynamics we have the convergence result of Theorem 4.3.1, that is, every agent A_i tracks its desired trajectory p_i^* despite the uncertainties. Hence, the cohesive whole motion of the formation is achieved in the asymptotic sense with the virtual leader-based formation scheme.*

Simulation results for this setting are given in Section 4.5. We emphasize that adaptive virtual leader based formation control of a multi-agent system is a straightforward extension of the trajectory tracking control law of single vehicle with parametric uncertainty and it is intended to be a base for further formation control algorithm studies. It can be further integrated with other formation control algorithms such as gradient based and sliding-mode based ones to accomplish other formation control objectives such as collision/obstacle

avoidance, formation expansion/contraction, rotation, and formation reconfiguration under parametric uncertainty in vehicle dynamics.

4.4.2 Adaptive CFSFC

We now relate the adaptive control algorithm of Section 4.3 to the CFSFC law (3.4) which is described in Section 3.3.2. Let A_1 be the flocking leader with the double integrator dynamics (2.2) setting $u_1 = 0$ and $v_1(0) = v_c$ where v_c is a constant vector. Each follower agent $A_i,\ i = (2, \ldots, N)$ is assumed to have the special case of the dynamic model (4.22) where $r = 2$. Observe that (4.22) with $r = 2$ and $x_{i,2} = v_i$ is equivalent to the double integrator agent model (2.2) where the acceleration input is not free, but a function of unknown parameters.

Further, we choose the flocking graph $\mathcal{G}_f$ and the formation shape graph $\mathcal{G}_{sh}$ as described in Section 3.3.2. Let ν_i be the linear control term of agent $A_i,\ i = (2, \ldots, N)$. For agent $A_i,\ i = (2, \ldots, N)$, we propose the control rule (4.6) together with (4.8)-(4.11), and the linear control term ν_i generated as follows:

$$\begin{aligned} \bar{\nu}(t) &= [\nu_2(t), \cdots, \nu_N(t)] \\ &= -\left(\bar{L} \otimes I_2\right) v_r(t) - \nabla V(p_r(t)), \end{aligned} \tag{4.23}$$

where $p_r,\ v_r$ are defined in (3.3). Convergence properties of the algorithm is summarized in the following proposition.

Proposition 4.4.1. *Consider the adaptive CFSFC system of $N > 2$ agents with the flocking and formation shape graphs as described in Section 3.3.2. Let the agent A_1 be the leader with the velocity vector v_c. Then, the velocities of agents $A_i,\ i = \{2, \cdots, N\}$, asymptotically converge to v_c, and the desired formation shape is converged asymptotically.*

Proof. For the special case $r = 2$ assumed in this section, the dynamics of agent A_i controlled by (4.6) is

$$\begin{aligned} \dot{p}_{i,j} &= v_{i,j}, \\ \dot{v}_{i,j} &= \nu_{i,j} - \tilde{\theta}_{i,j}^{\top} \bar{\phi}_i. \end{aligned}$$

From Lemma 4.3.1, we have that $\tilde{\theta}_{i,j}^{\top} \bar{\phi}_i$ converges to zero asymptotically for all i, j. Combining this fact with the perfect convergence property of the linear control term (4.23), we conclude the result. □

In Section 4.5, we simulate the behavior of a three-agent system driven by the aforementioned decentralized control law applied at each agent.

4.5 Simulations and Results

In this section, we give the simulation results of the adaptive formation control schemes designed in Section 4.4.

Virtual Leader-based Control Scheme:
Consider a three-agent formation system with the agent dynamics (4.22) with $r = 2$ and $m = 3$. Assume $p_i, v_i \in \mathbb{R}^3$. The values of the unknown functions α_i and β_i are chosen as follows:

$$\alpha_i(t) = \begin{bmatrix} 0.1\cos(0.1t) \\ 0.2\cos(0.05t) \\ 0.2\cos(0.05t) \end{bmatrix}, \ \beta_i = \begin{bmatrix} 0.8 & 0.1 & 0.3 \\ 0.03 & 2 & 0.5 \\ 0.08 & 0.2 & 1 \end{bmatrix},$$

for all $i = \{1, 2, 3\}$. The time variations in the entries of α_i are very small, obeying Assumption 1-iv. It is worth to note that the entries of α_i do not need to be periodic signals, they can be any bounded signals such as piece-wise constants. We also emphasize that different α_i, β_i can be selected for different vehicles. The initial positions for the agents are chosen such that they constitute a triangular shape: $p_1(0) = [9, 5, 0]^\top$, $p_2(0) = [1, 5, 0]^\top$, $p_3(0) = [3, 8, 0]^\top$. This initial formation configuration is also the desired configuration of the three agent system. Since the main aim of the adaptive virtual leader-based formation control scheme is formation maintaining and cohesive whole motion, it is suitable to initiate the formation with the desired configuration. The reference path for the virtual leader is given as follows:

$$p_v^*(t) = \begin{bmatrix} 5.05 + 0.3t - 0.05\cos(2t) \\ 8.8 - 3.8\cos(0.5t) \\ 1 - \cos(0.5t) \end{bmatrix}.$$

Parameter values for the linear control law (4.15) are chosen as $c_1 = 15$, $c_0 = 25$

resulting in the following control vector for each agent A_i:

$$\nu_i(t) = \begin{bmatrix} 0.2\cos(2t) + c_1\dot{\hat{e}}_{i,1} + c_0 e_{i,1} \\ 0.95\cos(0.5t) + c_1\dot{\hat{e}}_{i,2} + c_0 e_{i,2} \\ 0.25\cos(0.5t) + c_1\dot{\hat{e}}_{i,3} + c_0 e_{i,3} \end{bmatrix},$$

where $\dot{\hat{e}}_{i,j}$ are generated with the Luenberger observer as explained in Section 4.3.2. Initial values of the estimated parameters are chosen as

$$\hat{\alpha}_i(0) = \begin{bmatrix} 0.09 \\ 0.18 \\ 0.17 \end{bmatrix}, \ \hat{\beta}_i(0) = \begin{bmatrix} 0.9 & 0.15 & 0.25 \\ 0.02 & 2.2 & 0.5 \\ 0.1 & 0.17 & 1.1 \end{bmatrix},$$

for $i = 1, 2, 3$. In Fig. 4.2, 4.3, and 4.4, the simulation results are illustrated. Although the formation is dispersed at the first few seconds because of the uncertainties in agent dynamics, the agents form the formation in finite time again and track their trajectories perfectly.

Adaptive CFSFC:

In this part, we simulate the adaptive formation control scheme proposed in Section 4.4.2 for a three-agent formation system. The agent A_1 is selected as the flocking leader with the double integrator dynamics (2.2) and the dynamics of the follower agents A_2 and A_3 are given by (4.22) with $r = m = 2$. Assume $p_i, v_i \in \mathbb{R}^3$. The values of the unknown functions α_i and β_i are chosen as

$$\alpha_i(t) = \begin{bmatrix} 0.1\cos(0.05t) \\ 0.2\cos(0.01t) \end{bmatrix}, \ \beta_i = \begin{bmatrix} 0.8 & 0.5 \\ 0.5 & 1.5 \end{bmatrix}$$

for $i = \{2, 3\}$. Notably, time variations in the entries of α_i are very small, obeying Assumption 1-iv. The initial positions for the agents are chosen as $p_1(0) = [1, 0]^\top$, $p_2(0) = [4, 0]^\top$, $p_3(0) = [\frac{5}{2}, \frac{3\sqrt{3}}{2}]^\top$. Desired configuration of the formation is a triangular shape with edge length 3, i.e., $d^*_{12} = d^*_{23} = d^*_{13} = 3$. Since the main aim of the adaptive CFSFC is formation maintaining and cohesive whole motion, it is suitable to initiate the formation with the desired configuration. Initial values of the estimated parameters are chosen as

$$\hat{\alpha}_i(0) = \begin{bmatrix} 0.15 \\ 0.27 \end{bmatrix}, \ \hat{\beta}_i(0) = \begin{bmatrix} 0.75 & 0.45 \\ 0.02 & 1.2 \end{bmatrix}$$

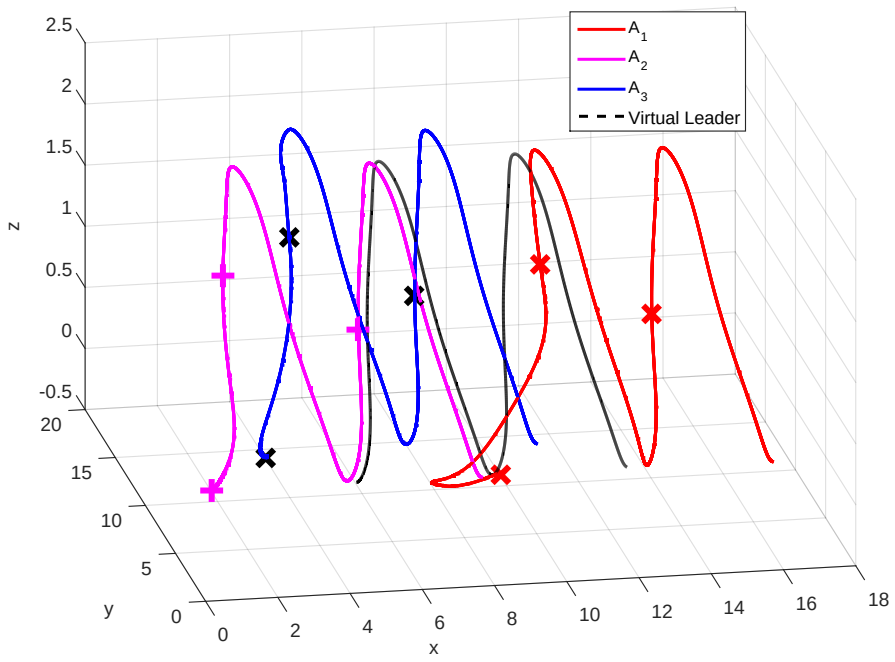

Figure 4.2: Adaptive virtual leader based controller: Movement of the three-agent system.

for $i = \{2, 3\}$. The velocity of A_1 is given as $v_c = [3, 3]^\top$. In Fig. 4.5, 4.6, and 4.7, the simulation results are illustrated. It is clearly observed from the simulation results that the velocities of the followers A_2, A_3 converge to that of the leader, and at the same time they form the desired equilateral triangular formation shape in a small amount of time. The agents achieve these tasks despite the uncertainties in the agent dynamics.

4.6 Summary

In this chapter, we have studied adaptive formation control algorithms utilizing the features of the certainty equivalence principle. First, we have developed an indirect adaptive control framework for vehicles with high-order dynamics and parametric uncertainty to achieve reference signal tracking. Least-squares algorithm is used to estimate the uncertain parameters. Then, output feedback linearization based control law is applied in an indirect adaptive control scheme using the certainty equivalence principle. Derivative(s) of

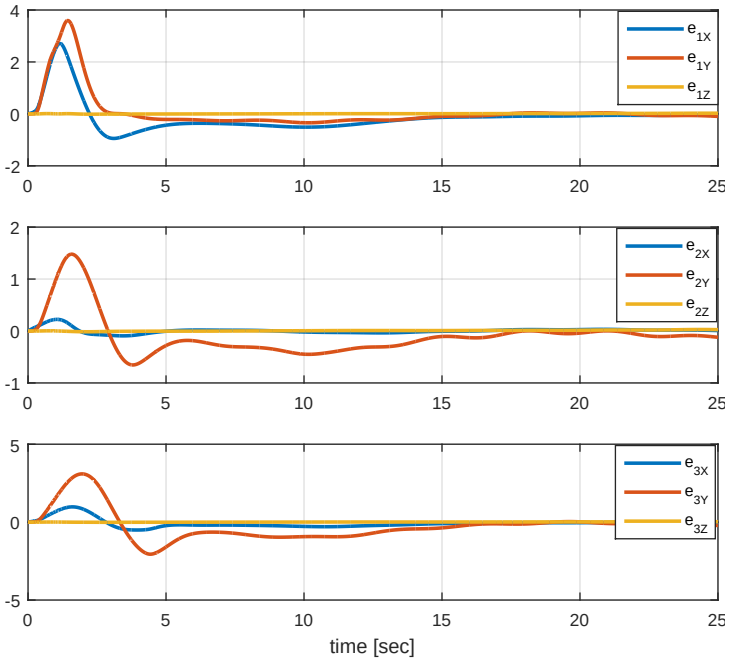

Figure 4.3: Adaptive virtual leader based controller: Output errors (e_1, e_2 and e_3).

the position errors have been obtained by Luenberger observer. Later, we have analyzed the adaptive formation control of these vehicles. As a straightforward extension of the single vehicle control case, we have considered the adaptive virtual-leader based formation control. As a more specific and realistic case, we have proposed the adaptive CFSCF control law for vehicles with second order uncertain dynamics. The indirect adaptive control method, that is, separation of the estimation and motion control parts, brings advantages in applications on different vehicle models. The adaptive control scheme covered in this chapter can further be applied to other formation control approaches such as sliding-mode and hierarchical cohesive motion control structures described in Chapter 3.

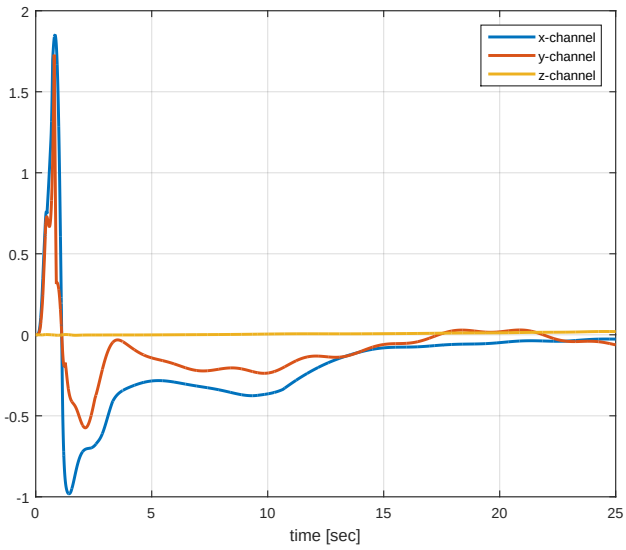

Figure 4.4: Adaptive virtual leader based controller: As indicated in Theorem 4.3.1, the term $\tilde{\theta}^\top \phi$ converges to zero (represented for A_1).

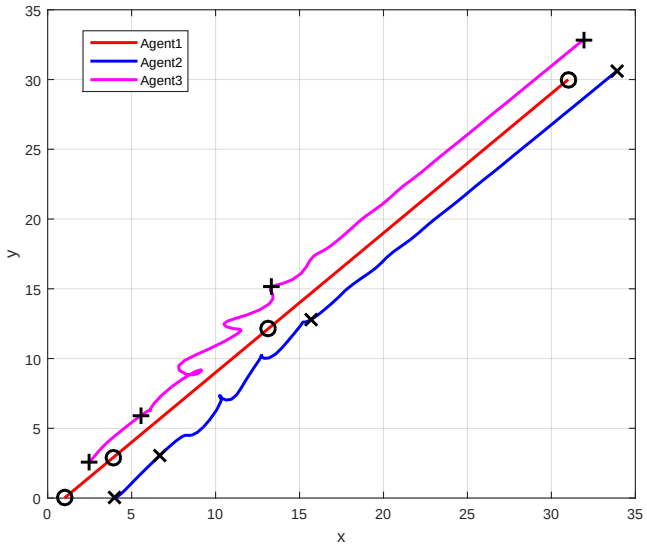

Figure 4.5: Adaptive CFSFC: Movement of the three-agent system.

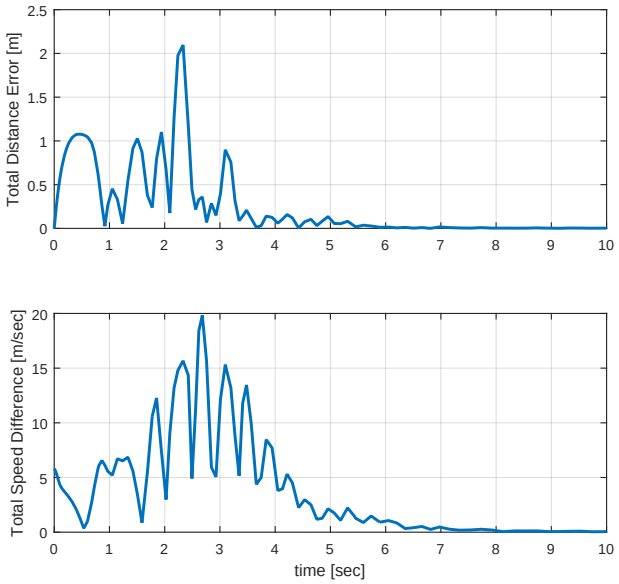

Figure 4.6: Adaptive CFSFC: Total distance errors, $|\sum_{i\neq j}(d_{ij}^{*}-d_{ij})|$; and total speed differences $|\sum_{i\neq j}(v_i-v_j)|$.

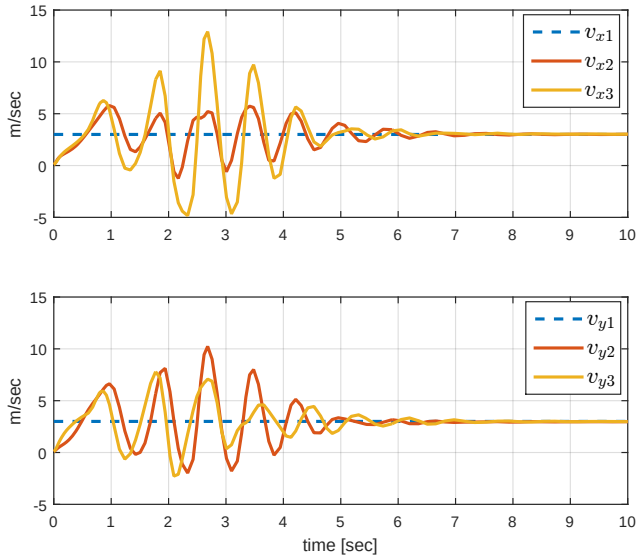

Figure 4.7: Adaptive CFSFC: Agent velocities.

Chapter 5

Formation Acquisition and Adaptive Station Keeping

5.1 Introduction

In Chapter 3 and Chapter 4, we consider the formation control of multi-vehicle systems. In connection with those chapters, here we study the problem of adding a mobile vehicle to a network of multi-vehicle system. We are interested in acquiring a new network of mobile vehicles by the addition of the mobile vehicle to the existing vehicles. Specifically, we consider the following scenario: Given an autonomous multi-vehicle system $\mathcal{S} = \{A_1, \cdots, A_N\}$ with vehicle positions p_i, the goal is to steer and add the mobile vehicle A to $\mathcal{S}$ in a way that A has distance d_i^* to each vehicle A_i. In this regard, we consider the following problem given in abstract terms.

Problem 5.1.1. *Consider a mobile sensory vehicle A with position $p_A \in \Re^n$, $n \in \{2, 3\}$, which is required to join a rigid formation of N vehicles $\mathcal{S} \triangleq \{A_1, \cdots, A_N\}$, $N > n$, with unknown position $p_i \in \Re^n$ for each A_i, and an unknown target position $p_A^* \in \Re^n$ for A within the formation. Assume that A_i are not collinear for $n = 2$ and not coplanar for $n = 3$. Assume also that the desired inter-vehicle distances $d_i^* \triangleq \|p_A^* - p_i\|$, the actual inter-vehicle distances $d_i(t) \triangleq \|p_A(t) - p_i\|$, and self-position p_A are available to A. The task is to define a control law to generate $\dot{p}_A(t)$ such that for any given initial position $p_A(0) = p_{A,0}$, $p_A(t)$ converges to p_A^* asymptotically.*

Remark 5.1.1. *There may also be the cases where the agents in $\mathcal{S}$ are persistently drifting in a rigid formation without violating distance constraints. As a result, the target point p_A^* may be persistently drifting and represented as a function of time, e.g., $p_A^*(t)$; however, we do not study that case in this chapter.*

It is worth to emphasize the second interpretation of Problem 5.1.1 in real-life applications as follows: There are N sensor stations with unknown positions p_i and a target signal source with unknown position p_A^*. A mobile sensory vehicle is desired to be steered to the target signal source autonomously, using the station-target distance measurements d_i^*, and the station-vehicle distance measurements $d_i(t)$.

Problem 5.1.1 is a special case of *target capture* (or *docking*) problem where a mobile vehicle is required to reach a specified target location autonomously using its sensing and/or communication capabilities such as continuous range measurements or bearing measurements or both, [18–20, 41]. Since the target location to be reached is not directly known in problems like Problem 5.1.1, one needs to follow an adaptive control approach. In [18] and [20], an adaptive switching control approach is applied to solve the second interpretation of Problem 5.1.1 for $N = 3$ and $n = 2$, without assuming the knowledge of the vehicle's own position y. It is assumed in these works that the mobile vehicle is modeled by single integrator kinematics and there exist small errors on the parameters d_i^* and the measurements $d_i(t)$. An analogue to this problem is considered in the localization literature where the objective is to estimate the unknown location of a signal source using distance measurements between the source and a set of sensors with known positions. [40] and [43] examine the geometric location set for the target that would guarantee certain gradient based localization algorithms to converge for given sensor station settings. The geometric sets are established to be nontrivial ellipsoidal and polytopic regions surrounding the sensor stations. In these papers, the performance of the gradient algorithms, which are based on a non-convex cost function, under noisy measurement cases is presented as well.

Circumnavigation, i.e., reaching a neighborhood of a target location and navigating around the target with a certain radius, is another research problem that is by nature closely related to target reaching and station keeping. [116] integrates the concepts of localization and motion control, as done in this chapter, to achieve a circumnavigation objective around a stationary target. A persistently drifting target situation is also considered in [116] with well-established convergence analysis, and this extension exhibits, in a sense, the robustness of the algorithm derived. [26] proposes an algorithm that steers a non-holonomic vehicle,

by controlling only its angular velocity, to a source to which the vehicle cannot measure its distance, but receives a signal from the source in the form of an unknown function of the distance. Employing extremum seeking and the techniques of averaging theory, circumnavigation around the target is achieved in that work.

In this chapter, we study Problem 5.1.1 assuming that the dynamics of the mobile autonomous vehicle is modeled by a single integrator kinematics. We partition the problem into two sub-problems; (i) localization of the stationary vehicles using range-only measurements, and (ii) motion control of the mobile vehicle. In the localization and the motion control parts, we employ least-squares (LS) based parameter estimation and a gradient control law, respectively. Using the certainty-equivalence approach, we then combine the two algorithms and synthesize an indirect adaptive control algorithm to achieve the objective. Our approach differs from [20] in that we assume N stationary vehicles with unknown positions and the position information of the vehicle with respect to some reference frame, while [20] solves the second interpretation of Problem 5.1.1 for the three sensor case without the assumption that the position of the mobile vehicle is known to it. As an advantage of the current work over [20], we may show the *modularity* property following from the nature of the indirect adaptive algorithm. To put it differently, any localization algorithm that achieves asymptotic convergence of the stationary vehicles position estimates to the correct values can be employed in place of the LS parameter estimation algorithm, while one may consider the replacement of the gradient-based motion control law by another controller which uniquely defines the target point based on the stationary vehicles locations.

The remainder of the chapter is organized as follows. In Section 5.2, a gradient-based control law which minimizes a convex cost function is synthesized for the fictitious case as if the locations of the stationary vehicles are known. Then, in Section 5.3, the localization algorithm used to localize the N stationary vehicles positions is presented. In Section 5.4, the localization algorithm and the motion control law are combined to derive the indirect adaptive control approach to solve Problem 5.1.1. Formal stability and convergence analysis take place in that section as well. Section 5.5 demonstrates the performance of the proposed controller via simulations, and finally, Section 5.6 offers conclusions.

5.2 Control Law Design: Known Station Positions Case

5.2.1 Problem Definition

Having the control and parameter identification parts of our design as specified in Section 5.1, we use a certainty equivalence approach to solve Problem 5.1.1. Accordingly, for control law construction, we first consider the fictitious case where the locations $p_1, \cdots, p_N \in \Re^n$ are perfectly known by the vehicle A. Following is the corresponding control problem statement for this fictitious case, which differs from Problem 5.1.1 only in the assumption on the vehicle's knowledge of stationary vehicle positions:

Problem 5.2.1. *Consider a mobile sensory vehicle A with position $p_A \in \Re^n$, $n \in \{2, 3\}$, which is required to join a rigid formation of N stationary vehicles $\mathcal{S} \triangleq \{A_1, \cdots, A_N\}$, $N > n$, with* "known" *position $p_i \in \Re^n$ for each A_i, and an unknown target position $p_A^* \in \Re^n$ for A within the formation. Assume that A_i are not collinear for $n = 2$ and not coplanar for $n = 3$. Assume also that the desired inter-vehicle distances $d_i^* \triangleq \|p_A^* - p_i\|$, the actual inter-vehicle distances $d_i(t) \triangleq \|p_A(t) - p_i\|$, and self-position p_A are available to A. The task is to define a control law to generate $\dot{p}_A(t)$ such that for any given initial position $p_A(0) = p_{A,0}$, $p_A(t)$ converges to p_A^* asymptotically.*

In Fig. 5.1, the scenario described in Problem 5.2.1 is depicted for the four stationary vehicles case. Two problems that are mathematically equivalent to the discrete-time version of Problem 5.2.1 have been defined (within localization context instead of motion control) and solved in [40, 43]. In these works, the non-convex weighted cost function

$$\overline{J}(p_A) = \frac{1}{4} \sum_{i=1}^{N} \lambda_{Ji} \left(d_i^2 - d_i^{*2} \right)^2 , \tag{5.1}$$

is used together with the gradient descent law to determine the ellipsoidal regions where practical localization of the signal source is achieved globally using only target-sensor distance measurements (the second interpretation of Problem 5.1 is solved in those works indeed, assuming the target and the stationary vehicles as the signal source and sensor stations, respectively). In (5.1), $\lambda_{Ji} > 0$ are certain design weights and each term $\lambda_{Ji} \left(d_i^2 - d_i^{*2} \right)^2$ penalizes the difference between d_i and d_i^*. The weights λ_{Ji} can be chosen

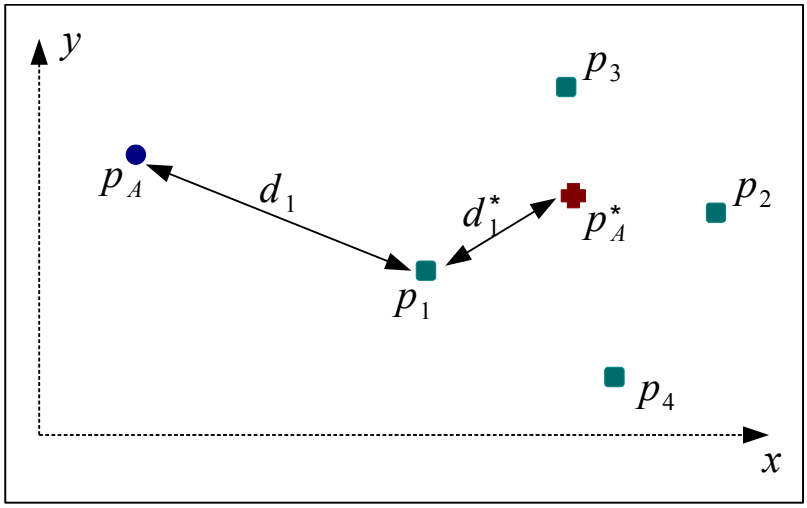

Figure 5.1: Depiction of the scenario in Problem 5.2.1 for a four-vehicle case.

based on the any additional *a priori* information that maybe available. For example, if it is known that certain d_i^* information is more reliable than others, then the corresponding λ_{Ji} can be chosen larger.

Here we use an approach similar to [40, 43], using an alternative convex cost function in place of (5.1) and applying the derivations in continuous time instead of discrete time, noting that one could also apply different techniques of extremum seeking literature. It is established in [46] that the cost function

$$J(p_A) = \frac{1}{2}\sum_{i=1}^{N-1}\left[(p_A - \xi_i)^\top e_i\right]^2, \tag{5.2}$$

where

$$\begin{aligned} e_i &\triangleq p_i - p_N, \\ \xi_i &\triangleq p_N + a_i e_i, \\ a_i &\triangleq \frac{\|e_i\|^2 + d_N^{*2} - d_i^{*2}}{2\|e_i\|^2}. \end{aligned} \tag{5.3}$$

is convex, and hence has a unique minimum, making it useful in many gradient search applications. The idea is based on defining the unique target point p_A^* as the intersection

of certain lines instead of intersection of circles with origins at stationary vehicle positions, for the sake of convexity.

Consider the stationary vehicle localization setting in Fig. 5.2. Specifically, in the formulation (5.3), we choose p_N as the reference point and denote the vector traversed from the p_N to the p_i by e_i. We note that selection of p_N among N vehicles is done randomly and the selection does not have any effect on the algorithm. Let l_{iN} denote the line passing through the two intersection points of the two non-concentric circles $\mathcal{C}(p_i, d_i^*)$ and $\mathcal{C}(p_N, d_N^*)$, viz., the circle with center p_i and radius d_i^* and the circle with center p_N and radius d_N^*, respectively. This line is called the *radical axis* of the circle pair $\mathcal{C}(p_i, d_i^*)$, $\mathcal{C}(p_N, d_N^*)$ [87], and has the property that any point x on l_{iN} has equal powers with respect to the circles $\mathcal{C}(p_i, d_i^*)$, $\mathcal{C}(p_N, d_N^*)$, i.e.,

$$\|x - p_i\|^2 - d_i^{*2} = \|x - p_N\|^2 - d_N^{*2}. \tag{5.4}$$

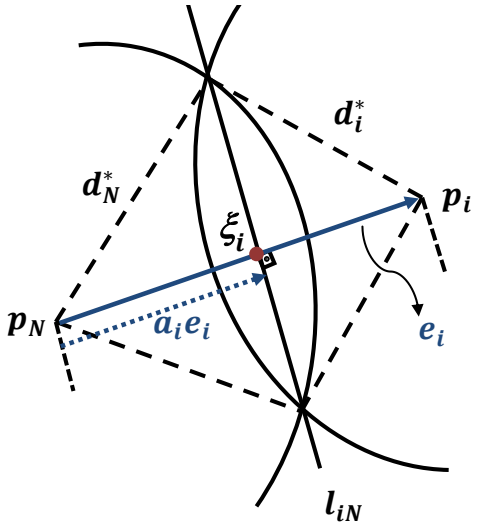

Figure 5.2: Illustration of the formulation (5.3) [46].

The intersection of the $N-1$ radical axes $l_{1N}, \cdots, l_{N-1,N}$ is y^*, which is the unique point satisfying

$$(p_A - \xi_i)^\top e_i = 0, \quad \forall i = \{1, \cdots, N-1\}. \tag{5.5}$$

Hence, we have the following lemma.

Lemma 5.2.1. *For the setting of Problem 5.2.1, p_A^* is the unique, global minimum of the cost function (5.2).*

Proof. This result for the 2D case is already established in [46]. The 3D extension is straightforward observing that the cost function (5.2) with the vectors e_i, ξ_i of (5.3) is the same as in 2D and it carries the same properties as in the 2D case. Nevertheless, it is worth noting that in the 3D case, the radical axes are replaced by radical planes and the cost function (5.2) is minimized at the intersection of the $N-1$ radical planes. □

Remark 5.2.1. *[46] uses an alternative convention for pairing the stationary vehicles, where radical axes for circle pairs $\mathcal{C}(p_i, d_i^*)$, $\mathcal{C}(p_{i+1}, d_{i+1}^*)$ are used to uniquely determine the target location. This selection leads to $e_i = p_{i+1} - p_i$ and $\xi_i = p_i + a_i e_i$, where $a_i = \dfrac{\|e_i\|^2 + d_i^{*2} - d_{i+1}^{*2}}{2\|e_i\|^2}$, as an alternative to (5.3). We emphasize that further alternative formulations exist. Leaving the optimal selection for the graph structures of the stationary vehicle set as a future work, we use the formulation (5.3) in this chapter.*

Observe that with the cost function (5.2), the gradient based control rule for vehicle velocity to reach y^* is given by

$$\begin{aligned} \dot{p}_A = -\frac{\partial J(p_A)}{\partial p_A} &= -\sum_{i=1}^{N-1} \left[(p_A - \xi_i)^\top e_i\right] e_i \\ &= -Ap_A + b, \end{aligned} \tag{5.6}$$

where

$$\begin{aligned} A &\triangleq \sum_{i=1}^{N-1} e_i e_i^\top = EE^\top, \quad b \triangleq \sum_{i=1}^{N-1} e_i e_i^\top \xi_i = EZ, \\ E &\triangleq [e_1, \ldots, e_{N-1}], \quad Z \triangleq \left[e_1^\top \xi_1, \ldots, e_{N-1}^\top \xi_{N-1}\right]^\top. \end{aligned} \tag{5.7}$$

Note that the control law (5.6) requires only the knowledge of the stationary vehicle positions p_i and the desired distances d_i^*, $i = 1, \cdots, N$.

Proposition 5.2.1. *The control law (5.6) with the parameters being defined in (5.3) solves Problem 5.2.1.*

Proof. Since the cost function (5.2) is convex, the only minimum of J is global. Hence, the vector p_A converges to the global minimum in the limit with the gradient rule (5.6) regardless of the initial condition. □

Corollary 5.2.1. *The unique minimum of the quadratic cost function* (5.2) *is given by*

$$p_A^* = A^{-1}b. \tag{5.8}$$

In (5.8)*, since we assume noncollinear and noncoplanar stationary vehicle positions, it follows from the geometry of the stationary vehicles that the matrix A is invertible.*

5.2.2 Comparison with Other Cost Functions

The cost function (5.1) can be considered as an alternative to (5.2) and the corresponding gradient vehicle velocity control rule for employing (5.1) is found as

$$\dot{p}_A = -\frac{\partial \overline{J}(p_A)}{\partial p_A} = \sum_{i=1}^{N} \lambda_{Ji}\left(d_i^{*2} - \|p_A - p_i\|^2\right)(p_A - p_i). \tag{5.9}$$

It is established in [40, 43] that (5.9) leads to global convergence of p_A to p_A^*, provided that p_A^* is within a certain ellipsoidal region defined by $p_1, \cdots, p_N$. However, when p_A^* is outside of this region, (5.1) has multiple stable local minima; and depending on the value of $p_A(0)$, p_A may converge to one of the false stable minimizers instead of p_A^* [40, 43, 109]. Hence, the control law (5.9) does not provide a global solution to Problem 5.2.1 for certain p_A^* settings.

5.3 Adaptive Signal Source Localization

If the mobile vehicle A knows the stationary vehicle positions p_i, it will converge to the target point described by the unique minimum of the function (5.2) with the gradient control law (5.6). However, in the setting of Problem 5.1.1, the stationary vehicle positions p_i are unknown. The vehicle A can only measure the distances d_i to the stationary vehicles. Accordingly, we propose use of a scheme that first estimates the (relative) stationary vehicle positions and then uses the produced estimates in place of the actual positions $p_1, \cdots, p_N$,

applying the certainty equivalence principle [82]. We revisit the adaptive source localization algorithms covered in [28] and [40] to comply with this objective. A formal definition of the localization task is described in the following.

Problem 5.3.1. *Consider a set of vehicles* $\mathcal{S} = \{A_1, \cdots, A_N\}$ *with unknown positions* $p_1, \cdots, p_N \in \Re^n$*, where* $n \in \{2, 3\}$ *and* $N > n$*, and a mobile sensory vehicle* A *with known position* $p_A \in \Re^n$*. Generate the vehicle position estimates* $\hat{p}_1, \cdots, \hat{p}_N$ *using the vehicle's own position* p_A*, and the inter-vehicle distance measurements* $d_i(t) = \|p_A(t) - p_i\|$*,* $i = 1, \cdots, N$*.*

Problem 5.3.1 has been addressed and solved with adaptive estimation methods based on gradient and LS approaches in [28, 39, 41]. In [28], the problem (for a single stationary vehicle A_i) is solved for mobile sensory vehicle A with single-integrator kinematics, using a gradient-based localization algorithm. In [28], both stationary and slowly drifting S cases are studied. In [41], the vehicle not only localizes S, but also moves to reach S. We generate the station position estimates $\hat{p}_1, \cdots, \hat{p}_N$, employing N identical estimators using the localization algorithm of [39, 41], where estimator i is fed by d_i for $i = 1, \ldots, N$.

5.3.1 The Localization Algorithm

We first revisit the LS based localization algorithm proposed in [39] in parallel to the gradient algorithm of [41] for estimating position p_i of each S_i in Problem 5.3.1. We first assume that p_i is constant. The linear parametric model developed in [39, 41] is based on the identity

$$\frac{1}{2}\frac{\mathrm{d}}{\mathrm{d}t}\left(\|p_A(t)\|^2 - d_i^2\right) = p_i^\top \dot{p}_A(t). \tag{5.10}$$

The implementation of a localization algorithm based on (5.10) would require generating the derivative of $d_i(t)$, however, this would bring some numerical problems especially when the noise level in measurements is high. Instead, we use the following filtered version of (5.10) as a parametric model:

$$z_i(\cdot) \equiv p_i^\top \phi(\cdot), \tag{5.11}$$

$$z_i(t) \triangleq \dot{\zeta}_i(t) = -\alpha\zeta_i(t) + \frac{1}{2}\left(p_A^\top(t)p_A(t) - d_i^2(t)\right), \tag{5.12}$$

$$\phi(t) \triangleq \dot{\varphi}(t) = -\alpha\varphi(t) + p_A(t), \tag{5.13}$$

where the notation $f_1(\cdot) \equiv f_2(\cdot)$ for two functions f_1, f_2 indicates that there exist $M_1,\ M_2 > 0$ such that for all $t \geq 0$, $\|f_1(t) - f_2(t)\| \leq M_1 e^{-M_2 t}$; $\alpha > 0$, $\zeta_i(0) \in \Re$, and $\varphi(0) \in \Re^n$ are arbitrary design parameters.

We propose use of the following modified form of the localization algorithm proposed and analyzed in [39], for Problem 5.3.1 (and for Problem 5.1.1), considering parametrization (5.11):

$$\dot{\hat{p}}_i(t) = \text{Proj}_{R,\hat{p}_i(t)}\left(P(t)\left(z_i(t) - \hat{z}_i(t)\right)\phi(t)\right), \tag{5.14}$$

$$\dot{P}(t) = \begin{cases} \beta P(t) - P(t)\phi(t)\phi(t)^\top P(t), & \lambda_{\max}(P(t)) < \rho_{\max} \\ 0, & \text{otherwise,} \end{cases} \tag{5.15}$$

$$P(t_r^+) = P_0 = \rho_0 I,$$

$$\hat{z}_i(t) = \hat{p}_i^\top(t)\phi(t), \tag{5.16}$$

with arbitrary initial estimate $\hat{p}_i(0)$ satisfying $\|\hat{p}_i(0)\| \leq R$ for a pre-set upper-bound R, where $\beta > 0$ is the constant forgetting factor, P is the adaptive gain matrix with the initial condition $P(0) = P_0 = \rho_0 I$, and t_r^+ is the resetting time instant defined by the condition $\lambda_{\min}(P(t_r)) = \rho_{\min}$ for some design coefficients $\rho_0 > \rho_{\min} > 0$. The modified LS gain update rule (5.15) with resetting guarantees that $\rho_{\min} I \leq P(t) \leq \rho_{\max} I$ for all $t \geq 0$ [82]. In (5.14), $\text{Proj}_{R,\hat{p}_i}(\cdot)$ stands for a parameter projection operator [82] used to satisfy $\|\hat{p}_i(t)\| \leq R$ for all t, and is defined for a given estimate vector θ, raw adaptive law input v (having the same dimension as θ), and scalar threshold $M_\theta > 0$ by

$$\text{Proj}_{M_\theta,\theta}(v) = \begin{cases} v & \text{if } \|\theta\| < M_\theta, \\ & \text{or if } \|\theta\| = M_\theta \text{ and } v^\top\theta \leq 0, \\ v - \dfrac{\theta\theta^\top}{M_\theta^2} v & \text{otherwise.} \end{cases}$$

Above and in the sequel, where we propose an alternative parametric model/estimation setting to reduce computational cost, we make the following assumption:

Assumption 5.3.1. *The target position p_A^*, the global station positions p_i, and the relative positions $e_i = p_i - p_N$ satisfy $\|p_A^*\| \leq R$, $\|p_i\| \leq R$ and $\|e_i\| \leq R$ for some known $R > 0$.*

Depending on the accuracy of the a priori information, R in Assumption 5.3.1 can be selected arbitrarily large.

5.3.2 Direct Estimation of e_i

The localization algorithm (5.14) generates the estimates of the N stationary vehicle positions. In this subsection, in order to reduce computational cost, we introduce an alternative parametric model to generate the estimates of the relative positions $e_i = p_i - p_N,\ i \in \{1, \ldots, N-1\}$. Evaluating (5.10) for $i = N$, one has

$$\frac{1}{2}\frac{\mathrm{d}}{\mathrm{d}t}\left(\|p_A(t)\|^2 - (d_N(t))^2\right) = p_N^\top \dot{p}_A. \tag{5.17}$$

For $i \in \{1, \ldots, N-1\}$, subtracting (5.17) from (5.10) gives

$$\frac{1}{2}\frac{\mathrm{d}}{\mathrm{d}t}\left((d_N(t))^2 - (d_i(t))^2\right) = e_i^\top \dot{p}_A. \tag{5.18}$$

Analogously to Section 5.3.1, we use the following filtered version of (5.18) as the parametric model:

$$z_{iN}(\cdot) \equiv e_i^\top \phi(\cdot), \tag{5.19}$$

$$z_{iN}(t) \triangleq \dot{\zeta}_{iN}(t) = -\alpha \zeta_{iN}(t) + \frac{1}{2}\left((d_N(t))^2 - (d_i(t))^2\right), \tag{5.20}$$

where ϕ is defined in (5.13).

Based on Assumption 5.3.1, we propose use of the following localization algorithm for estimation of e_i based on the parametric model (5.19):

$$\begin{aligned} \dot{\hat{e}}_i(t) &= \mathrm{Proj}_{R,\hat{e}_i(t)}\left(P(t)\left(z_{iN}(t) - \hat{z}_{iN}(t)\right)\phi(t)\right), \\ \hat{z}_{iN}(t) &= \hat{e}_i^\top(t)\phi(t), \end{aligned} \tag{5.21}$$

with arbitrary initial estimate $\hat{e}_i(0)$ satisfying $\|\hat{e}_i(0)\| \leq R$, where P is the adaptive gain matrix driven by (5.15) and $\mathrm{Proj}_{R,\hat{e}_i}(\cdot)$ is as in (5.17). The estimate $\hat{p}_N$ is generated using the parametric model (5.11),(5.12) and applying (5.14) for $i = N$ directly, i.e.,

$$z_N(\cdot) \equiv p_N^\top \phi(\cdot), \tag{5.22}$$

$$z_N(t) \triangleq \dot{\zeta}_N(t) = -\alpha \zeta_N(t) + \frac{1}{2}\left(p_A^\top(t)p_A(t) - d_N^2(t)\right), \tag{5.23}$$

$$\dot{\hat{p}}_N(t) = \mathrm{Proj}_{R,\hat{p}_N(t)}\left(P(t)\left(z_N(t) - \hat{p}_N^\top(t)\phi(t)\right)\phi(t)\right). \tag{5.24}$$

Based on the estimates $\hat{e}_i$ and $\hat{p}_N$ generated by (5.21), (5.24), we set the estimates $\hat{A}, \hat{b}$ of A, b in (5.8) as follows:

$$\hat{A} = \begin{cases} \hat{E}\hat{E}^\top, & \text{if } \lambda_{\min}(\hat{E}\hat{E}^\top) > \varepsilon_A \\ \hat{E}\hat{E}^\top + (\varepsilon_A - \lambda_{\min}(\hat{E}\hat{E}^\top))I, & \text{otherwise} \end{cases} \tag{5.25}$$

$$\begin{aligned} \hat{b} &= \hat{E}\hat{Z} \\ \hat{E} &= [\hat{e}_1, \ldots, \hat{e}_{N-1}], \quad \hat{Z} = \left[\hat{e}_1^\top \hat{\xi}_1, \ldots, \hat{e}_{N-1}^\top \hat{\xi}_{N-1}\right]^\top \\ \hat{\xi}_i &= \hat{p}_N + \hat{a}_i \hat{e}_i \\ \hat{a}_i &= \frac{\|\hat{e}_i\|^2 + d_N^{*2} - d_i^{*2}}{2\|\hat{e}_i\|^2}. \end{aligned} \tag{5.26}$$

where $\varepsilon_A > 0$ is a small design constant. Noting that $\hat{E}\hat{E}^\top$ is positive semi-definite, the switching law (5.25) guarantees that $\hat{A}$ is a continuous function of time, and $\hat{A}(t)$ is positive definite with minimum eigenvalue $\lambda_{\min}(\hat{A}(t)) \geq \varepsilon_A$ for all $t \geq 0$. The system matrix estimates $\hat{A}$ and $\hat{b}$ in (5.26) will be used in Section 5.4.1 for dynamic reference trajectory generation within the adaptive control scheme to be designed.

5.3.3 Stability and Convergence of the Localization Algorithm

In this subsection, we present the stability and convergence properties of the localization algorithm of Section 5.3.2, which will later be used in determining the control laws and design of the overall adaptive control scheme. We denote the filtering errors by

$$\delta_i(t) \triangleq e_i^\top \phi(t) - z_i(t), \quad i \in \{1, \ldots, N-1\}, \tag{5.27}$$

$$\delta_N(t) \triangleq p_N^\top \phi(t) - z_N(t), \tag{5.28}$$

and the estimation errors by

$$\tilde{e}_i(t) \triangleq \hat{e}_i(t) - e_i, \quad i \in \{1, \ldots, N-1\}, \tag{5.29}$$

$$\tilde{p}_N(t) \triangleq \hat{p}_N(t) - p_N. \tag{5.30}$$

Convergence properties of the localization algorithm are stated in the following lemma.

Lemma 5.3.1. *Consider the localization algorithm (5.21), (5.24) with the parametric models (5.19), (5.22). Then the following properties hold:*

i. $\dot{\delta}_i(t) = -\alpha\delta_i(t)$, *and hence* $\delta_i(t)$ *exponentially converges to zero as* $t \to \infty$ *for* $i = 1, \ldots, N$.

ii. $\dot{\tilde{e}}_i(t) = -P(t)\phi(t)\phi^\top(t)\tilde{e}_i(t) - P(t)\phi(t)\delta_i(t)$ *for* $i = 1, \ldots, N-1$, *and* $\dot{\tilde{p}}_N(t) = -P(t)\phi(t)\phi^\top(t)\tilde{p}_N(t) - P(t)\phi(t)\delta_N(t)$.

iii. *For all* $t \geq 0$, $P(t)$ *is symmetric positive definite and satisfies* $\rho_{\min} I \leq P(t) \leq \rho_{\max} I$ *where* $\rho_{\min}$ *and* $\rho_{\max}$ *are as in (5.14).*

iv. *The error signals* $\tilde{e}_i$, $\tilde{x}_N$, *and the estimates* $\hat{e}_i$, $\hat{p}_N$, $\hat{A}$, $\hat{b}$ *are bounded.*

v. *The* $n \times n$ *matrix* $\hat{A}(t)$ $(\forall t \geq 0)$ *is symmetric positive definite.*

vi. *If the regressor signal* ϕ *is persistently exciting, i.e., if for every* $t \geq 0$ *and for some* $T_0 > 0$ *there exist some constants* α_1, α_2 *such that*

$$\alpha_1 I \leq \int_t^{t+T_0} \phi(\tau)\phi(\tau)^\top d\tau \leq \alpha_2 I, \tag{5.31}$$

then $\tilde{e}_i(t)$ $(i = 1, \ldots, N-1)$ *and* $\tilde{p}_N(t)$, *and hence* $\tilde{A} \triangleq \hat{A} - A$ *and* $\tilde{b} \triangleq \hat{b} - b$ *converge to zero exponentially as* $t \to \infty$.

Proof. In [39], (i),(ii), and (vi) are proven for the case of estimating the vector p_i by a single estimator. We invoke the result of [39] and state that those properties of the localization algorithm also hold here for e_i for all $i \in \{1, \ldots, N-1\}$ and p_N without loss of generality, and noting that the introduced modifications do not affect these properties. (iii) is a direct corollary of the initialization $P_0 = \rho_0 I$, the symmetry preservation property of the LS algorithm (5.14), and the bounding modification and covariance resetting used in this algorithm. Parameter projection guarantees (iv). (v) follows by definition of $\hat{A}$ in (5.25). □

Remark 5.3.1. *By (5.13), the relation between the signals* ϕ *and* $\dot{y}$ *is given by:*

$$\dot{\phi}(t) = -\alpha\phi(t) + \dot{p}_A(t).$$

Note that the persistence of excitation condition (5.31) on ϕ also requires the persistence of excitation of $\dot{p}_A$. This can be interpreted as the signal $\dot{p}_A$ should persistently span $\Re^n$, $n = \{2, 3\}$, and avoid linear trajectories in $\Re^2$ and planar trajectories in $\Re^3$. However, this is contrary to the main goal which is reaching the target and stopping. We deal with this issue in the next section.

5.4 Adaptive Motion Control for Unknown Station Positions

In this section, we combine the motion control law of Section 5.2 and the parameter estimation (or localization) algorithm of Section 5.3.2 to constitute the adaptive controller as in Fig. 5.3 and propose a systematic solution for Problem 5.1.1.

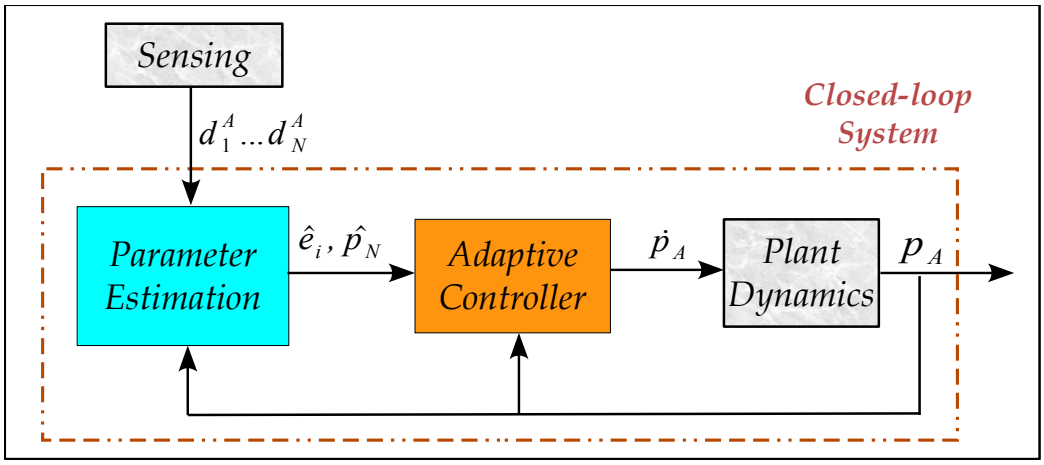

Figure 5.3: The indirect adaptive control scheme.

5.4.1 The Adaptive Control Scheme

Note that the control law (5.6) requires only the signals e_i, $i = 1, \cdots, N-1$, and p_N, and the distance measurements d_i, $i = 1, \cdots, N$. We design our adaptive control scheme based on this control law, Proposition 5.2.1, and certainty equivalence principle; replacing

the signals $e_1, \cdots, e_{N-1}, p_N$ by their estimates generated by the localization algorithm in Section 5.3.2. We define a new (estimate) cost function, which can be defined in terms of these estimates, as

$$J_{est}(p_A) = \frac{1}{2} \sum_{i=1}^{N-1} \left[(p_A - \hat{\xi}_i)^\top \hat{e}_i \right]^2. \tag{5.32}$$

Based on (5.32), we generate the following trajectory, starting at an arbitrary initial location $\hat{p}_A(0) = \hat{p}p_{A,0}$:

$$\dot{\hat{p}}_A(t) = -\frac{\partial J_{est}(\hat{p}_A)}{\partial \hat{p}_A} = -\hat{A}(t)\hat{p}_A(t) + \hat{b}(t), \tag{5.33}$$

where $\hat{A}$ and $\hat{b}$ are defined in (5.25)-(5.26).

The aim in the remainder of the design will be forming a control law which will generate $\dot{p}_A$ such that (i) p_A and $\dot{p}_A$ are bounded; (ii) the persistence of excitation condition in (5.31) is satisfied, and hence exponential convergence of $\hat{A}$ and $\hat{b}$ to A and b, respectively, is guaranteed; and (iii) y asymptotically tracks $\hat{p}_A$. To meet all of these requirements, we propose the following control law:

$$\dot{p}_A(t) = \dot{\hat{p}}_A(t) - \kappa(p_A(t) - \hat{p}_A(t)) + f\left(\|D^* - D(t)\|_\infty\right) \dot{\sigma}_a(t) \tag{5.34}$$

$$\dot{\sigma}_a(t) = H(t)\sigma_a(t), \tag{5.35}$$

where $D^* = [d_1^*, \cdots, d_N^*]^\top$, $D = [d_1, \cdots, d_N]^\top$, $\kappa > 0$ is a design constant. The auxiliary signal σ_a in the control law (5.34)-(5.35) is introduced for the purpose of the persistence of excitation of $\dot{p}_A(t)$, being motivated by the design procedure of [41] and [116], where the function f and the matrix H are selected to satisfy the following assumptions.

Assumption 5.4.1. *$f : \Re^+ \to \Re^+$ is a strictly increasing, differentiable, bounded function that satisfies $f(0) = 0$ and $f(x) \leq x, \ \forall x > 0$.*

Assumption 5.4.2. *i. There exists a $T > 0$ such that for all $t \geq 0$*

$$H(t + T) = H(t). \tag{5.36}$$

ii. $H(t)$ is skew-symmetric for all t and differentiable everywhere.

iii. The derivative of σ_a in (5.35) is persistently exciting for any nonzero value of $\sigma_a(0)$, that is, there exist positive T_1, α_i such that for all $t \geq 0$ there holds

$$\alpha_1 \|\sigma_a(0)\|^2 I \leq \int_t^{t+T_1} \dot{\sigma}_a(\tau)\dot{\sigma}_a(\tau)^\top d\tau \leq \alpha_2 \|\sigma_a(0)\|^2 I.$$

iv. For every $\theta \in \Re^n$, and every $t \in [0, \infty)$, there exists a time instant $t_1(t, \theta) \in [t, t+T_1]$ such that $\theta^\top \dot{\sigma}_a(t_1) = 0$.

Some matrices H satisfying Assumption 5.4.2 are given in [41] and [116] for both 2D and 3D cases. For instance, in 2D, the matrix $H \in \Re^{2\times 2}$ can be chosen in the form of

$$H = hJ, \quad h \in \{\Re \setminus \{0\}\}, \quad J = \begin{bmatrix} 0 & 1 \\ -1 & 0 \end{bmatrix}. \tag{5.37}$$

A constant 3 by 3 matrix cannot however be found which satisfies the requirements of Assumption 5.4.2. In [41] and [116], the following switching matrix is given as an example to matrices satisfying Assumption 5.4.2 in 3D:

$$H(t) = \begin{cases} g\left(\frac{r_{T_1}(t)}{\rho}\right) H_1, & 0 \le r_{T_1}(t) \le \bar{T}_1 \\ H_1, & \bar{T}_1 \le r_{T_1}(t) \le \bar{T}_2 \\ \left(1 - g\left(\frac{r_{T_1}(t)-\bar{T}_2}{\rho}\right)\right) H_1, & \bar{T}_2 \le r_{T_1}(t) \le \bar{T}_3 \\ g\left(\frac{r_{T_1}(t)-\bar{T}_3}{\rho}\right) H_2, & \bar{T}_3 \le r_{T_1}(t) \le \bar{T}_4 \\ H_2, & \bar{T}_4 \le r_{T_1}(t) \le \bar{T}_5 \\ \left(1 - g\left(\frac{r_{T_1}(t)-\bar{T}_5}{\rho}\right)\right) H_2, & \bar{T}_5 \le r_{T_1}(t) \le \bar{T}_6 \end{cases} \tag{5.38}$$

Here, for a suitably small $\rho > 0$,

$$\begin{aligned} &\bar{T}_1 = \rho, \quad \bar{T}_2 = \rho + \frac{\pi}{|h_1|}, \quad \bar{T}_3 = 2\rho + \frac{\pi}{|h_1|}, \\ &\bar{T}_4 = 3\rho + \frac{\pi}{|h_1|}, \quad \bar{T}_5 = 3\rho + \frac{\pi}{|h_1|} + \frac{\pi}{|h_2|}, \\ &T_1 = \bar{T}_6 = 4\rho + \frac{\pi}{|h_1|} + \frac{\pi}{|h_2|}, \end{aligned} \tag{5.39}$$

and $r_{T_1}(t) = t - K_{T_1}(t)T_1$ where $K_{T_1}(t)$ is the largest integer k satisfying $t \ge kT_1$,

$$H_1 = \begin{bmatrix} 0 & 0 \\ 0 & h_1 J \end{bmatrix}, \quad H_2 = \begin{bmatrix} h_2 J & 0 \\ 0 & 0 \end{bmatrix},$$

h_1, h_2 are real nonzero scalars, J is as in (5.37), and

$$g(t) = \begin{cases} 0, & t < 0 \\ \frac{1}{2}(1 - \cos(\pi t)) & 0 \le t \le 1 \\ 1 & t > 1. \end{cases}$$

Lemma 5.4.1. *Consider* $\sigma_a(t) : \Re \to \Re^n$, $n = \{2, 3\}$ *in* (5.35), *with* $H(t) : \Re \to \Re^{n\times n}$, $n = \{2, 3\}$ *and* T_1 *defined as follows:*

- *For* $n = 2$, $H(t)$ *is defined as in* (5.37) *with* $T_1 = \frac{\pi}{h}$.
- *For* $n = 3$, $H(t)$ *is defined as in* (5.38) *with* T_1 *as in* (5.39).

Then, $\sigma_a(t)$ *obeys Assumption 5.4.2.*

Proof. The result is a direct corollary of Theorem 5.1 and Theorem 5.2 of [41], and Section 8 of [116]. □

We have the following lemma.

Lemma 5.4.2 ([41])**.** *Consider* (5.35) *with* $\sigma_a : \Re \to \Re^n$ *and* $H(t) : \Re \to \Re^{n\times n}$, $n = \{2, 3\}$, *satisfying Assumption 5.4.2. Then,*

i. $\|\sigma_a(t)\| = \|\sigma_a(0)\|$ *for all* t.

ii. There exists a finite constant $\bar{\sigma}_a$ *such that* $\|\dot{\sigma}_a(t)\| \leq \bar{\sigma}_a$ *for all* t.

Assumption 5.4.3. κ *is such that* $\kappa > \bar{\sigma}_a$.

5.4.2 Stability and Convergence

In Section 5.3.3, we have established that the signals $\tilde{p}_N$, $\tilde{e}_i$, $i \in \{1, \ldots, N-1\}$, and $\hat{e}_i$, δ_i for all i are bounded. In this subsection, we show that the output vector p_A and the regressor signal ϕ are also bounded, and prove the convergence of the vehicle to the target location.

Before stating the main stability and convergence result, observe that for the target tracking error

$$\varepsilon_A(t) \triangleq p_A(t) - p_A^*, \tag{5.40}$$

by applying the triangular inequality to the sides of the triangle with vertices $p_A(t)$, p_A^*, p_i, one has $\|\varepsilon_A(t)\| + d_i^* \geq d_i(t)$ and $\|\varepsilon_A(t)\| + d_i(t) \geq d_i^*$ for all $i \in \{1, \cdots, N\}$. Thus,

$$\|\varepsilon_A(t)\| \geq \max_{i\in\{1,\cdots,N\}} |d_i^* - d_i(t)| = \|D^* - D(t)\|_\infty. \tag{5.41}$$

Theorem 5.4.1. *Consider Problem 5.1.1 and use of the adaptive control scheme composed of the localization algorithm (5.21), (5.24); the trajectory generation law (5.33); and the control law (5.34),(5.35) to solve this problem. Let Assumptions 5.3.1, 5.4.1, 5.4.2, 5.4.3 hold. Furthermore assume that there exists a time instant $t_{rm} > 0$ after which no covariance resetting occurs in update of $P(t)$ in (5.21), (5.24). Then:*

i. All the closed loop signals, including $\hat{p}_A,\ p_A, \dot{\hat{p}}_A,\ \dot{p}_A,\ \phi,\ \dot{\phi}$, are bounded.

ii. $p_A(t)$ converges to p_A^* asymptotically.

Proof. See Appendix A. □

5.5 Simulations

In this section, we present the simulation results of the adaptive control system synthesized in Section 5.4, combination of the gradient control rule of Section 5.2 and the localization algorithm of Section 5.3. We assume there is a set $\mathcal{S} = \{S_1, S_2, S_3\}$ of three stationary vehicles which are positioned at the following locations:

$$p_1 = [2,\ 0]^\top,\ p_2 = [10,\ 0]^\top,\ p_3 = [6,\ 6]^\top.$$

For all simulations, the estimation parameters are chosen as follows:

$$\beta = 0.9,\ \rho_0 = 10,\ \rho_{min} = 0.001,\ \rho_{\max} = 100,\ R = 5000,$$
$$\epsilon_A = 0.01.$$

In what follows, we simulate the system for different cases of system and controller parameters. For all cases, we show the motion of the mobile vehicle, the distance error $\|p_A - p_A^*\|$ between the mobile vehicle and the target, and the distance errors between the estimated parameters and their actual values, $\|p_A - \hat{p}_A\|$, $\|e_i - \hat{e}_i\|$, $(i = 1, 2)$, and $\|p_3 - \hat{p}_3\|$.

Case 1:
In this scenario, we assume the target is at the interior of the triangle that the stationary vehicles constitute by letting $p_A^* = [8,\ 2]^\top$, resulting in the distance values $d_1^* = 6.3246,\ d_2^* =$

2.8284, $d_3^* = 4.4721$ between the target and the stationary vehicles. The initial estimation parameter values are chosen as follows:

$$\hat{p}_1(0) = [2,\ 3]^\top,\ \hat{p}_2(0) = [2,\ 3]^\top,\ \hat{p}_3(0) = [2,\ 1]^\top,$$
$$p_A(0) = [-10,\ -20]^\top.$$

The design coefficients are chosen as follows:

$$\kappa = 10, \quad \sigma_a(0) = [2,\ 0]^\top, \quad H = J,$$

where J is as in (5.37). With these values, we get the responses in Figures 5.4 and 5.5. It is clearly observed from these results that the mobile vehicle converges to the target location with the proposed control algorithm asymptotically.

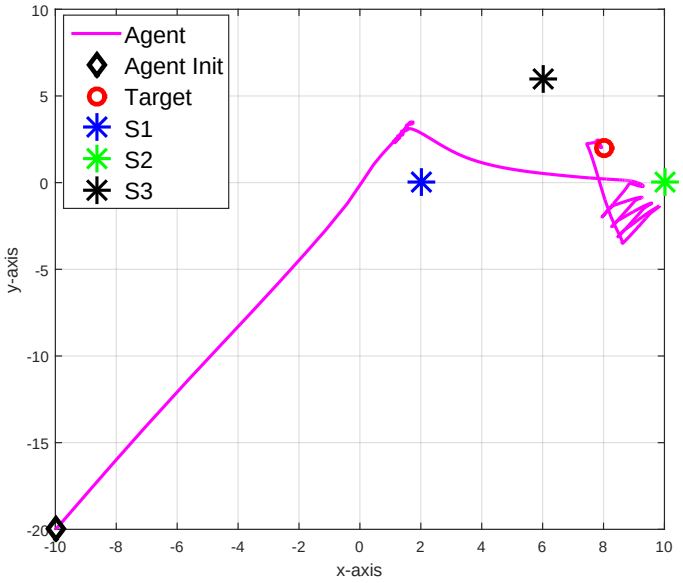

Figure 5.4: Case 1: No noise, non-collinear stationary vehicle positions, $\kappa = 10,\ H = J$. Agent motion and the stationary vehicle positions.

Case 2:

In order to present the global convergence property of the proposed control law, we now assume that the target is located outside the triangle that the sensor stations constitute by letting $p_A^* = [7,\ -2]^\top$. We also change the initial location of the vehicle to $p_A(0) =$

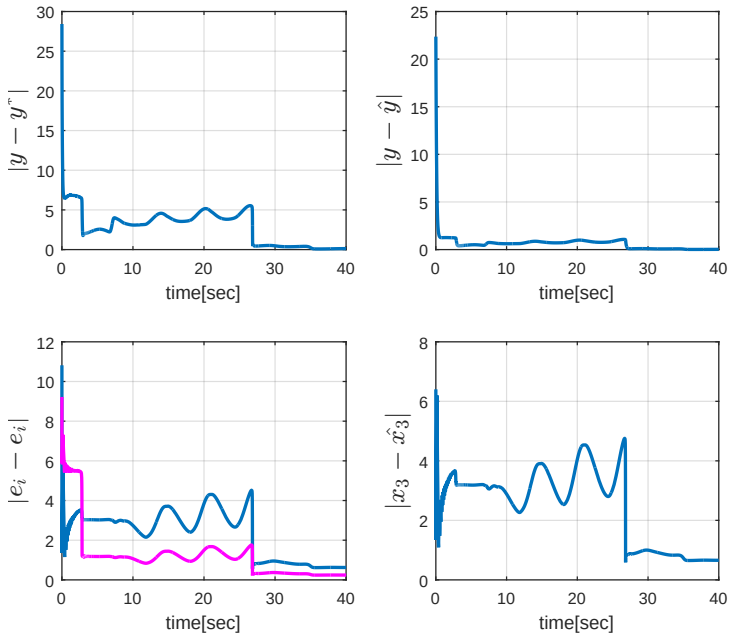

Figure 5.5: Case 1: No noise, non-collinear stationary vehicle positions, $\kappa = 10$, $H = J$. The vehicle converges to the target point asymptotically.

$[-10,\ 20]^\top$. The other variable values are kept the same as in Case 1. The results for this setting are illustrated in Figures 5.6 and 5.7. Since the proposed convergence result is global, the mobile vehicle converges to the target regardless of the initial location of the vehicle or the target's location.

Case 3:
In this case, we simulate the system for $\kappa = 50$ by letting all other variable values the same as in Case 1. The results are shown in Figure 5.8 and 5.9. As κ determines how the position p_A of the vehicle converges to its estimate $\hat{p}_A$, increasing this coefficient fastens the convergence of the distance $\|p_A - \hat{p}_A\|$ to zero.

Case 4:
Here, we keep the variable values the same as in Case 1 except for $H = 5J$. In Figures 5.10 and 5.11, the simulation results are depicted. As expected, this increased the oscillations on the motion of the mobile vehicle in both $x-axis$ and $y-axis$, thus resulting in circular paths with diminishing radius on the $x-y$ graph of the motion. As the control law (5.34)

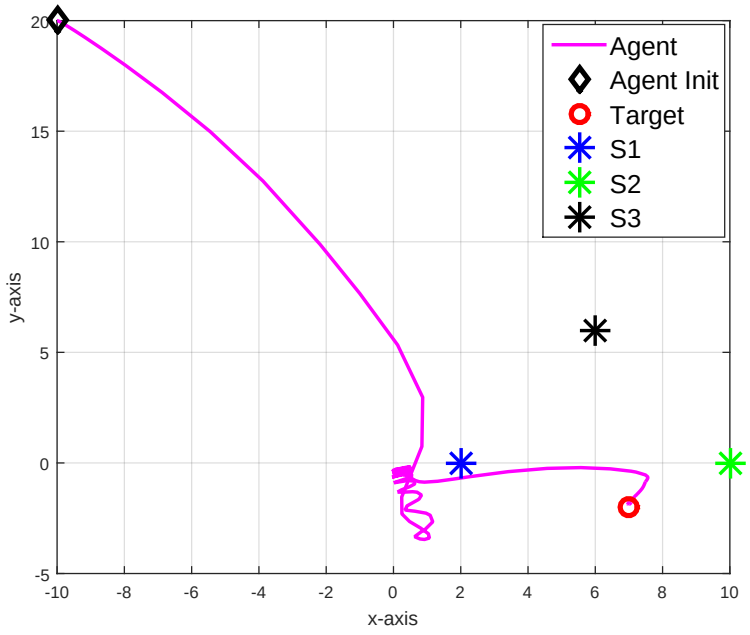

Figure 5.6: Case 2: No noise, non-collinear stationary vehicle positions, $\kappa = 10$, $H = J$. Agent motion and the stationary vehicle positions for different initial and target locations.

suggests, since the magnitude of the f function diminishes with time, the effect of the oscillations caused by the $\dot{\sigma}_a$ term disappears asymptotically, therefore the mobile vehicle converges to the target.

Case 5:

This scenario tests the robustness of the proposed control law to noise. We assume all coefficient values are as in Case 1, and the distance measurements $d_i(t)$ for all $i = \{1, 2, 3\}$ are corrupted by a zero-mean Gaussian noise such that $d_i^{cor}(t) = d_i(t) + X(t)$, where $X(t) \sim \mathcal{N}(0, 0.05)$. The results are depicted in Figures 5.12 and 5.13. Even though noise adds small ripples to the motion of the vehicle, the vehicle eventually converges to a neighborhood of the target asymptotically.

Case 6:

In Problem 5.1.1 of Section 5.2, we assume non-collinear stationary vehicles on $\Re^2$ or non-coplanar stationary vehicles on $\Re^3$. The best scenario in which this assumption is satisfied

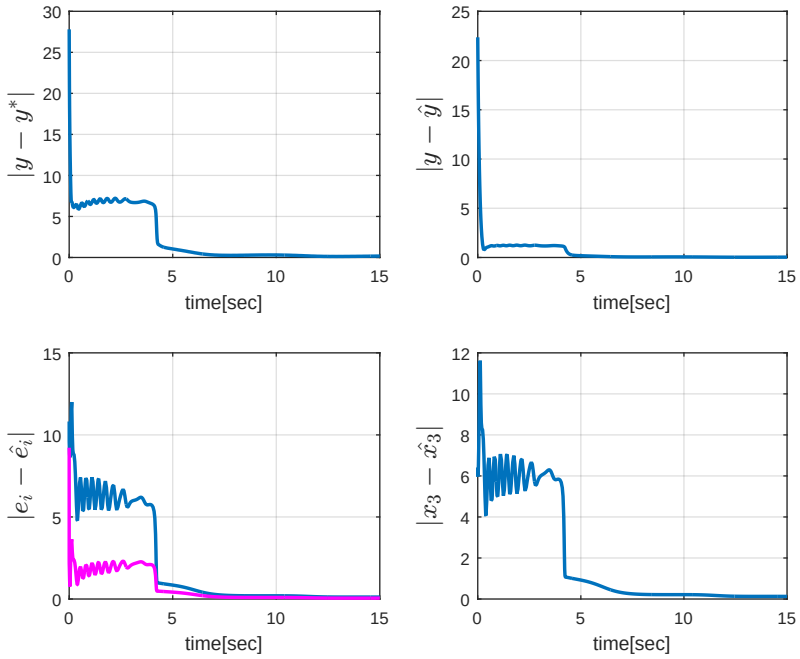

Figure 5.7: Case 2: No noise, non-collinear stationary vehicle positions, $\kappa = 10$, $H = J$. The vehicle converges to the target point asymptotically regardless of the initial and target locations.

for a three-vehicle case is when the stationary vehicles constitute an equilateral triangle, and in the simulations so far we let the three stationary vehicles form a triangle close to an equilateral one. In this scenario, we consider an "almost" collinear stationary vehicles case under noisy measurements. We assume the target is at $p_A^* = [12,\ 0.5]^\top$ and the stationary vehicles are positioned at the following locations:

$$p_1 = [2,\ 0]^\top,\ p_2 = [9,\ 1]^\top,\ p_3 = [16,\ 0]^\top.$$

We keep all other coefficient values the same as in Case 1 and add measurement noise to $d_i(t)$ for all $i = \{1, 2, 3\}$ as in Case 5. The results are depicted in Figure 5.14 and 5.15. The distance error in the transient part of the motion is large compared to the previous cases, and the terms e_i $(i = 1, 2)$ do not converge to their actual values. One reason for this transient behavior is that e_1 and e_2 are almost parallel, and hence, the matrix A in (5.7) is close to a singular one.

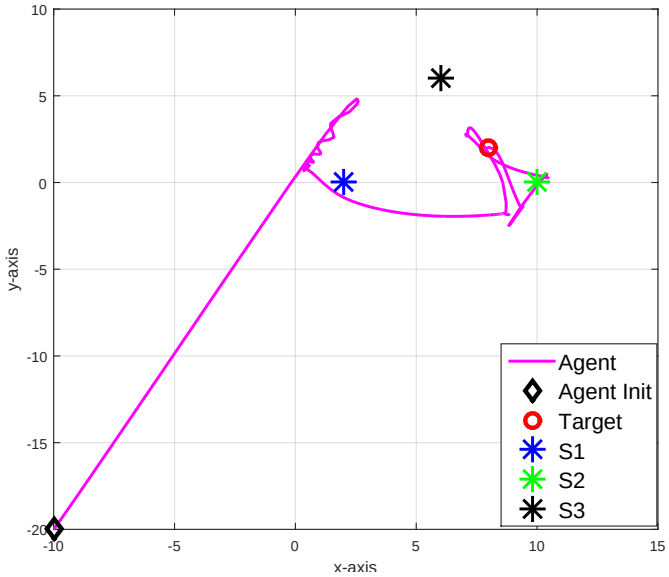

Figure 5.8: Case 3: No noise, non-collinear stationary vehicle positions, $\kappa = 50$, $H = J$. Agent motion and the stationary vehicle positions with increased κ.

5.6 Summary

We synthesize an indirect adaptive control scheme for an autonomous mobile vehicle with known position to reach an unknown target location whose distances to a set of stationary vehicles are measured and broadcast to the vehicle. Employing the modularity and flexibility properties of the indirect adaptive control technique, we decompose the main task into two sub-objectives: localization of the target and motion control of the mobile vehicle. We apply the LS estimation algorithm for the localization objective, and gradient-based control law for the motion control objective. Lyapunov stability analysis is the tool we employ to obtain the globally asymptotically convergence results which are valid for both the two and three-dimensional space.

Robustness to measurement noise is well observed in numerous simulations. Even for the almost collinear stationary vehicles case, we obtain acceptable simulation results. Nevertheless, formal robustness analysis and modification of the proposed algorithm for enhancing robustness is left as a future work item. One may consider minimization of other alternative convex cost functions that can uniquely define the target. Convergence

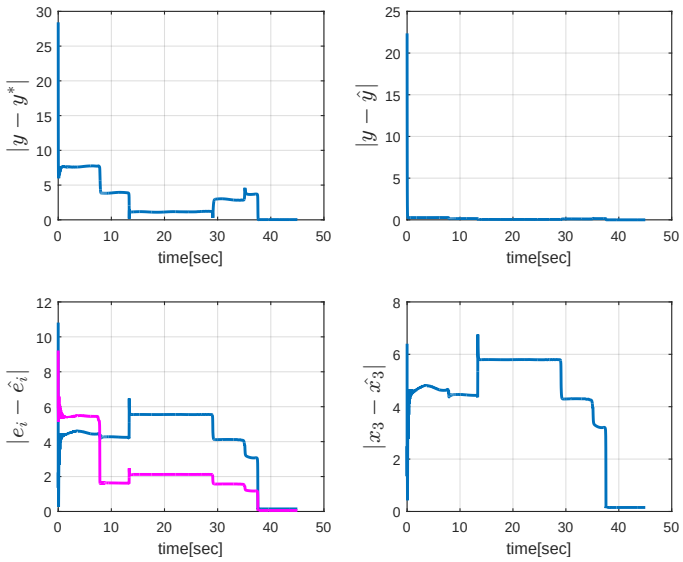

Figure 5.9: Case 3: No noise, non-collinear stationary vehicle positions, $\kappa = 50$, $H = J$. Increasing κ fastens the convergence of y to $\hat{y}$.

properties for these alternatives can also be obtained accordingly.

Results of this chapter can easily be applied to real-life scenarios where vehicle-target distance measurements are not directly obtained by the mobile vehicle. In this regard, extension of the results obtained in this chapter to cover the persistently drifting vehicles case is certainly a good path to continue.

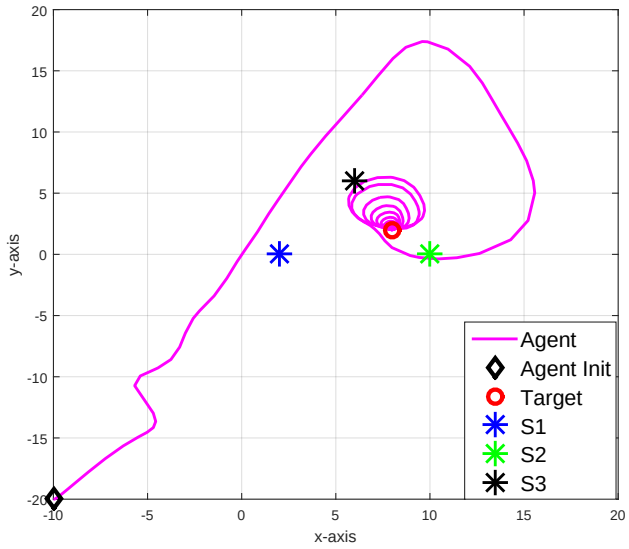

Figure 5.10: Case 4: No noise, non-collinear stationary vehicle positions, $\kappa = 10$, $H = 5J$. Increasing h causes an increase in the artificial oscillation on the $x - y$ graph comparing to the $H = J$ case.

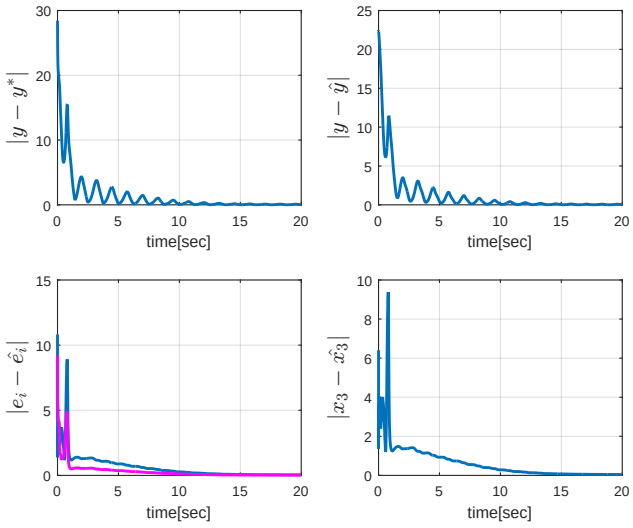

Figure 5.11: Case 4: No noise, non-collinear stationary vehicle positions, $\kappa = 10$, $H = 5J$. There are ripples in the transient motion, but the vehicle converges to the target asymptotically.

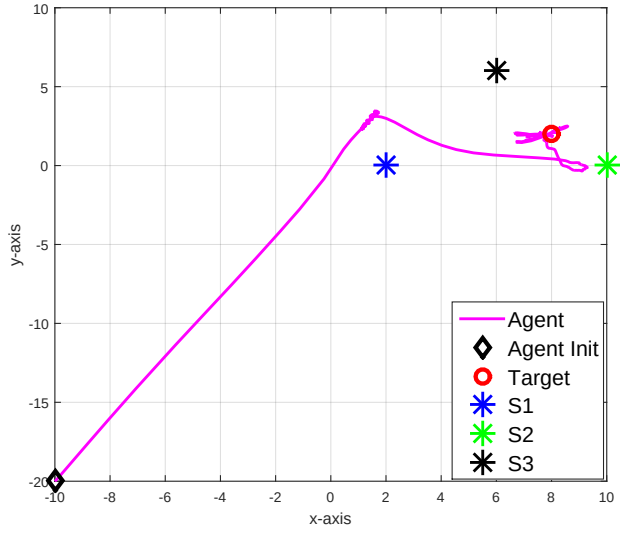

Figure 5.12: Case 5: With noise, non-collinear stationary vehicle positions, $\kappa = 10$, $H = J$. Agent motion and the stationary vehicle positions when noise exists in measurement.

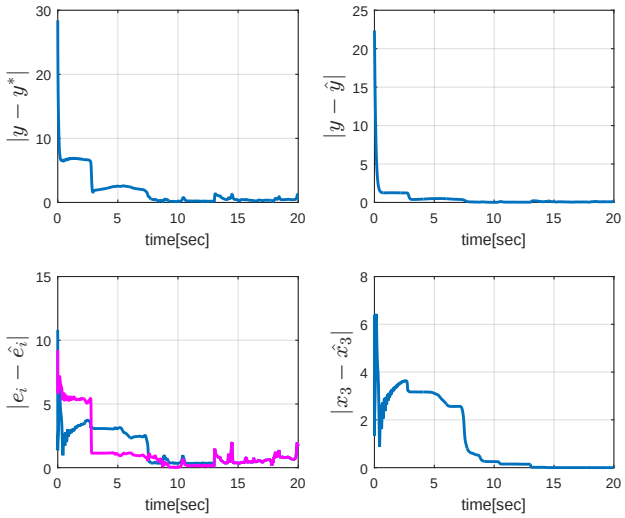

Figure 5.13: Case 5: With noise, non-collinear stationary vehicle positions, $\kappa = 10$, $H = J$. Noise added to the measurements $d_i(t)$ causes chattering on the vehicle motion; however, the vehicle converges to the target's neighborhood.

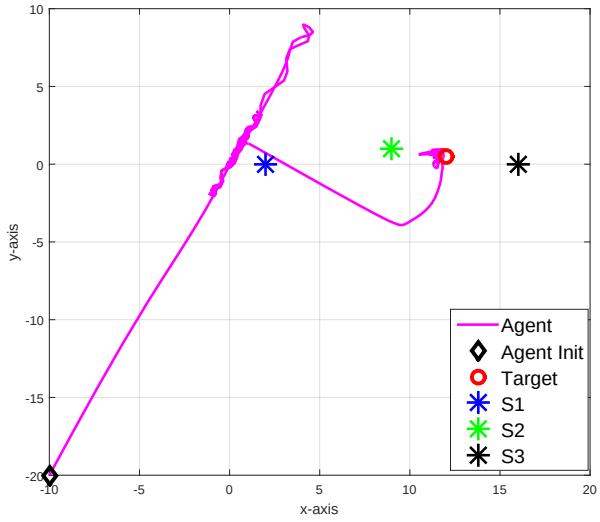

Figure 5.14: Case 6: No noise, almost collinear stationary vehicle positions, $\kappa = 10$, $H = J$. Agent motion and the stationary vehicle positions when stationary vehicles form an almost collinear triangle.

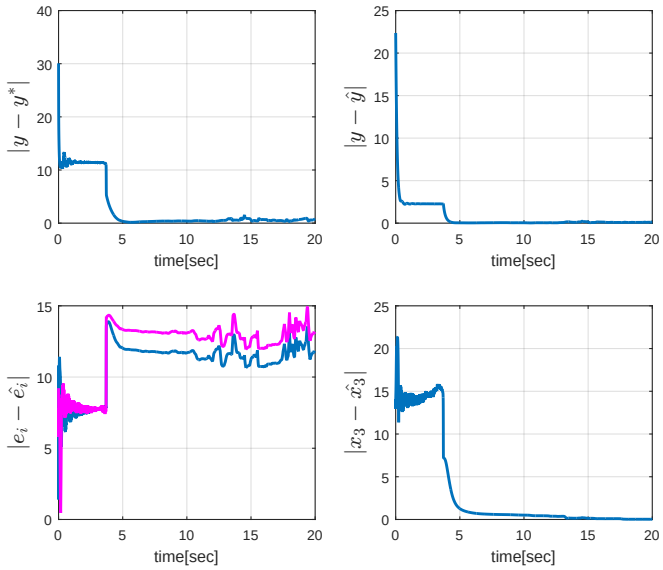

Figure 5.15: Case 6: No noise, almost collinear stationary vehicle positions, $\kappa = 10$, $H = J$. Transient behavior of the vehicle is worse than previous cases because of the almost collinear stationary vehicle positions. The vehicle still reaches to a close neighborhood of the target.

Chapter 6

Station Keeping without Self-Location Information

6.1 Introduction

In Chapter 5, we have proposed a motion control law that achieves the station keeping of an autonomous mobile vehicle A with single integrator kinematics. With this control law, the mobile vehicle A is added to a stationary multi-vehicle network $\mathcal{S}$ to form a new multi-vehicle system by steering it to a target location which is implicitly defined by its distances to vehicles in the network whose positions are also unknown. In Chapter 5, A has been assumed to have the stationary vehicle-target distances d_i^*, stationary vehicle-mobile vehicle distances $d_i(t)$, and its self-position $p_A(t)$. In this chapter, we redesign the proposed station keeping scheme for the more challenging case where the vehicle A has non-holonomic motion dynamics, does not know its self-location $p_A(t)$, but has access to inter-agent distance measurements $d_i(t)$. In practical autonomous vehicle settings, this corresponds to consideration of unavailability of GPS. As the first step to solve this objective, we start with solving the *target capture* (also referred to as *target docking* or *target pursuit*) problem under the same measurement assumptions, then we modify the target capture control law for solving the station keeping problem.

The target capture problem has been studied in a collection of recent works, see for example [26,41], and the references therein. [41] combines the localization algorithm of [28]

and a motion control law to solve the target capture problem, assuming the availability of the range measurement to the target and the vehicle's own position in a reference frame. Our solution to the target capture problem differs from [41] in that we ask the question of how would it be if one applies a range-based motion control approach without localization algorithm to the target capture problem of a non-holonomic vehicle. We propose a switching-based control law inspired by the control approach of [22, 74] for the target capture problem. The switching between the control rules is based on the range measurement and the range rate signal. We first present the control law for a general case where the range measurement and its time derivative are available to the controller. We then present the stability and convergence properties of the control system. Later, we use linear filtering approach to acquire the range rate and use this filtered version of the range rate signal in the control law. Finally, we derive the station keeping control law by modifying the target capture control law such that the error signal is redefined as the difference between the actual and desired mobile vehicle-stationary vehicle distances.

Rest of the chapter is organized as follows. In Section 6.2, the target capture problem for the non-holonomic agent setting without self-location information is defined formally and the motion control law assuming perfect range-rate measurement for the non-holonomic vehicle is proposed. Stability and convergence results of the proposed control law are given in the same section. In Section 6.3, the way the range-rate is obtained and the modified motion control law are presented. In Section 6.4, the station keeping of the non-holonomic vehicle is considered. Section 6.5 demonstrates the performance of the control designs via simulations. Section 6.6 is on the conclusions and future directions.

6.2 Target Capture Problem and Control Design

In this section, we give the formal definition of the target capture problem and present the proposed control law to solve this problem for a mobile non-holonomic vehicle assuming that the range and range-rate measurements are available to the vehicle.

6.2.1 Problem Definition

Consider a non-holonomic vehicle A with the dynamics

$$\dot{p}_A = v\left[\cos(\theta_h),\ \sin(\theta_h)\right]^\top, \quad \dot{\theta} = \omega, \tag{6.1}$$

where $p_A(t) \triangleq [x_A(t),\ y_A(t)]^\top : \Re_+ \to \Re^2$ and $\theta_h(t) : \Re_+ \to [0, 2\pi)$ are the unknown position vector and the known heading angle of the vehicle in the global coordinate frame, and $u(t) \triangleq [v(t),\ \omega(t)]^\top : \Re_+ \to \Re^2$ is the control input of the vehicle. Consider also a target T with unknown constant position $p_T = [x_T,\ y_T]^\top \in \Re^2$. We denote the range (distance) between A and T by

$$d_{AT}(t) \triangleq \|p_A(t) - p_T\|, \tag{6.2}$$

and we assume that $d_{AT}(0) > \epsilon_d$ where ϵ_d is a very small threshold to be defined in the sequel. This configuration is illustrated in Fig. 6.1. Another representation of the

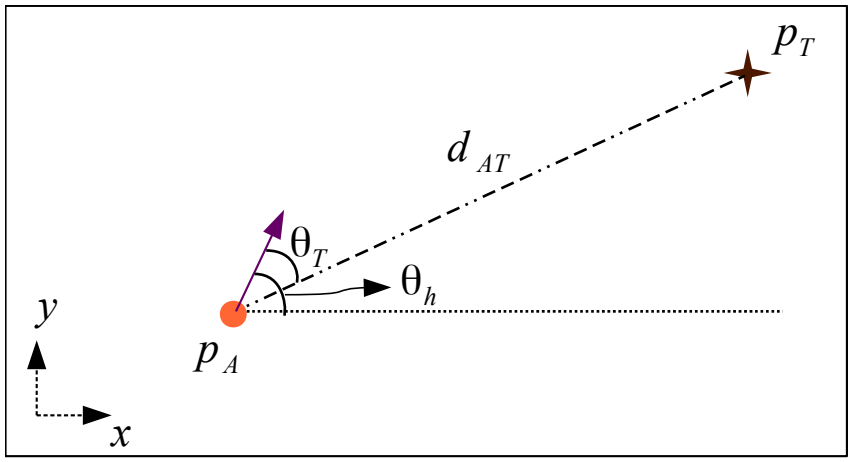

Figure 6.1: Illustration of the vehicle-target configuration.

dynamics (6.1) uses a time-varying coordinate system centered at A, and the unknown angle $\theta_T \in [0, 2\pi)$ from the vector $p_T - p_A$ to the current heading of A [22]:

$$\dot{d}_{AT}(t) = -v(t)\cos(\theta_T(t)), \tag{6.3}$$

$$\dot{\theta}_T(t) = \omega(t) + \frac{1}{d_{AT}(t)} v(t)\sin(\theta_T(t)). \tag{6.4}$$

We focus on driving the non-holonomic vehicle A to the ϵ_d-neighborhood of the target for sufficiently small $\epsilon_d > 0$ and stop the vehicle in this region. Let this region be denoted by $\mathcal{B}_{\epsilon_d}(T) := \{p(t) \mid \|p(t) - p_T\| \leq \epsilon_d\}$.

Problem 6.2.1. *Consider a non-holonomic vehicle A with motion dynamics (6.1) and a stationary target T with unknown location p_T. Given the range measurement $d_{AT}(t)$ in (6.2), with $d_{AT}(0) > \epsilon_d$, and its time derivative $\dot{d}_{AT}(t)$, find a control law $u(t) = [v(t),\ \omega(t)]^\top$ so that A asymptotically converges to the ϵ_d neighborhood $\mathcal{B}_{\epsilon_d}(T)$ of T.*

A similar problem is considered in [26] in the context of extremum seeking, carrying expense of added sinusoid search signals. Here we will follow a more direct approach similar to that of [22, 74] for the target capture problem.

6.2.2 Control Law

In this subsection we derive the base control law we propose, assuming that range-rate $\dot{d}_{AT}(t)$ is perfectly available for measurement. In later sections we will discuss the implementation without having $\dot{d}_{AT}$ information directly. Inspired by the circumnavigation control design in [22, 74], we propose the control law

$$u = [v,\ \omega]^\top, \tag{6.5}$$

where

$$v(t) = \begin{cases} \bar{v}, & \text{if } d_{AT}(t) > \epsilon_d \\ 0, & \text{otherwise,} \end{cases} \tag{6.6}$$

$$\omega(t) = \begin{cases} \left(\text{sgn}(\dot{d}_{AT}(t)) + 1 + 2\dfrac{v(t)}{d_{AT}(t)}\right)\sigma\left(\dfrac{-\dot{d}_{AT}(t)}{v(t)}\right), & d_{AT}(t) > \epsilon_d \\ 0, & \text{otherwise,} \end{cases} \tag{6.7}$$

with

$$\sigma(x) = \begin{cases} 1 - e^{\gamma(x+\epsilon_\theta - 1)}, & \text{if } x < 1 - \epsilon_\theta \\ 0, & \text{otherwise,} \end{cases} \tag{6.8}$$

Here $\sigma\left(-\dot{d}_{AT}/v(t)\right) = \sigma(\cos(\theta_T))$ is a function that satisfies the regulation of the angle θ_T, $\bar{v}$ can be considered as the maximum speed that the vehicle can reach, and $\gamma > 0$.

The function sgn is defined such that $\text{sgn}(x) = 1$ for $x > 0$, $\text{sgn}(x) = -1$ for $x < 0$, and $\text{sgn}(0) = 0$. The coefficients $\epsilon_d,\ \epsilon_\theta > 0$ are sufficiently small and serve as thresholds. To put it differently, if the vehicle enters the disc $\mathcal{B}_{\epsilon_d}$, which is a very small region, the vehicle is desired to stop. Section 6.2.3 provides detailed description on these coefficients.

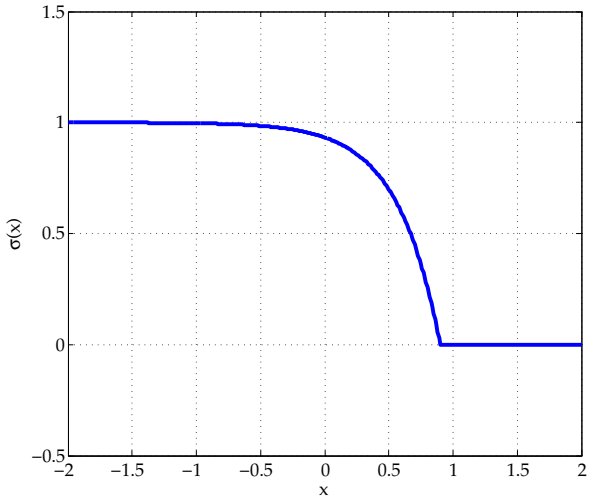

Figure 6.2: The σ function.

6.2.3 Stability and Convergence

In this subsection we provide stability and convergence analysis of the proposed control law (6.5)–(6.8), together with a formal discussion of the intuition behind the selection of switching rules (6.6)–(6.8). The key component in the control law is the steering ω law (6.7). The aim is to drive θ_T to zero, corresponding to the direction in which the approach rate $-\dot{d}_{AT}$ is maximized. This aim can be reformulated as maximizing $\cos(\theta_T)$, which is indirectly measured in terms of $\dot{d}_{AT}$ and v via (6.3) as

$$\cos(\theta_T) = \frac{-\dot{d}_{AT}}{v(t)}. \tag{6.9}$$

The function σ is used to penalize the deviation of θ_T from its desired value zero, as depicted in Fig. 6.2. (6.7) guides the agent A to rotate with a rate dependent on $d_{AT},\ v,$

and the sign of $\dot{d}_{AT}$ as long as A is outside the target vicinity ball $\mathcal{B}_{\epsilon_d}(T)$, unless θ_T gets sufficiently close to zero, which is quantified by comparing (6.9) with $1-\epsilon_\theta$. The switches to zero in the control inputs (6.6) and (6.7) assure that the vehicle stops once it enters the disc $\mathcal{B}_{\epsilon_d}(T)$.

We now present the main result of this section.

Proposition 6.2.1. *Consider Problem 6.2.1 and the control law (6.5)-(6.8) for the vehicle A. Then, the following properties hold:*

(i) The dynamics of θ_T has an isolated equilibrium at $\theta_T = 0$, and a unique stable equilibrium at $\theta_T = \theta_\epsilon \in (0, \frac{\pi}{2})$, which satisfies

$$\sin(\theta_\epsilon) = 2\sigma(\cos(\theta_\epsilon)) \tag{6.10}$$

and

$$cos(\theta_\epsilon) < 1 - \theta_\epsilon. \tag{6.11}$$

(ii) The vehicle A asymptotically converges to the disc $\mathcal{B}_{\epsilon_d}(T)$.

Proof. (i) By assumption of Problem 6.2.1, we have $d_{AT}(0) > \epsilon_d$. Substituting (6.7) into (6.4) gives

$$\dot{\theta}_T(t) = (1 - \text{sgn}(\cos(\theta_T)))\,\sigma(\cos(\theta_T(t))) + \frac{v(t)}{d_{AT}(t)}\left(2\sigma(\cos(\theta_T(t))) + \sin(\theta_T(t))\right). \tag{6.12}$$

We now analyze $\dot{\theta}_T(t)$ for different cases for the parameter $\theta_T(t)$ for any t:

1. $\theta_T(t) = 0$: $\dot{\theta}_T(t) = \dfrac{v(t)}{d_{AT}(t)}\left(2\sigma(1) + 0\right) = 0.$

2. $\theta_T(t) \in (0, \frac{\pi}{2})$: $\dot{\theta}_T(t) = \dfrac{v(t)}{d_{AT}(t)}\left(2\sigma(\cos(\theta_T(t))) + \sin(\theta_T(t))\right)) > 0.$

3. $\theta_T(t) = \dfrac{\pi}{2}$: $\dot{\theta}_T(t) = \sigma(0) + \dfrac{v(t)}{d_{AT}(t)}\left(2\sigma(0) + 1\right) > 0.$

4. $\theta_T(t) \in (\frac{\pi}{2}, \frac{3\pi}{2})$:

$$\dot{\theta}_T(t) = 2\sigma(\cos(\theta_T)) + \frac{v(t)}{d_{AT}(t)}\left(2\sigma(\cos(\theta_T(t))) + \sin(\theta_T(t))\right)$$
$$> 2\sigma(0) + \frac{v(t)}{d_{AT}(t)}\left(2\sigma(0) + \sin(\theta_T(t))\right) > 0.$$

5. $\theta_T(t) = \frac{3\pi}{2}$: $\dot{\theta}_T(t) = \sigma(0) + \frac{v(t)}{d_{AT}(t)}\left(2\sigma(0) - 1\right) > 0.$

6. $\theta_T(t) \in (\frac{3\pi}{2}, 2\pi)$: $\dot{\theta}_T(t) = \frac{v(t)}{d_{AT}(t)}\left(2\sigma(\cos(\theta_T(t))) + \sin(\theta_T(t))\right).$

We further examine the behavior of $\dot{\theta}_T$ when $\theta_T \in (\frac{3\pi}{2}, 2\pi)$ by partitioning this interval into three sets: $\theta_T \in (\frac{3\pi}{2}, 2\pi - \theta_\epsilon)$, $\theta_T = 2\pi - \theta_\epsilon$, and $\theta_T \in (2\pi - \theta_\epsilon, 2\pi)$, where the unique θ_ϵ satisfies (6.10):

6.a. $\theta_T(t) \in (\frac{3\pi}{2}, 2\pi - \theta_\epsilon)$: $\dot{\theta}_T(t) = \frac{v(t)}{d_{AT}(t)}\left(2\sigma(\cos(\theta_T)) + \sin(\theta_T(t)))\right) > 0.$

6.b. $\theta_T(t) = 2\pi - \theta_\epsilon$: $\dot{\theta}_T(t) = 0.$

6.c. $\theta_T(t) \in (2\pi - \theta_\epsilon, 2\pi)$: $\dot{\theta}_T(t) < 0.$

Thus, θ_ϵ is a stable equilibrium of the θ_T dynamics. Considering all of the six possible cases, Cases 1-6, above we have that either $\theta_T(0) = 0$ and thus $\theta_T(t) = 0$ for all $t \geq 0$, or $\theta_T(0) \neq 0$ and thus $\theta_T \to 2\pi - \theta_\epsilon$.

(6.10) is established by the $\dot{\theta}_T$ properties for cases 3, 4, 6. (6.11) and uniqueness of $\theta_\epsilon \in (0, \frac{\pi}{2})$ follows from direct analysis of the function $2\sigma(\cos(\theta_\epsilon)) - \sin(\theta_\epsilon)$.

(ii) It follows from (i) that if $\theta_T(0) = 0$ then $\theta_T(t) = 0$ for all $t \geq 0$, so $\dot{d}_{AT}(t) = -\bar{v}$ and there necessarily exists a time instant $T_f > 0$ such that $d_{AT}(T_f) \leq \epsilon_d$. If $\theta_T(0) \in (0, 2\pi - \theta_\epsilon)$, then $\theta_T(t)$ monotonically increases for all $t \geq 0$, and there holds $\theta_T(t) \to 2\pi - \theta_\epsilon$ and $\dot{d}_{AT}(t) \to -\bar{v}\cos(\theta_\epsilon)$ as $t \to \infty$. If $\theta_T(0) \in (2\pi - \theta_\epsilon, 2\pi)$, then again $\theta_T(t) \to 2\pi - \theta_\epsilon$ and thus $\dot{d}_{AT}(t) \to -\bar{v}\cos(\theta_\epsilon)$ as $t \to \infty$.

For the analysis of the transient behavior of d_{AT}, one can take the integral of both sides of (6.3):

$$d_{AT}(t) = d_{AT}(0) - \int_0^t v(\tau)\cos(\theta_T(\tau))\mathrm{d}\tau, \tag{6.13}$$

which, when the vehicle is outside $\mathcal{B}_{\epsilon_d}(T)$, amounts to

$$d_{AT}(t) = d_{AT}(0) - \bar{v}\int_0^t \cos(\theta_T(\tau))\mathrm{d}\tau. \tag{6.14}$$

It is easily seen that since $\bar{v} > 0$, the range term $d_{AT}(t)$ increases when $\theta_T \in (\frac{\pi}{2}, \frac{3\pi}{2})$, decreases when $\theta_T \in (0, \frac{\pi}{2})$ or $\theta_T \in (\frac{3\pi}{2}, 2\pi)$, and remains constant when $\theta_T = \frac{\pi}{2}$ or $\theta_T = \frac{3\pi}{2}$. From the analysis above, we have that $\dot{d}_{AT}$ eventually converges to $-\bar{v}\cos(\theta_\epsilon)$ and monotonically decreases afterwards. Hence, depending on the initial condition $d_{AT}(0)$, the range term d_{AT} may increase in some finite time interval, but eventually starts decreasing and satisfies $d_{AT}(t) \leq \epsilon_d$, for all $t \geq t_\epsilon$, for some finite time instant $t_epsilon$. Therefore, we conclude that the vehicle A asymptotically converges to the disc $\mathcal{B}_{\epsilon_d}(T)$. □

The phase portrait of θ_T is illustrated in Fig. 6.3. All the solutions starting from the initial condition $\theta_T \neq 0$ converges to $\theta_T = \theta_\epsilon$.

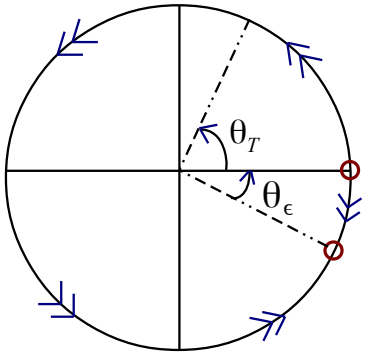

Figure 6.3: The phase portrait of θ_T: There are two equilibrium points one of which is at $\theta_T = 0$ and the other is at $\theta_T = \theta_\epsilon$.

6.3 Control without Range Rate Information

The control design in Section 6.2 has assumed that the range rate $\dot{d}_{AT}$ is available. This, in general, is not the case due to sensing limitations of the vehicle agent A. When the range rate information is not available, one possible attempt is approximating $\dot{d}_{AT}$ via digital signal processing of d_{AT} measurement samples. However, it is a well known fact that this process is not an efficient way since even small noise on the measurement data may cause the $\dot{d}_{AT}$ approximation errors become significantly large. Other typical approaches to obtain first and higher order derivative estimates of a measured signal include high gain and sliding mode observer design [89]. In [22], the range rate estimates are proposed to be obtained using a sliding mode observer. Here, we propose use of a first order filter instead, as a simpler and lower gain solution.

Consider the following first order filtering:

$$z(t) = \dot{\zeta}(t) = -\alpha\zeta(t) + \alpha d_{AT}(t), \tag{6.15}$$

where $\zeta,\ z \in \Re$ are the states of the linear filtering with arbitrary scalar initial conditions and $\alpha > 0$ is a design coefficient. Observe that the signals ζ and z are the filtered version of the signals d_{AT} and $\dot{d}_{AT}$, respectively. We use these signals in place of d_{AT} and $\dot{d}_{AT}$ inside the control law (6.5) to eliminate the range-rate signal requirement, i.e., we propose the control law (6.5) with (6.6), (6.8), and the modified angular velocity control

$$\omega(t) = \begin{cases} \left(\text{sgn}(z(t)) + 1 + 2\dfrac{v(t)}{\zeta(t)}\right)\sigma\left(\dfrac{-z(t)}{v(t)}\right), & d_{AT}(t) > \epsilon_d \\ 0, & \text{otherwise.} \end{cases} \tag{6.16}$$

6.4 Range-Based Station Keeping

6.4.1 Problem Definition

In this section, we adapt the control algorithm derived in Section 6.3 to the station keeping problem defined in Problem 5.1.1 for the setting where the vehicle A has non-holonomic motion dynamics and cannot measure its self-location. For having the problems well-defined and for convenience of the analysis, we focus on 2-dimensional case $n = 2$. The

main task is steering A to the target location p_A^* asymptotically using only the continuous mobile vehicle-stationary vehicle range information $d_i(t)$. For this setting, we write the system dynamics as

$$\begin{aligned} \dot{d}_i(t) &= -v(t)\cos(\theta_{hi}(t)), \\ \dot{\theta}_{hi}(t) &= \omega(t) + \frac{1}{d_i(t)} v(t)\sin(\theta_{hi}(t)). \end{aligned} \tag{6.17}$$

where $i = \{1, \cdots, N\}$ and $\theta_{hi} \in [0, 2\pi)$ is the angle from the vector $(x_i - y)$ to the current heading of A. Here, d_i and θ_{hi} can be considered as the analogue of the range term d_{AT} and the angle θ_T of (6.3)-(6.4). We define the error term to be minimized in magnitude as the difference between the desired and actual values of the inter-vehicle distances of A, i.e., we use

$$e_A(t) \triangleq \frac{1}{\sqrt{N}} \left\| D(t) - D^* \right\|, \tag{6.18}$$

where D, D^* are as defined in (5.34), and the term $\sqrt{N}^{-1}$ serves as the normalization signal. We derive the time derivative $\dot{e}_A$ of e_A by filtering in a similar way to (6.15).

Remark 6.4.1. *In the error definition* (6.18)*, infinity norm of the distance differences, i.e.,* $\left\| D(t) - D^* \right\|_\infty$*, can also be used. In that case, the normalization term* $\sqrt{N}^{-1}$ *can be eliminated.*

We consider the following problem:

Problem 6.4.1. *Consider a mobile* non-holonomic vehicle *A with position $p_A \in \Re^2$ and heading angle $\theta_h \in [0, 2\pi)$ which is required to join a rigid formation of N vehicles $\mathcal{S} = \{A_1, \cdots, A_N\}$, $N > 2$, with unknown constant positions $p_i \in \Re^2$ for each A_i, and an unknown target position $p_A^* \in \Re^2$ for A within the formation. Assume that A_i are not collinear. Assume also that only the desired inter-vehicle distances d_i^* and the the actual inter-vehicle distances $d_i(t)$ are available to A. The task is to define a control law to generate $u = [v,\ \omega]^\top$ such that for any given initial position $p_A(0)$, $p_A(t)$ converges to p_A^* asymptotically.*

6.4.2 Control Law

We use the control law derived in Section 6.2 with some modifications to solve Problem 6.4.1 as follows:

$$u = [v,\ \omega]^\top, \tag{6.19}$$

where

$$v(t) = \begin{cases} \bar{v}\left(1 - \sigma\left(\dfrac{-\dot{e}_A}{\bar{v}}\right)\right), & \text{if } e_A(t) > \epsilon_d \\ 0, & \text{otherwise,} \end{cases} \tag{6.20}$$

$$\omega(t) = \begin{cases} \left(\text{sgn}(\dot{e}_A(t)) + 1 + 2\dfrac{v(t)}{e_A(t)}\right)\sigma\left(\dfrac{-\dot{e}_A(t)}{v(t)}\right), & e_A(t) > \epsilon_d \\ 0, & \text{otherwise.} \end{cases} \tag{6.21}$$

In (6.20)-(6.21), the function $\sigma(\cdot)$ and the terms $\bar{v} > 0,\ \epsilon_d$ are as defined in Section 6.2.2. Since we have N different stationary vehicles, the idea of converging the angle θ_{hi} to the vicinity of zero by controlling the angular velocity ω while keeping the translational velocity v constant as in Section 6.2 does not apply here directly. Instead, we design the control term v such that the translational velocity of A decreases if the error term e_A starts increasing, otherwise it moves with the maximum translational speed $\bar{v}$. Leaving the full stability and convergence analysis of the closed-loop system as a future work, we present the simulation results of the proposed control law (6.20), (6.21) in the next section.

6.5 Simulations

In this section, we present the simulation results for the target capture and station keeping of A with the proposed controllers.

Target Capture: For the target capture objective, the following parameter values are used:

$$\begin{aligned} &p_T = [20,\ 30]^\top \text{m}, \quad p_A(0) = [0,\ 0]^\top \text{m}, \\ &\epsilon_d = 0.2\text{m}, \quad \epsilon_\theta = 0.1, \quad \gamma = 3, \quad \alpha = 20, \quad \bar{v} = 2\text{m/sec}. \end{aligned} \tag{6.22}$$

Fig. 6.4-6.6 represent the behavior of A with the control law (6.5)-(6.8) for 100 seconds. The vehicle successfully achieves the objective, i.e., it enters the disc $\mathcal{B}_{\epsilon_d}(T)$ in a finite time (22 seconds) and stops as soon as it reaches there. Fig. 6.5 shows the range measurement d_{AT} (top), and the range rate $\dot{d}_{AT}$ and the filtered signal z (bottom).

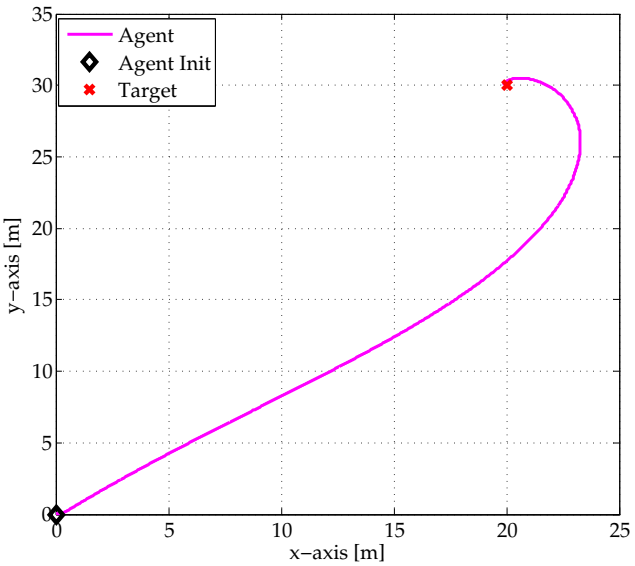

Figure 6.4: Vehicle motion on the plane with the control law (6.5)-(6.8).

Station Keeping: We assume there are three sensor stations located at the following positions:

$$p_1 = [20,\ 20]^\top \text{ m}, \quad p_2 = [25,\ 20]^\top \text{ m}, \quad p_3 = [23,\ 25]^\top \text{ m}.$$

The target location is at $p_A^* = [23,\ 22]^\top$ m. As can be seen in Fig. 6.7 and 6.8, the vehicle reaches the target location while the error e_A decays asymptotically.

6.6 Summary

In this chapter, we have considered the station keeping problem for a non-holonomic vehicle where the self-location information is not available to the vehicle. We have initially studied

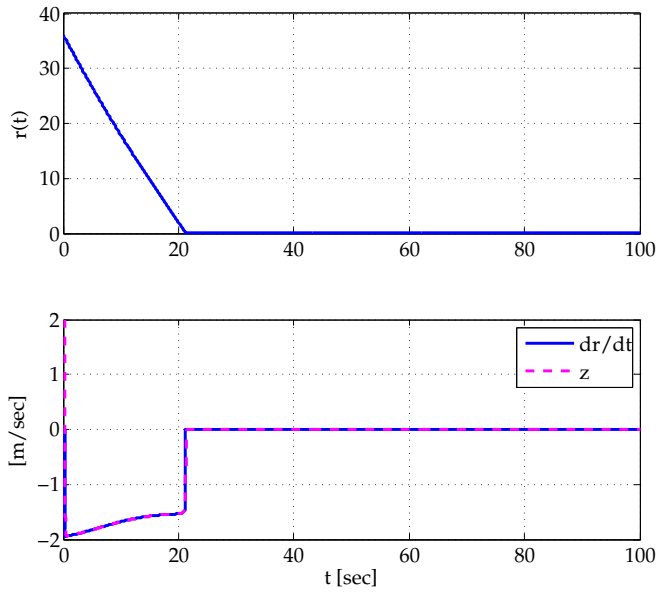

Figure 6.5: The range measurement r (top), and the derivative of the range measurement $\dot{r}$ and the filtered signal z (bottom).

the target capture problem for the same measurement settings. For the target capture task, we have proposed a switching-based control law that requires only the continuous range measurements between the agent and the target. The switching between the control rules are based on the range measurement and the range rate, where the range rate is obtained via filtering of the range measurement signal. The full stability and convergence analysis is presented for the target capture part. Later, we have considered the station keeping problem where the target location is not sensed by the vehicle directly, but it is known by the vehicle that the target is at specified distances to vehicles in a rigid formation whose positions are also unknown. By redesigning the target capture control law, we have synthesized a controller for the station keeping task that uses only the inter-vehicle distances. Studying the stability and convergence properties of the station keeping control law proposed in this chapter is a worthy topic to pursue on.

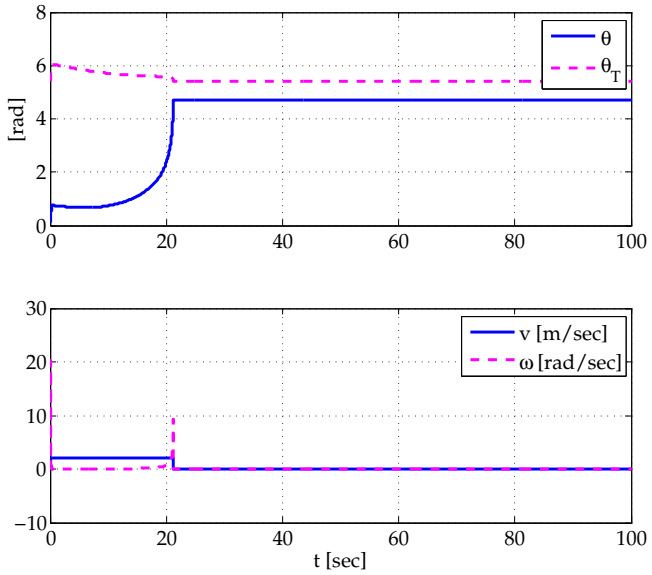

Figure 6.6: The heading angle θ_h in the global coordinate frame and the control input u.

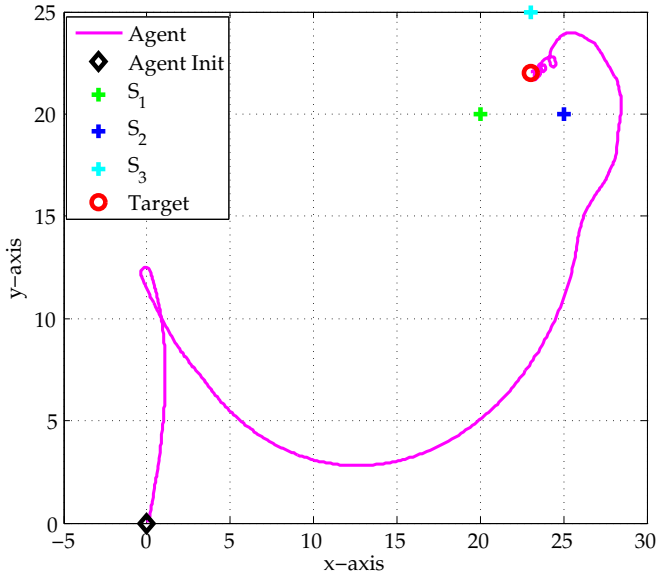

Figure 6.7: Vehicle motion and positions of the sensors and the target.

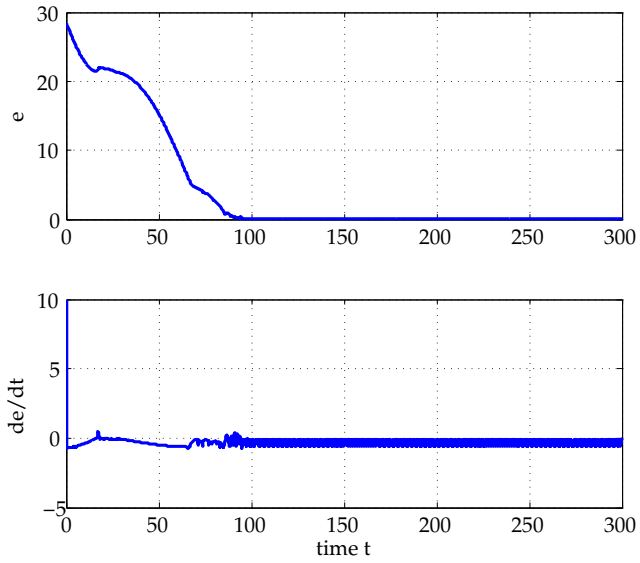

Figure 6.8: The error term e and its time derivative $\dot{e}$.

Chapter 7

Concluding Remarks

We have considered the adaptive formation control of multi-vehicle systems by addressing different particular subproblems. The literature on this subject has been analyzed in detail, and some of most effective works have been presented with discussions on the results and their applicability to the real-time systems. A rich literature exists for formations accepting undirected sensing and constraint graphs in terms of both formation stabilization and flocking. However, *it has been observed that less results have been proposed for the cohesive motion control problem of acyclic minimally persistent formations for general cases, i.e., formations with four or more agents.* Only a few of these works demonstrate limited stability and convergence results without giving transient error analysis for individual vehicles.

In this thesis, we have focused on deriving adaptive control frameworks for a set of interrelated formation control problems. We have defined the problem of cohesive motion control of minimally persistent formations formally and reviewed the recent results on this topic. With carefully selected state variables representing inter-agent behaviors in the formation, a linear system model has been derived assuming each vehicle is modeled by holonomic point agent kinematics. The cohesive motion control problem has been converted to a regulation problem in the interest of gaining new perspectives on the objective and defining the system well for controller derivations. We have established an exponentially stabilizing control law which is completely distributed. Speed limitations on the vehicles and possible control methods to solve the problem have also been studied.

Additionally, we have discussed the formation control problem for the case of high-order

vehicle dynamics with parametric uncertainties. Deriving a parametric model from the system dynamics, we have followed the indirect adaptive control approach that estimates the uncertain parameters by least-squares estimation algorithm and employ these estimates in the adaptive motion control law, applying the certainty equivalence principle. The control law is composed of feedback linearization together with a linear control law. Full stability analysis for individual agents have been provided. Simulation results show that the designed controller perform well in tracking of reference signals for each individual vehicle. Later, we have studied a distributed extension of the proposed adaptive control scheme to the cohesive motion control problem of the aforementioned type of mobile vehicles using two different approaches. *We have concluded that the vehicles achieve the formation control objectives with the proposed controllers even in the existence of parametric uncertainties in vehicle system dynamics.*

Furthermore, we have examined the formation acquisition objective in the context of station keeping control. We have studied the objective of adding an autonomous mobile vehicle to a multi-vehicle system so that the new vehicle is positioned at desired distances from the existing vehicles. The mobile vehicle is assumed to have some restrictions on sensing: It only has its own position and continuous distance measurements to the vehicles in the multi-vehicle network. At the high level, we have studied this implicitly defined problem in two parts: localization and motion control. We have derived an estimation method and a control law to address each part and then combined them in an indirect adaptive control scheme, establishing formal stability and convergence results. *The proposed control approach is modular and adaptive in the sense that different localization algorithms and motion control laws can be employed in the proposed control law as long as the new algorithms satisfy certain conditions by virtue of the certainty equivalence principle.*

Finally, we have studied the station keeping problem for a non-holonomic vehicle without self-location information, as a more-realistic scenario of the station keeping objective. At the outset, using an alternative system dynamics formulation, we have proposed a control law to the target capture problem establishing convergence of the mobile vehicle to a small neighborhood of the target point. We have then modified the target capture motion control law for the station keeping problem. *The proposed control laws therein can be applied in real-time application scenarios where the mobile vehicle bears non-holonomic constraints and low-cost range sensors are mounted on the mobile vehicle instead of complicated sensors such as GPS.*

On the whole, this thesis comprises four different, correlated formation control problems and their solution methods with formal analysis. The results can be enhanced for more specific application scenarios. Some possible future works are listed below:

The linear system dynamics (3.19) is a base motion model describing the inter-agent motion behaviors at the high-level. (3.19) can be integrated with low-level control algorithms for more specific application scenarios. In addition, further distributed control laws can be designed to solve the regulation problem in Section 3.4 in an optimal and robust fashion.

Real-time experiments are planned to be performed, having the proposed algorithms implemented on ground robots and quadrotors. In those experimental settings, uncertain constant parameters in the dynamics of the ground robots or quadrotors can be handled on-line using the approach in Chapter 4.

The results established in this thesis are mostly based on the assumption of perfect sensing of measured quantities such as distances and relative positions for the vehicles. In real-time applications, sensor measurements are prone to noise. The results can be extended with filtering techniques so that the proposed methods would be robust in the case of noise-corrupted measurement cases.

In Chapter 5, we have proposed a control algorithm for the adaptive station keeping problem of a point agent kinematics to constitute a base for further extensions. The algorithm is shown to be robust to measurement noise in simulations, but formal robustness analysis is left as a future work.

In Chapter 6, we have studied the station keeping objective for the non-holonomic vehicle model assuming self-location information is not available to the vehicle. The adaptive station keeping results can be extended to cover more specific and complex vehicle dynamic models which carry non-holonomic kinematic constraints. For instance, the angular velocity control of the vehicle is given in (6.21); if there is a dynamic constraint on the angular velocity, it can be controlled with an integrated low-level control law producing the desired angular velocity.

APPENDICES

Appendix A

Proof of Theorem 5.4.1

(i) Boundedness of the parameter estimates $\hat{e}_i$, $\hat{p}_N$, $\hat{A}$, $\hat{b}$ and the estimation errors $\tilde{e}_i$, $\tilde{p}_N$, $\tilde{A}$, $\tilde{b}$ has already been established in Lemma 5.3.1. Boundedness of σ_a and $\dot{\sigma}_a$ has been established in Lemma 5.4.2. To see the boundedness of $\hat{p}_A$ and $\dot{\hat{p}}_A$, consider the Lyapunov function

$$V_{p_A}(t) = \frac{1}{2}\hat{p}_A^\top(t)\hat{p}_A(t).$$

The time derivative of V_{p_A} is derived as

$$\dot{V}_{p_A}(t) = -\hat{p}_A^\top(t)\hat{A}(t)\hat{p}_A(t) + \hat{p}_A^\top(t)\hat{b}(t).$$

Since, from Lemma 5.3.1 (iv), $\|\hat{b}(t)\| \leq b_{\max}$ for some $b_{\max} > 0$ and for all t, (5.25) guarantees that

$$\begin{aligned}\dot{V}_{p_A}(t) &\leq -\varepsilon_A\hat{p}_A^\top(t)\hat{p}_A(t) + b_{\max}\|\hat{p}_A(t)\| \\ &= -\left(\varepsilon_A\|\hat{p}_A(t)\| - b_{\max}\right)\|\hat{p}_A(t)\|.\end{aligned} \tag{A.1}$$

(A.1) implies that $\dot{V}_{p_A}(t) < 0$ for $\|\hat{p}_A(t)\| > \frac{b_{\max}}{\varepsilon_A}$, and hence $\hat{p}_A$ is bounded. This, together with boundedness of $\hat{A}$ and $\hat{b}$, implies that $\dot{\hat{p}}_A$ is bounded as well.

To establish boundedness of p_A and $\dot{p}_A$, define $e_p(t) \triangleq p_A(t) - \hat{p}_A(t)$ and rewrite (5.34) in terms of e_p:

$$\dot{e}_p(t) = -\kappa e_p(t) + f\left(\|D^* - D(t)\|_\infty\right)\dot{\sigma}_a(t). \tag{A.2}$$

In (A.2), by Assumption 5.4.3, the constant κ satisfies $\kappa > \bar{\sigma}_a > 0$; and by Assumption 5.4.1 and Lemma 5.4.2, $f\left(\|D^* - D(t)\|_\infty\right)\dot{\sigma}_a(t)$ is bounded. Hence, we have e_p and $\dot{e}_p$ are bounded. Since $\hat{p}_A$ and $\dot{\hat{p}}_A$ are bounded, this further implies boundedness of p_A and $\dot{p}_A$. Consequently, boundedness of ϕ and $\dot{\phi}$ follows from (5.13).

(ii) We examine the trajectories of the signals $\tilde{e}_i$, $\tilde{p}_N$ over time, for $t \geq t_{rm}$, following the steps of the proof of Theorem 4.1 of [41] with minor modifications. Consider the Lyapunov-like function

$$V(t) = \sum_{i=1}^{N-1}\left(\frac{3}{\alpha}\delta_i^2(t) + \tilde{e}_i^\top(t)P^{-1}(t)\tilde{e}_i(t)\right) + \frac{3}{\alpha}\delta_N^2(t) + \tilde{p}_N^\top(t)P^{-1}(t)\tilde{p}_N(t), \tag{A.3}$$

with $\gamma_\delta > \dfrac{\rho_{\min}}{4\alpha} > 0$. Using the system equations in Lemma 5.3.1 (ii), the time derivative of V is derived as

$$\begin{aligned}\dot{V}(t) = \sum_{i=1}^{N-1}\Bigg(-3\delta_i^2(t) - \tilde{e}_i^\top(t)\left(2\phi(t)\phi^\top(t) - \frac{dP^{-1}}{dt}\right)\tilde{e}_i(t) - 2\tilde{e}_i^\top(t)\phi(t)\delta_i(t)\Bigg) \\ - 3\delta_N^2(t) - \tilde{p}_N^\top(t)\left(2\phi(t)\phi^\top(t) - \frac{dP^{-1}}{dt}\right)\tilde{p}_N(t) - 2\tilde{p}_N^\top(t)\phi(t)\delta_N(t)\end{aligned} \tag{A.4}$$

Defining $\nu_i \triangleq \tilde{e}_i^\top\phi$ for $i = 1, \ldots, N-1$ and $\nu_N \triangleq \tilde{p}_N^\top\phi$, and noting that, from (5.15), for $t \geq t_{rm}$

$$\frac{dP^{-1}}{dt} = \begin{cases} -\beta P^{-1} + \phi\phi^\top, & \text{if } \lambda_{\max}(P(t)) < \rho_{\max}, \\ 0, & \text{otherwise,}\end{cases}$$

(A.4) implies that

$$\begin{aligned}\dot{V}(t) &\leq \sum_{i=1}^{N-1}\left(-3\delta_i^2(t) - \nu_i^2(t) - 2\nu_i(t)\delta_i(t)\right) - 3\delta_N^2(t) - \nu_N^2(t) - 2\nu_N(t)\delta_N(t) \\ &\leq \sum_{i=1}^{N}\left(-\delta_i^2(t) - \frac{1}{2}\nu_i^2(t)\right) \leq 0, \ \forall t \geq t_{rm};\end{aligned} \tag{A.5}$$

and further for any $t \geq t_{rm}$ at which $\lambda_{\max}(P(t)) < \rho_{\max}$ and, hence, $\frac{dP^{-1}}{dt} \neq 0$,

$$\dot{V}(t) \leq \sum_{i=1}^{N}\left(-\delta_i^2(t) - \frac{1}{2}\nu_i^2(t)\right) - \beta\sum_{i=1}^{N-1}\tilde{e}_i^\top(t)P^{-1}(t)\tilde{e}_i(t) - \beta\tilde{p}_N^\top(t)P^{-1}(t)\tilde{p}_N(t) \leq -k_V V(t) \tag{A.6}$$

for $k_V = \min(\alpha/3,\ \beta)$. Using (A.5),(A.6), from LaSalle-Yoshizawa Theorem, we have that the lumped signal $\left[\delta_1, \cdots, \delta_N, \tilde{e}_1^\top, \cdots, \tilde{e}_{N-1}^\top, \tilde{p}_N^\top,\ \phi^\top\right]^\top$ converges to the set

$$\Omega = \left\{ \left[\delta_1, \cdots, \delta_N, \tilde{e}_1^\top, \cdots, \tilde{e}_{N-1}^\top, \tilde{p}_N^\top,\ \phi^\top\right]^\top \mid \dot{V} = 0,\ \delta_i = 0,\ \nu_i = 0 \right\}. \tag{A.7}$$

Note that on Ω we have

$$\begin{aligned} \dot{\tilde{e}}_i(t) &= \dot{\hat{e}}_i(t) = -P(t)\phi(t)\phi^\top(t)\tilde{e}_i(t) - P(t)\phi(t)\delta_i(t) = 0, \\ \dot{\tilde{p}}_N(t) &= \dot{\hat{p}}_N(t) = -P(t)\phi(t)\phi^\top(t)\tilde{p}_N(t) - P(t)\phi(t)\delta_N(t) = 0. \end{aligned}$$

Therefore, $\tilde{e}_i(t) = \bar{e}_i$ and $\tilde{p}_N(t) = \bar{p}_N$, for some constant vectors $\bar{e}_i$, $\bar{p}_N$. This further implies that $\hat{A}(t) = \bar{A}$ and $\hat{b}(t) = \bar{b}$, for a constant matrix $\bar{A}$ and a constant vector $\bar{b}$. Furthermore, because of continuity of $\hat{A}$ and the fact that $\lambda_{min}(\hat{A}(t)) \geq \epsilon_A$ for all t, $\bar{A}$ is positive definite as well, and hence

$$\hat{p}_A(t) \to \bar{A}^{-1}\bar{b}, \quad \dot{\hat{p}}_A(t) \to 0 \tag{A.8}$$

asymptotically as well.

We now show that along the trajectories on Ω, $p_A(t)$ converges to p_A^* asymptotically. Taking the time derivative of $\bar{e}_i^\top\phi$ and $\bar{p}_N^\top\phi$ on Ω yields

$$\frac{\mathrm{d}}{\mathrm{d}t}\left(\bar{e}_i^\top\phi(t)\right) = \bar{e}_i^\top\dot{\phi}(t) \ = \ 0 \quad \forall i \in \{1, \cdots, N-1\}, \tag{A.9}$$

and

$$\frac{\mathrm{d}}{\mathrm{d}t}\left(\bar{p}_N^\top\phi(t)\right) = \bar{p}_N^\top\dot{\phi}(t) \ = \ 0. \tag{A.10}$$

This, together with (5.13), leads to

$$-\alpha\bar{e}_i^\top\phi(t) + \bar{e}_i^\top\dot{p}_A(t) = \bar{e}_i^\top\dot{p}_A(t) \ = \ \frac{\mathrm{d}}{\mathrm{d}t}\left(\bar{e}_i^\top p_A(t)\right) \ = \ 0 \quad \forall i \in \{1, \cdots, N-1\}, \tag{A.11}$$

and

$$-\alpha\bar{p}_N^\top\phi(t) + \bar{p}_N^\top\dot{p}_A(t) = \bar{p}_N^\top\dot{p}_A(t) \ = \ \frac{\mathrm{d}}{\mathrm{d}t}\left(\bar{p}_N^\top p_A(t)\right) \ = \ 0 \tag{A.12}$$

on Ω.

Hence, with (5.34), (A.8), (A.11), and (A.12), on Ω there holds:

$$\bar{e}_i^\top(\dot{p}_A - \dot{\hat{p}}_A) = -\kappa\bar{e}_i^\top(p_A(t) - \hat{p}_A(t)) + f(D^*, D(t))\bar{e}_i^\top\dot{\sigma}_a(t) = 0 \quad \forall i \in \{1, \cdots, N-1\}, \tag{A.13}$$

$$\bar{p}_N^\top(\dot{p}_A - \dot{\hat{p}}_A) = -\kappa\bar{p}_N^\top(p_A(t) - \hat{p}_A(t)) + f(D^*, D(t))\bar{p}_N^\top\dot{\sigma}_a(t) = 0. \tag{A.14}$$

(A.13) and (A.14) imply that

$$f(D^*, D(t))\bar{e}_i^\top\dot{\sigma}_a(t) = m_1, \tag{A.15}$$

$$f(D^*, D(t))\bar{p}_N^\top\dot{\sigma}_a(t) = m_2, \tag{A.16}$$

where m_1, m_2 are finite constants. Because of Assumption 5.4.2-(iv), $m_1 = m_2 = 0$, that is

$$f(D^*, D(t))\bar{e}_i^\top\dot{\sigma}_a(t) = f(D^*, D(t))\bar{p}_N^\top\dot{\sigma}_a(t) = 0 \tag{A.17}$$

on Ω. To see that

$$\bar{e}_i = \bar{p}_N = 0, \tag{A.18}$$

we use contradiction. Assume that (A.18) does not hold. Then, because of Assumption 5.4.2-(iii), we necessarily have that $f(D^*, D(t)) = 0$ which is equivalent to $p_A = p_A^*$. Thus, by the equation $\kappa\bar{e}_i^\top(p_A(t) - \hat{p}_A(t)) = 0$, there holds $\bar{e}_i^\top = \bar{p}_N^\top = 0$, which contradicts the assumption.

Now, in order to conclude that $p_A(t)$ asymptotically converges to p_A^* along the trajectories in Ω, we define the Lyapunov function

$$L(t) = \frac{1}{2}\varepsilon_p^\top(t)\varepsilon_p(t), \tag{A.19}$$

where ε_p is defined in (5.40). Then,

$$\dot{L} = -2\kappa L + f(D^*, D(t))\varepsilon_p\dot{\sigma}_a \tag{A.20}$$

$$\leq -2\kappa L + f(D^*, D(t))\|\varepsilon_p\|\|\dot{\sigma}_a\| \tag{A.21}$$

$$\leq -2\kappa L + \|\varepsilon_p\|^2\|\dot{\sigma}_a\| \tag{A.22}$$

$$= -2\left(\kappa - \|\dot{\sigma}_a\|\right)L, \tag{A.23}$$

where we have applied (5.41). Under Assumption 5.4.3 we have that $\dot{L}(t) \leq 0$. Since the largest invariant set satisfying (A.23) in Ω is constituted by $p_A(t) = p_A^*$, from LaSalle's Invariance Principle, we conclude that $\varepsilon_y(t)$ converges to 0 and hence, $p_A(t)$ converges to p_A^* asymptotically.

Appendix B

Proof of Lemma 3.6.2

(i). To show the exponential stability of the leader agent to the way-point $p_{1f}[k]$, we consider

$$V_1(t) = \frac{1}{2}\left(\delta_{1f}^\top(t)\delta_{1f}(t)\right)^2 \tag{B.1}$$

as the Lyapunov function candidate. The time derivative of (B.1) is

$$\begin{aligned}
\dot{V}_1(t) &= \delta_{1f}^\top(t)\dot{\delta}_{1f}(t) && \text{(B.2)}\\
&= \bar{v}_1 f_{12}\delta_{1f}^\top(t)\frac{-\delta_{1f}(t)}{\|\delta_{1f}(t)\|} && \text{(B.3)}\\
&= -\bar{v}_1 f_{12}\|\delta_{1f}(t)\| && \text{(B.4)}\\
&\leq 0. && \text{(B.5)}
\end{aligned}$$

Since, by definition, $f_{12}(t) > 0$ for all t, the largest invariant set in $\mathcal{D}_1 := \left\{[\tilde{x}_{1f},\ \tilde{y}_{1f}]^\top \mid \dot{V}_1(t) = 0\right\}$ is $\mathcal{D}_1$ itself. From the LaSalle Invariance Principle [71], δ_{1f} asymptotically convergences to zero.

(ii). Consider the positive definite, radially unbounded Lyapunov function

$$V_2(t) = \frac{1}{4}\left(\delta_{12}^\top(t)\delta_{12}(t)\right)^2. \tag{B.6}$$

The time derivative of (B.6) is

$$\dot{V}_2(t) = \left(\tilde{x}_{12}^2 + \tilde{y}_{12}^2\right)\left(\tilde{x}_{12}\dot{\tilde{x}}_{12} + \tilde{y}_{12}\dot{\tilde{y}}_{12}\right) \tag{B.7}$$

$$= \left(\tilde{x}_{12}^2 + \tilde{y}_{12}^2\right)\left(\tilde{x}_{12}\left(\bar{v}_1 f_{12}\frac{x_{1f}}{\|\delta_{1f}\|} - \dot{x}_2\right) + \tilde{y}_{12}\left(\bar{v}_1 f_{12}\frac{y_{1f}}{\|\delta_{1f}\|} - \dot{y}_2\right)\right) \tag{B.8}$$

Substituting the control rule (3.39) into (B.7) we get

$$\begin{aligned}
\dot{V}_2(t) &= \left(\tilde{x}_{12}^2 + \tilde{y}_{12}^2\right)\left[\tilde{x}_{12}\left(\bar{v}_1 f_{12}\frac{x_{1f}}{\|\delta_{1f}\|} - \bar{v}_1 f_{12}\frac{\tilde{x}_{12}}{\|\delta_{12}\|} - \alpha_2\frac{\tilde{x}_{12}}{\|\delta_{12}\|}\right)\right. \\
&\quad \left. + \tilde{y}_{12}\left(\bar{v}_1 f_{12}\frac{y_{1f}}{\|\delta_{1f}\|} - \bar{v}_1 f_{12}\frac{\tilde{y}_{12}}{\|\delta_{12}\|} - \alpha_2\frac{\tilde{y}_{12}}{\|\delta_{12}\|}\right)\right] \\
&= \left(\tilde{x}_{12}^2 + \tilde{y}_{12}^2\right)\left(\bar{v}_1 f_{12}\left(\frac{x_{1f}}{\|\delta_{1f}\|}\tilde{x}_{12} + \frac{y_{1f}}{\|\delta_{1f}\|}\tilde{y}_{12}\right) - \right. \\
&\quad \left.\left(\bar{v}_1 + (1 - f_{12})\,\alpha_2\right)\left(\frac{\tilde{x}_{12}^2}{\|\delta_{12}\|} + \frac{\tilde{y}_{12}^2}{\|\delta_{12}\|}\right)\right) \\
&\leq \left(\tilde{x}_{12}^2 + \tilde{y}_{12}^2\right)\left(\bar{v}_1 f_{12}\left\|\frac{x_{1f}}{\|\delta_{1f}\|}\tilde{x}_{12} + \frac{y_{1f}}{\|\delta_{1f}\|}\tilde{y}_{12}\right\| - \left(\bar{v}_1 + (1 - f_{12})\,\alpha_2\right)\|\delta_{12}\|\right) \\
&\leq \left(\tilde{x}_{12}^2 + \tilde{y}_{12}^2\right)\left(\bar{v}_1 f_{12}\left\|\frac{1}{\|\delta_{1f}\|}[x_{1f},\ y_{1f}]^\top\right\|\|\delta_{12}\| - \left(\bar{v}_1 + (1 - f_{12})\,\alpha_2\right)\|\delta_{12}\|\right) \\
&= \|\delta_{12}\|^3\left(\bar{v}_1 f_{12} - \bar{v}_1 - (1 - f_{12})\,\alpha_2\right) \\
&\leq 0.
\end{aligned} \tag{B.9, B.10}$$

The last inequality follows from that $\|\delta_{12}(t)\|^3 \geq 0$, $(\bar{v}_1 f_{12} - \bar{v}_1) \leq 0$, and $-(1 - f_{12})\,\alpha_2 \leq 0$ for all t. Consider the set

$$\mathcal{D}_2 := \left\{[\tilde{x}_{12},\ \tilde{y}_{12}]^\top \mid \dot{V}_2(t) = 0\right\}. \tag{B.11}$$

Note that in $\mathcal{D}_2$ we have $\tilde{x}_{12} = \tilde{y}_{12} = 0$, and the largest invariant set contained in $\mathcal{D}_2$ is itself. Then, from the LaSalle Invariance Principle [71], asymptotic convergence of δ_{12} follows.

(iii). Since in the limit we have that $\|\delta_{12}(t)\|$ converges to zero and since $f_{12} = 1 \iff \|\delta_{12}(t)\| = 0$, it follows that f_{12} converges to 1 as $t \to \infty$. This implies (3.40).

References

[1] B.D.O. Anderson, C. Yu, B. Fidan, and J.M. Hendrickx, "Rigid Graph Control Architectures for Autonomous Formations, " *IEEE Control Systems Magazine,* vol.28, no.6, pp.48,63, December 2008.

[2] B.D.O. Anderson, C. Yu, S. Dasgupta, and S. Morse, "Control of a three-coleader formation in the plane, " *Systems & Control Letters,* vol.56, no.9-10, pp.573–578, May 2007.

[3] B.D.O. Anderson, Z. Lin, and M. Deghat, "Combining distance-based formation shape control with formation translation, " in L. Qiu, J. Chen, T. Iwasaki, and H. Fujioka (Eds.), *Developments in Control Theory Towards Glocal Control,* pp.121–130, 2012.

[4] B.D.O. Anderson, S. Mou, A. S. Morse, U. Helmke, "Decentralized gradient algorithm for solution of a linear equation, " *arXiv:1509.04538,* 2015.

[5] M. Arcak, "Passivity as a Design Tool for Group Coordination, " *IEEE Trans. Automatic Control,* vol. 52, no. 8, pp. 1380-1390, August 2007.

[6] R.C. Arkin, *Behavior-based Robotics,* MIT press, 1998.

[7] H. Bai, M. Arcak, and J.T. Wen, *Cooperative Control Design: A Systematic, Passivity-based Approach,* New York: Springer, 2011.

[8] H. Bai, M. Arcak, and J.T. Wen, "Adaptive design for reference velocity recovery in motion coordination, " *Systems & Control Letters,* vol.57, no.8, pp.602–610, February 2008.

[9] H. Bai, M. Arcak, and J.T. Wen , "Adaptive motion coordination: Using relative velocity feedback to track a reference velocity, " *Automatica,* vol.45, no.4, pp.1020–1025, January 2009.

[10] R. Balakrishnan and K. Ranganathan, *A Textbook of Graph Theory,* Springer Science & Business Media, 2012.

[11] T. Balch and R. C. Arkin, "Behavior-based formation control for multirobot teams, " *IEEE Transactions on Robotics and Automation,* vol.14, no.6, pp.926–939, December 1998.

[12] I. Bayezit and B. Fidan, "Distributed cohesive motion control of flight vehicle formations, " *IEEE Trans. Industrial Electronics,* vol.60, no.12, pp.5763–5772, December 2013.

[13] R. Bellman, *Stability Theory of Differential Equations,* New York: Dover Publication, 1969.

[14] D. S. Bernstein, *Matrix Mathematics,* Princeton University Press, 2009.

[15] O. Brown and P. Eremenko, "Fractionated space architectures: a vision for responsive space, " in *Proc. AIAA, 4th Responsive Space Conference,* April 2006.

[16] O. Brown, P. Eremenko, and M. Bille, "Fractionated space architectures: tracing the path to reality, " in *Proc. 23rd Annual AIAA/USU Conference on Small Satellites,* August 2009.

[17] F. Bullo, J. Cortes, and S. Martinez, *Distributed Control of Robotic Networks: A Mathematical Approach to Motion Coordination Algorithms,* Princeton University Press, 2009.

[18] M. Cao and A. S. Morse, "Station keeping in the plane with range-only measurements, " in *Proc. the 2007 American Control Conference,* New York, July 2007.

[19] M. Cao and A. S. Morse , "Maintaining an autonomous agent's position in a moving formation with range-only measurements, " *Proc. of The 2007 European Control Conference,* Kos, Greece, July 2007.

[20] M. Cao and A. S. Morse, "An adaptive approach to the range-only station-keeping problem, " *Int. J. Adapt. Control Signal Process,* vol.26, pp.757–777, February 2012.

[21] M. Cao C. Yu, and B.D.O. Anderson, "Formation control using range-only measurements, " *Automatica,* vol. 47, no. 4, pp. 776–781, April 2011.

[22] Y. Cao, "UAV circumnavigating an unknown target using range measurement and estimated range rate, " in *Proc. American Control Conference,* pp. 4581–4586, June 2014.

[23] Y. Cao, W. Ren, and Z. Meng, "Decentralized finite-time sliding mode estimators and their applications in decentralized finite-time formation tracking, " *Systems & Control Letters,* vol. 59, no.9, pp. 522–529, September 2010.

[24] X. Chen and Y. Li, "Stability on adaptive nn formation control with variant formation patterns and interaction topologies, " *International Journal of Advanced Robotic Systems,* vol.5, no.1, pp.69–82, 2008.

[25] K. Choi, S.J. Yoo, J.B. Park, and Y.H. Choi, "Adaptive formation control in absence of leader's velocity information, " *IET Control Theory and Applications,* vol.4, no.4, pp.521-528, 2010.

[26] J. Cochran and M. Krstic, "Nonholonomic source seeking with tuning of angular velocity, " *IEEE Trans. Automatic Control,* vol. 54, no. 4, pp. 717–731, April 2009.

[27] J. Cortes, "Global and robust formation-shape stabilization of relative sensing networks, " *Automatica,* vol.45, no.12, pp.2754–2762, December 2009.

[28] S.H. Dandach, B. Fidan, S. Dasgupta, and B.D.O. Anderson, "A continuous time linear adaptive source localization algorithm, robust to persistent drift, " *Systems & Control Letters,* vol.58, no.1, pp.7–16, January 2009.

[29] A.K. Das, R. Fierro, V. Kumar, J.P. Ostrowski, J. Spletzer, and C.J. Taylor, "A vision-based formation control framework, " *IEEE Trans. Robotics and Automation,* vol. 18, no. 5, pp. 813-825, October 2002.

[30] M. Deghat, I. Shames, B.D.O. Anderson, and C. Yu, "Localization and circumnavigation of a slowly moving target using bearing measurements, " *IEEE Trans. Automatic Control,* vol.59, no.8, pp.2182–2188, Aug. 2014.

[31] M. Deghat, I. Shames, and B.D.O. Anderson, "Safe autonomous agent formation operations via obstacle collision avoidance, " *Asian Journal of Control,* vol.17, no.5, pp.1473-1483, September 2015.

[32] J.P. Desai, J.P. Ostrowski, and V. Kumar, "Modeling and control of formations of nonholonomic mobile robots, " *IEEE Trans. Robotics and Automation,* vol. 17, no. 6, pp. 905-908, December 2001.

[33] J.P. Desai, J.P. Ostrowski, and V. Kumar, "Controlling formations of multiple mobile robots, " in *Proc. IEEE International Conference on Robotics and Automation,* pp.2864–2869 May 1998.

[34] D.V. Dimarogonas and K.H. Johansson, "On the stability of distance-based formation control, " in *Proc. 47th IEEE Conference on Decision and Control,* pp.1200–1205, December 2008.

[35] D.V. Dimarogonas and K.J. Kyriakopoulos, "A connection between formation infeasibility and velocity alignment in kinematic multi-agent systems, " *Automatica,* vol.44, no.9, pp.2648–2654, September 2008.

[36] S. Duran and V. Gazi, "Adaptive formation control and target tracking in a class of multi-agent systems, " in *Proc. American Control Conference,* pp.75–80, June–July 2010.

[37] M. Egerstedt and X. Hu, "Formation constrained multi-agent control, " *IEEE Transactions on Robotics and Automation,* vol.17, no.6, pp.947–951, December 2001.

[38] S. El-Ferik, A. Qureshi, and F.L. Lewis, "Neuro-adaptive cooperative tracking control of unknown higher-order affine nonlinear systems, " *Automatica,* vol.50, no.3, pp.798–808, March 2014.

[39] B. Fidan, A. Çamlıca, and S. Güler, "Least-squares-based adaptive target localization by mobile distance measurement sensors, " *Int. J. Adapt. Control Signal Process,* vol.29, no.2, pp.259–271, February 2015.

[40] B. Fidan, S. Dasgupta, and B.D.O. Anderson, "Guaranteeing practical convergence in algorithms for sensor and source localization, " *IEEE Trans. Signal Processing,* vol. 56, no. 9, pp. 4458–4469, September 2008.

[41] B. Fidan, S. Dasgupta, and B.D.O. Anderson, "Adaptive range-measurement-based target pursuit, " *Int. J. Adapt. Control and Signal Process.,* vol. 27, no. 1–2, pp. 66–81, January 2013.

[42] B. Fidan, S.Dasgupta, and B.D.O. Anderson, "Guaranteeing practical convergence in algorithms for sensor and source localization, " *IEEE Trans. Signal Processing,* vol.56, no.9, pp.4458–4469, September 2008.

[43] B. Fidan, S. Dasgupta, and B.D.O. Anderson, "Realistic anchor positioning for sensor localization, " in V.D. Blondel, S.P. Boyd and H. Kimura (eds.), *Recent Advances in Learning and Control,* LNCIS, vol. 371, Springer-Verlag, pp.79–94, 2008.

[44] B. Fidan, B.D.O. Anderson, C. Yu, and J.M. Hendrickx, "Persistent autonomous formation and cohesive motion control, " in P.A. Ioannou and A. Pitsillides (eds.), *Modeling and Control of Complex Systems,* CRC Press, December, 2010.

[45] B. Fidan, V. Gazi, S. Zhai, N. Cen, and E. Karatas, "Single-view distance-estimation-based formation control of robotic swarms, " *IEEE Trans. Industrial Electronics,* vol.60, no.12, pp.5781–5791, December 2013.

[46] B. Fidan and F. Kiraz, "On convexification of range measurement based sensor and source localization problems, " *Ad Hoc Networks,* vol.20, pp.113–118, September 2014.

[47] V. Gazi, *Stability Analysis of Swarms,* Dissertation: The Ohio State University, 2002.

[48] V. Gazi, "Formation control of a multi-agent system using nonlinear servomechanism, " *International Journal of Control,* vol. 78, no. 8, pp. 554–565, May 2005.

[49] V. Gazi, "Swarm aggregations using artificial potentials and sliding mode control, " *IEEE Trans. Robotics,* vol. 21, no. 6, pp. 1208–1214, December 2005.

[50] V. Gazi, "Distributed adaptive output agreement in a class of multi-agent systems, " in *Proc. 9th Asian Control Conference,* pp. 1485–1491, Istanbul, Turkey, June 2013.

[51] V. Gazi, "Adaptive formation control and target tracking in a class of multi-agent systems: formation maneuvers, " in *Proc. International Conference on Control, Automation and Systems (ICCAS),* pp. 78–85, Gwangju, Korea, October 2013.

[52] V. Gazi, "Distributed output agreement in a class of uncertain linear heterogeneous multi-agent dynamic systems, " in *Proc. European Control Conference,* pp. 177–183, 2014.

[53] V. Gazi and K.M. Passino, "Stability Analysis of Swarms, " *IEEE Trans. Automatic Control,* vol.48, no.4, pp.692–697, April 2003.

[54] V. Gazi and K.M. Passino, "Stability analysis of social foraging swarms, " *IEEE Transactions on Systems, Man, and Cybernetics: Part B,* vol.34, no.1, pp.539–557, Feb. 2004.

[55] V. Gazi and K.M. Passino, "A class of attraction/repulsion functions for stable swarm aggregations, " *International Journal of Control,* vol.77, no.18, pp.1567-1579, 2004.

[56] V. Gazi and K.M. Passino, *Swarm Stability and Optimization,* Springer-Verlag, 2011.

[57] V. Gazi and B. Fidan, "Coordination and control of multi-agent dynamic systems: models and approaches", in E. Sahin, W. M. Spears and A. F. T. Winfield (Eds.), *Lecture Notes in Computer Science (LNCS) 4433,* Springer-Verlag, pp. 71–102, 2007.

[58] V. Gazi and B. Fidan, "Adaptive formation control and target tracking in a class of multi-agent systems: formation maneuvers, " in *Proc. 13th International Conference on Control, Automation and Systems (ICCAS),* pp. 78–85, 2013.

[59] V. Gazi, B. Fidan, R. Ordonez, and M. I. Koksal, "A target tracking approach for non-holonomic agents based on artificial potentials and sliding mode control, " *Journal of Dynamic Systems, Measurement and Control,* vol. 134, no. 6, November 2012.

[60] V. Gazi, M. İ. Köksal, and B. Fidan, "Aggregation in a swarm of non-holonomic agents using artificial potentials and sliding mode control, " in *Proc. European Control Conference,* pp. 1485–1491, Kos, Greece, July 2007.

[61] E. Gül and V. Gazi, "Adaptive internal model based formation control of a class of multi-agent systems, " in *Proc. American Control Conference,* pp. 4800–4805, 2010.

[62] E. Gül and V. Gazi, "Adaptive internal model based distributed output agreement in a class of multi-Agent dynamic systems, " in *Proc. Special International Conference on Complex Systems: Synergy of Control, Computing, and Communications,* 2011.

[63] E. Gül and V. Gazi, "Adaptive internal model based formation control of a class of multi-agent systems with switched exosystems, " in *Proc. Chinese Control and Decision Conference,* pp. 6–13, May 2012.

[64] S. Güler, B. Fidan, S. Dasgupta, B.D.O. Anderson, and I. Shames, "Adaptive source localization based station keeping of autonomous vehicles, " *IEEE Trans. Automatic Control,* (submitted).

[65] S. Güler, N. Köksal, B. Fidan, and V. Gazi, "Indirect adaptive formation control of multi-agent systems with uncertain dynamics, " *Asian Journal of Control,* (submitted).

[66] S. Güler, B. Fidan, and V. Gazi, "Adaptive swarm coordination and formation control, " in Y. Tan (edt.), *Handbook of Research on Design, Control, and Modeling of Swarm Robotics,* IGI Global, December 2015.

[67] S. Güler and B. Fidan, "Range based target capture and station keeping of nonholonomic vehicles without GPS, " in *Proc. European Control Conference,* Linz, Austria, pp.2970–2975, July 2015.

[68] S. Güler, N. Köksal, and B. Fidan, "Adaptive control of a three-agent surveillance swarm with constant speed constraint, " in *Proc. 9th Asian Control Conference (ASCC),* June 2013.

[69] S. Güler, N. Köksal, B. Fidan, and V. Gazi, "Indirect adaptive formation control with nonlinear dynamics and parametric uncertainty, " in *Proc. 9th Asian Control Conference (ASCC),* June 2013.

[70] F. Hadaegh, W.M. Lu, and P. Wang, "Adaptive control of formation flying spacecraft for interferometry, " in *Proc. IFAC Symposium on Large Scale Systems: Theory and Applications,* Patras, Greece, July 1998.

[71] W.M. Haddad and V. Chellaboina, *Nonlinear Dynamical Systems and Control: A Lyapunov-based Approach,* Princeton University Press, 2008.

[72] Y.Hanada, G. Lee, and N.Y. Chong, "Adaptive flocking of a swarm of robots based on local interactions, " in *Proc. IEEE Swarm Intelligence Symposium (SIS),* 2007.

[73] A.R. Hashemi, Y. Cao, G. Yin, and D. Casbeer, "UAV circumnavigation using noisy range-based measurements without GPS information, " *ASME Journal of Dynamic Systems, Measurement, and Control,* June 2014.

[74] A. Hashemi, Y. Cao. D. Casbeer, and G.Y. Yin, "UAV circumnavigation of an unknown target without location information using noisy range-based measurements, " in *Proc. American Control Conference (ACC),* pp.4587,4592, June 2014.

[75] J.M. Hendrickx, B. Fidan, C. Yu, B.D.O. Anderson, and V.D. Blondel, "Formation reorganization by primitive operations on directed graphs, " *IEEE Trans. Automatic Control,* vol. 53, no. 4, pp. 968–979, May 2008.

[76] J.M. Hendrickx, B.D.O. Anderson, J.C. Delvenne, and V.D. Blondel, "Directed graphs for the analysis of rigidity and persistence in autonomous agent systems, " *IEEE Trans. Automatic Control,* vol. 17, no. 10–11, pp. 960–981, July 2007.

[77] J.P. Hespanha, *Linear Systems Theory,* Princeton University Press, 2009.

[78] Z.G. Hou, L. Cheng, and M. Tan, "Decentralized robust adaptive control for the multiagent system consensus problem using neural networks, " *IEEE Trans. Systems, Man, and Cybernetics, Part B: Cybernetics,* vol. 39, no. 3, pp. 636–647, June 2009.

[79] J. Hu and W.X. Zheng, "Adaptive tracking control of leaderfollower systems with unknown dynamics and partial measurements, " *Automatica,* vol.50, no.5, pp.1416–1423, May 2014.

[80] *IEEE Signal Processing Magazine*, July 2005.

[81] I-A. F. Ihle, M. Arcak, and T.I. Fossen, "Passivity-based designs for synchronized path-following, " *Automatica,* vol.43, no.9, pp.1508–1518, September 2007.

[82] P. Ioannou and B. Fidan, *Adaptive Control Tutorial,* SIAM, 2006.

[83] P. Ioannou and A. Pitsillides, *Modeling and Control of Complex Systems,* Taylor & Francis, December 2007.

[84] B. Jackson and T. Jordan, "Connected rigidity matroids and unique realizations of graphs, " *Journal of Combinatorial Theory, Series B,* vol.94, no.1, pp.1–29, May 2005.

[85] D. Jin and L. Gao, "Stability analysis of swarm based on double integrator model, " in D. S. Huang, K. Li, and G.W. Irwin (Edt.), *Proc. ICIC 2006, Lecture Notes in Bioinformatics (LNBI),* Springer-Verlag, Berlin Heidelberg, 2006.

[86] D. Jin and L. Gao, "Stability analysis of a double integrator swarm model related to position and velocity, " *Transactions of the Institute of Measurement and Control,* vol.30, no.3, pp.275-293, 2008.

[87] R. Johnson, *Advanced Euclidean Geometry,* Dover Publications, 2007.

[88] S.S. Joshi, "Multilevel adaptation for autonomous mobile robot formations, " *Guidance, Navigation, and Control Conference,* Denver, CO, USA, August 2000.

[89] H.K. Khalil, *Nonlinear Systems,* Third Edition, New Jersey: Prentice Hall, 1996.

[90] T. Kim and T. Sugie, "Cooperative control for target-capturing task based on a cyclic pursuit strategy, " *Automatica,* vol.43, no.8, pp.1426–1431, June 2007.

[91] L. Krick, M.E. Broucke, and B.A. Francis, "Stabilization of infinitesimally rigid formations of multi-robot networks, " *International Journal of Control,* vol.82, no.3, pp.423–439, March 2009.

[92] J. Lawton, R.B. Beard, and F.Y. Hadaegh, "An Adaptive Control Approach to Satellite Formation Flying With Relative Distance Constraints, " in *Proc. American Control Conference (ACC),* pp. 1545–1549, June 1999.

[93] N.E. Leonard and E. Fiorelli, "Virtual leaders, artificial potentials and coordinated control of groups, " in *Proc. the 40th IEEE Conference on Decision and Control,* pp. 2968–2973. 2001.

[94] G. Lee and N. Y. Chong, "Adaptive flocking of robot swarms: algorithms and properties, " *IEICE Transactions on Communications,* vol. E91-B, no. 9, pp. 2848–2855, 2008.

[95] H.C. Lim and H. Bang, "Adaptive control for satellite formation flying under thrust misalignment, " *Acta Astronautica,* vol.65, pp.112–122, July-August 2009.

[96] G. Mao and B. Fidan, *Localization Algorithms and Strategies for Wireless Sensor Networks: Monitoring and Surveillance Techniques for Target Tracking,* IGI Global, 2009.

[97] S. Mou and A. S. Morse, "A fixed-neighbor, distributed algorithm for solving a linear algebraic equation, " in *Proc. European Control Conference,* pp.2269-2273, 2013.

[98] S. Mou, J. Liu, and A. S. Morse, "A distributed algorithm for solving a linear algebraic equation, " in *Proc. the 51st Annual Allerton Conference on Communication, Control and Computing,* pp.267-274, 2013.

[99] S. Mou, J. Liu, and A. S. Morse, "A distributed algorithm for solving a linear algebraic equation, " *IEEE Trans. Automatic Control,* vol.60, no.11, pp.2863-2878, November 2015.

[100] K.K. Oh and H. Ahn, "Formation control of mobile agent groups based on localization, " in *Proc. IEEE International Symposium on Intelligent Control (ISIC),* pp.822–827, September 2011.

[101] K.K. Oh and H. Ahn, "Formation control of mobile agents based on distributed position estimation, " *IEEE Trans. Automatic Control,* vol.58, no.3, pp.737–742, March 2013.

[102] K.K. Oh and H. Ahn, "Formation control of mobile agents based on inter-agent distance dynamics, " *Automatica,* vol.47, no.10, pp.2306-2312, October 2011.

[103] C. W. Reynolds, "Flocks, herds, and schools: A distributed behavioral model, " *Computer Graphics,* vol.21, no.4, pp.25–34, July 1987.

[104] H. Rezaee, F. Abdollahi and H. A. Talebi, "H-infinity based motion synchronization in formation flight with delayed communications, " *IEEE Trans. Industrial Electronics,* vol.61, no.11, pp.6175-6182, November 2014.

[105] R. Olfati-Saber, "Flocking for multi-agent dynamic systems: algorithms and theory, " *IEEE Trans. Automatic Control,* vol.51, no.3, pp.401–420, March 2006.

[106] R. Olfati-Saber, J.A. Fax, and R.M. Murray, "Consensus and cooperation in networked multi-agent systems, " *Proceedings of the IEEE,* vol.95, no.1, pp.215–233, January 2007.

[107] R. Olfati-Saber and R.M. Murray, "Distributed cooperative control of multiple vehicle formations using structural potential functions, " in *Proc. IFAC World Congr.,* Barcelona, Spain, June 2002.

[108] R. Olfati-Saber and R.M. Murray, "Consensus problems in networks of agents with switching topology and time-delays, " *IEEE Transactions on Automatic Control,* vol.49, no.9, pp.1520–1533, September 2004.

[109] M.-C. Park, Z. Sun, K.-K. Oh, B.D.O. Anderson, and H.-S. Ahn, "Finite-time convergence control for acyclic persistent formations, " in *Proc. IEEE Multi-conference on Systems and Control,* pp.1608–1613, Antibes, France, October 2014.

[110] K.M. Passino and S. Yurkovich, *Fuzzy Control,* Addison-Wesley Longman, 1998.

[111] Z. Peng, Z.C. Wang, X. Hu, and W. Lan, "Adaptive dynamic surface control for formations of autonomous surface vehicles with uncertain dynamics, " *IEEE Trans. Control Systems Technology,* vol.21, no.2, pp.513–520, March 2013.

[112] B. Ranjbar-Sahraei, F. Shabaninia and A. Nemati and S.-D. Stan, "A novel robust decentralized adaptive fuzzy control for swarm formation of multi-agent systems, " *IEEE Trans. Industrial Electronics,* vol.59, no.8, pp.3124–3134, August 2012.

[113] S. Sandeep, B. Fidan, and B. Yu, "Decentralized cohesive motion control of multi-agent formations, " in *Proc. the 14th Mediterranean Conference on Control and Automation,* June 2006.

[114] S. Seshagiri and H.K. Khalil, "Output feedback control of nonlinear systems using RBF neural networks, " *IEEE Trans. Neural Networks,* vol.11, no.1, pp.69–79, January 2000.

[115] A. Serrani, A. Isidori, and L. Marconi, "Semiglobal nonlinear output regulation with adaptive internal model, " *IEEE Trans. Automatic Control,* vol.46, no.8, pp.1178-1194, 2001.

[116] I. Shames, S. Dasgupta, B. Fidan, and B.D.O. Anderson, "Circumnavigation using distance measurements under slow drift, " *IEEE Trans. Automatic Control,* vol.57, no.4, pp.889–903, April 2012.

[117] D.D. Siljak, *Decentralized Control of Complex Systems,* Courier Corporation, July 2013.

[118] R. Skjetne, T.I. Fossen, and P.V. Kokotovic, "Robust output maneuvering for a class of nonlinear systems, " *Automatica,* vol.40, no.3, pp.373–383, March 2004.

[119] M.W. Spong, S. Hutchinson, and M. Vidyasagar, *Robot Modeling and Control,* Wiley, 2005.

[120] J.T. Spooner and K.M. Passino, "Stable adaptive control using fuzzy systems and neural networks, " *IEEE Trans. Fuzzy Systems,* vol.4, no.3, pp.339–359, August 1996.

[121] J.T. Spooner, M. Maggiore, R. Ordonez, and K.M. Passino, *Stable Adaptive Control and Estimation for Nonlinear Systems: Neural and Fuzzy Approximator Techniques,* Wiley, 2002.

[122] Y. Su and J. Huang, "Cooperative global adaptive output regulation for nonlinear uncertain multi-agent systems with iiss inverse dynamics, " *Asian Journal of Control,* vol.17, no.1, pp.14–22, January 2015.

[123] H. Su, X. Wang, and Z. Lin, "Flocking of multi-agents with a virtual leader, " *IEEE Trans. Automatic Control,* vol. 54, no. 2, pp. 293–307, February 2009.

[124] T. Summers, C. Yu, S. Dasgupta, and B.D.O. Anderson, "Control of minimally Persistent leader-remote-follower and coleader formations in the plane, " *IEEE Trans. Automatic Control,* vol.56, no.12, pp.2778–2792, December 2011.

[125] H.G. Tanner, A. Jadbabaie, and G.J. Pappas, "Flocking in fixed and switching networks, " *IEEE Trans. Automatic Control,* vol.52, no.5, pp.863–868, May 2007.

[126] H.G. Tanner, G.J. Pappas, and V. Kumar, "Leader-to-formation stability, " *IEEE Trans. Robotics and Automation,* vol.20, no.3, pp.443–455, June 2004.

[127] A.R. Teel, R. Kadiyala, P. Kokotovic, and S. Sastry, "Indirect techniques for adaptive input-output linearization of non-linear systems, " *Int. J. of Control,* vol.53, no.1, pp.193–222, January 1991.

[128] K.G. Vamvoudakis, F.L. Lewis, and G.R. Hudas, "Multi-agent differential graphical games: Online adaptive learning solution for synchronization with optimality, " *Automatica,* vol.48, no.8, pp.1598–1611, August 2012.

[129] W. Wang, D. Wang, Z. Peng, and H. Wang, "Cooperative adaptive fuzzy output feedback control for synchronization of nonlinear multi-agent systems in the presence of input saturation, " *Asian Journal of Control,* 2015, doi: 10.1002/asjc.1104.

[130] W. Wang, J. Huang, C. Wen, and H. Fan, "Distributed adaptive control for consensus tracking with application to formation control of non-holonomic mobile robots, " *Automatica,* vol.50, no.4, pp.1254–1263, April 2014.

[131] C. Weisheng, H. Shaoyong, and S.G. Shuzhi, "Consensus-based distributed cooperative learning control for a group of discrete-time nonlinear multi-agent systems using neural networks, " *Automatica,* vol.50, no.9, pp.2254–2268, September 2014.

[132] P. Wieland and F. Allgöver, "An internal model principle for consensus in heterogeneous linear multi-agent systems, " in *Proc. 1st IFAC Workshop on Estimation and Control in Networked Systems,* pp.7-12, Venice, Italy, 2009.

[133] P. Wieland, R. Sepulchre, and F. Allgöver, "An internal model principle for synchronization, " in *Proc. IEEE International Conference on Control and Automation (ICCA),* pp.285-290, Christchurch, New Zealand, 2009.

[134] P. Wieland, R. Sepulchre, and F. Allgöver, "An internal model principle is necessary and sufficient for linear output synchronization, " *Automatica,* vol.47, no.3, pp.1068–1074, March 2011.

[135] H.Xu and P.A. Ioannou, "Robust adaptive control of linearizable nonlinear single input systems with guaranteed error bounds, " *Automatica,* vol.40, no.11, pp.1905–1911, November 2004.

[136] J. Yao, R. Ordonez, and V. Gazi, "Swarm tracking using artificial potentials and sliding mode control, " *Journal of Dynamic Systems, Measurement, and Control,* vol.129, no.5, pp.749–754, September 2007.

[137] S.J. Yoo, "Distributed adaptive containment control of uncertain nonlinear multi-agent systems in strict-feedback form, " *Automatica,* vol.49, no.7, pp.2145–2153, July 2013.

[138] H. Yu and X. Xia, "Adaptive consensus of multi-agents in networks with jointly connected topologies, " *Automatica,* vol.48, no.8, pp.1783–1790, August 2014.

[139] C. Yu, B.D.O. Anderson, S. Dasgupta, and B. Fidan, "Control of minimally persistent formations in the plane, " *SIAM Journal on Control and Optimization,* vol.48, no.1, pp.206–233, February 2009.

[140] C. Yu, J.M. Hendrickx, B. Fidan, B.D.O. Anderson, and V.D. Blondel, "Three and higher dimensional autonomous formations: Rigidity, persistence and structural persistence, " *Automatica,* vol.43, no.3, pp.387–402, March 2007.

[141] L. Zhiyun, B. Francis, and M. Maggiore, "Necessary and sufficient graphical conditions for formation control of unicycles, " *IEEE Trans. Automatic Control,* vol.50, no.1, pp.121–127, January 2005.